MARTIN MARIETTA ENERGY SYSTEMS LIBRARIES
3 4456 0350614 1

CENTRAL RESEARCH LIBRARY
DOCUMENT COLLECTION

ORNL-2500
Part 3
Plant Design

cy. 3

THE ORNL GAS-COOLED REACTOR

OAK RIDGE NATIONAL LABORATORY

operated by

UNION CARBIDE CORPORATION

for the

U.S. ATOMIC ENERGY COMMISSION

CENTRAL RESEARCH LIBRARY
DOCUMENT COLLECTION
LIBRARY LOAN COPY
DO NOT TRANSFER TO ANOTHER PERSON
If you wish someone else to see this document, send in name with document and the library will arrange a loan.

ORNL-2500
Part 3
Plant Design

Contract No. W-7405-eng-26

THE ORNL GAS-COOLED REACTOR

By

The Staff

of the

Oak Ridge National Laboratory

DATE ISSUED

April 1, 1958

OAK RIDGE NATIONAL LABORATORY
Oak Ridge, Tennessee
operated by
UNION CARBIDE CORPORATION
for the
U.S. ATOMIC ENERGY COMMISSION

MARTIN MARIETTA ENERGY SYSTEMS LIBRARIES

3 4456 0350614 1

CONTENTS

SECTION 6. Gas System

SECTION 7. Instrumentation and Controls

SECTION 8. Operating Procedures

SECTION 9. Steam System

SECTION 6

GAS SYSTEM

6. GAS SYSTEM

Contents

6.1 Coolant 6.1
6.2 Heat Transfer Performance 6.8
6.3 Blowers 6.23
6.4 Piping 6.34
6.4.1 System Configuration 6.35
6.4.2 Material Selection 6.41
6.4.3 Fabrication Methods 6.42
6.4.4 Valves 6.43
6.4.5 Expansion Joints 6.44
6.4.6 Leak Tightness Considerations 6.46
6.4.7 Stress Analysis 6.49
6.5 Storage System 6.51
6.6 Helium Purification System 6.51

6. GAS SYSTEM

Because of the low volumetric heat capacity of gases relatively high pumping power requirements are inherent in any system using gaseous cooling media. Preliminary calculations for the GCR-2 design indicated that these would amount to 5 to 10% of the gross electric output. In an effort to minimize the unit cost of net electrical power there was, therefore, an incentive to minimize the coolant circuit pressure losses. The objective of minimum cost power also gives an incentive to extract as much heat as possible from the reactor in order to minimize capital costs per unit of output. These two competing objectives result in an optimum reactor power output and an optimum coolant pressure loss through the reactor.

6.1 Coolant

The first step in the analysis of the gas system was to investigate the effects of inlet and outlet gas temperatures and gas composition on pumping power for a system having a given loss coefficient. Table 6.1 summarizes the pertinent properties of various coolant media.

Relative gamma and total (gamma and beta) activities for the various gases are shown in Table 6.1. Since in some instances there are several isotopes as well as two elements involved, there are frequently several activation reactions possible, some of which decay emitting betas only, while others emit beta and gamma radiations. The activities listed in Table 6.1 are based upon thermal neutron activation of pure gases (i.e. impurities were not considered except for (n,p) reactions with O^{16}). Both the total number of disintegrations per unit volume of each gas as compared to CO_2 are shown as well as the number of disintegrations which can lead to gamma radiations as compared to that for CO_2. In using this data, it is noted that the ratio of total to gamma activity for CO_2 is 100.

Figure 6.1 shows the relative pumping power requirements as a function of reactor inlet temperature for carbon dioxide, helium, hydrogen, and nitrogen or carbon monoxide at a fixed-mean system pressure, and at a given reactor power. It is interesting to note that hydrogen

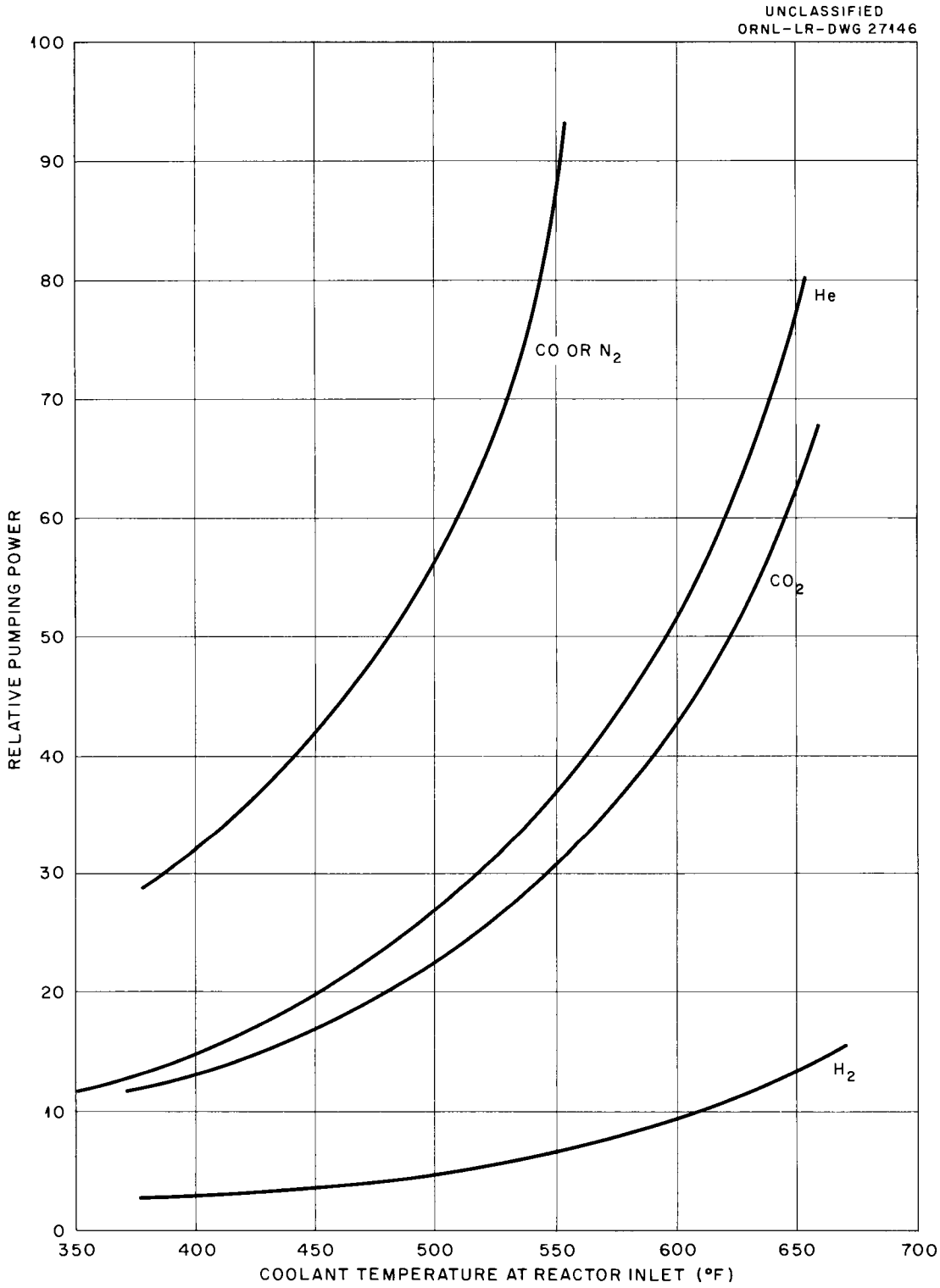

Fig. 6.1. Relative Coolant Pumping Power as a Function of Inlet Temperature.

TABLE 6.1

PROPERTIES OF GASES SUITABLE FOR REACTOR COOLING

Gas	H_2	He	N_2	Air	CO	CO_2	A
Molecular Weight	2	4	28	29	28	44	40
Thermal Conductivity, Btu/hr-ft^2-°F/ft							
200°F	0.125	0.097	0.018	0.018	0.017	0.013	0.012
700°F	0.199	0.135	0.028	0.028	0.027	0.028	0.018
1330°F		0.172	0.037	0.039		0.042	0.025
Viscosity centipoises							
200°F	0.010	0.023	0.020	0.021	0.020	0.017	0.027
700°F	0.015	0.033	0.031	0.032	0.031	0.028	0.041
1330°F	0.020	0.044	0.041	0.042	0.044	0.041	0.054
Specific Heat Btu/lb°F							
200°F	3.47	1.24	0.249	0.241	0.250	0.217	0.124
700°F	3.51	1.24	0.259	0.254	0.262	0.262	0.124
1330°F	3.60	1.24	0.279	0.272	0.283	0.295	0.124
Density at S.T.P., lb/ft^3	0.0052	0.0104	0.0727	0.0748	0.0727	0.114	0.104
Volumetric Specific Heat at S.T.P., Btu/ft^3-°F	0.0178	0.0129	0.0180	0.0179	0.0180	0.0238	0.0129
Relative Heat Transfer Coefficient Compared to He for same gas temperature and same power output	1.19	1.00	0.73	0.73	0.72	0.79	0.68
Relative pumping power compared to helium for same gas temperature and same power output	0.17	1.00	2.2	2.2	2.2	0.88	10
Relative Pumping Power Compared to He	0.17	1.0	4.0	4.0	4.0	1.8	24
Cost of Gas per 1000 ft^3 at S.T.P.	6	22.7	10	0	60	5	40
Relative Total Activity	4.53×10^{-4}	18.5	9294	7225	0.51	1.0	1392
Relative Gamma Activity	0	0	4.56×10^{-2}	1284	0.5	1.0	137,065

gives by far the lowest pumping power requirement. The pumping power for the various coolant gases shown in Fig. 6.1 was calculated on the basis of capacity of the gases to transport heat through a fixed system resistance without reference to the effect of gas composition on heat transfer coefficients and fuel element temperatures. If helium, carbon dioxide, and hydrogen were each used in a given fuel element channel configuration at the same inlet and outlet temperatures and power output, the heat transfer coefficient obtained with carbon dioxide would be approximately 0.79 that obtained with helium, and the resulting fuel capsule surface temperatures would run approximately 100°F hotter at the same power density. Hydrogen, in comparison, would give coefficients approximately 1.19 times that of helium, and the corresponding surface temperatures would be approximately 30°F lower. It is probable,however, in designing reactors for specific coolant gases, that the channel sizes would be adjusted, as described in Section 6.2, to fix the fuel capsule surface temperature for a given power density and coolant inlet and outlet temperatures. To maintain the same temperature difference between the fuel capsule surface and the coolant for the same power density, it is necessary to have the same heat transfer coefficient. To obtain the same heat transfer coefficient with carbon dioxide, the channel must be smaller than for helium. This tends to offset the effect of the higher heat capacity of carbon dioxide. The reverse is true for hydrogen. The relative pumping power for helium, carbon dioxide, and hydrogen calculated by this method is shown on Table 6.2 (referred to helium).

TABLE 6.2

RELATIVE PUMPING POWER FOR VARIOUS GASES WITH FUEL-CHANNEL SIZE ADJUSTED TO GIVE CONSTANT HEAT TRANSFER COEFFICIENT

Coolant temperature: 450°F inlet, 1000°F outlet,
Maximum fuel element temperature: 1200°F,
Thermal power level: 700 Mw

Gas	Heat Capacity	Weight Flow	Vol. Flow	Head Loss	Pumping Power
Helium	1.0	1.0	1.0	1.0	1.0
Carbon dioxide	0.218	4.6	0.418	0.386	1.78
Hydrogen	2.8	0.357	0.714	0.483	0.172

In addition to pumping power requirements, a determining factor in elimination of carbon dioxide as a coolant was its dissociation at the higher system temperatures which makes it suspect for use in contact with graphite. This effect was of little concern in design of the British gas-cooled reactors because of their lower temperature level.

Hydrogen is regarded with suspicion because of its flammability and its characteristic of diffusing into metals and causing embrittlement. In this regard, however, it should be remembered that large electrical machinery is almost universally hydrogen-cooled, and the Haber process for ammonia synthesis has been operating for over fifty years with hydrogen at pressures and temperatures higher than those planned for the subject reactor.

The thermodynamic properties of carbon monoxide and nitrogen would offer some advantages if the coolant gas were also the working fluid in a gas turbine power cycle, but their high-pumping power requirements definitely rule them out for use as simple cooling media.

The selection of helium as a coolant for the reactor naturally raises some important economic questions. These are:

1. Is there an adequate helium supply available?
2. Can the helium losses due to system leakage be limited to the extent that it will not be difficult to maintain a reasonable storage inventory?
3. Will the cost of the helium containment be low enough so that the ultimate power cost will be virtually unaffected?

For each of these questions an affirmative answer will be substantiated in this section.

The supply problem was explored through contacts with the Bureau of Mines, currently the only U. S. helium producers. Unclassified data concerning 1954 production show that the U. S. produced 190,000,000 standard cubic feet of helium and the AEC, Oak Ridge Operations, alone, utilized 15,000,000 SCF during this period. Since 1954 the U. S. capacity has been increased and is now approximately 300,000,000 ft^3 per year. Should multiple reactor installations of this type justify

an extension of this capacity, U. S. helium reserves could easily supply the need. A typical natural gas field in the U. S. contains 0.93% [1] helium in its mixture and is available in substantial quantities in the Texas gas fields.[2]

If the GCR-2 were built using helium as a coolant, it is conceivable that conditions could arise which would make it desirable to replace the helium with some other gas. From considerations discussed above carbon dioxide and hydrogen would be the most likely prospects for use in place of helium.

The use of carbon dioxide would necessitate modification of the gas system. The blowers for the helium plant would be designed to operate at a flow rate of 7920 cfs and a head of 10,000 ft with a drive motor of 6000 hp. Since the density of carbon dioxide is eleven times that of helium at the same temperature and pressure, pumping carbon dioxide with the existing blowers at design flow and head would require eleven times the pumping power, or 66,000 hp. In addition to the very large pumping power, this flow rate of carbon dioxide is much greater than that required to produce 700 Mw (T) without exceeding the fuel capsule surface temperature limit. Thus the most practical solution would be to replace the existing blowers with ones designed for the flow rate of carbon dioxide required to produce 700 Mw (T). Since the fuel channel diameter would be fixed and for the same channel diameter carbon dioxide gives a lower heat transfer coefficient than helium, the temperature difference between the gas and metal would have to be increased for the same power density. This would result in a lower exit temperature of carbon dioxide than for helium at the same thermal output, and consequently a lower thermal efficiency for the plant. The operating conditions for a thermal output of 700 Mw (T) using carbon dioxide as compared with helium and hydrogen are shown in Table 6.3.

[1] Encyclopedia Britannica, 11, 400 (1949).

[2] Bureau of Mines reports 7,000,000,000 ft^3 of proven reserves in the four fields currently being utilized, and many other fields which are not being used.

TABLE 6.3

EFFECTS OF DIFFERENT COOLANT GASES
ON THE PERFORMANCE OF THE ORNL GCR-2 REACTOR

Gas	Thermal Output, Mw (T)	Motor HP Per Blower	Gas Exit Temp., °F	Fuel Element Surface Temp. °F	Gross Elec. Power, Mw (E)	Net Elec. Power, Mw (E)
He	700	6,000	1,000	1,200	251	222
CO_2*	700	8,000	880	1,200	231	197
H_2	700	3,000	842	980	226	206
H_2	700	2,050	1,020	1,200	251	234
H_2	990	3,000	1,004	1,200	355	331

* The blowers would have to be replaced to permit operation with CO_2.

In addition to replacing the blowers, the blower drive motors would have to be replaced with 8,000 hp motors to produce 700 Mw (T) using carbon dioxide. The resulting gross electric power would be less than that for helium because of the lower exit temperature and the consequent lower thermal efficiency for carbon dioxide. The net electric power would be less by an even greater amount because of the increased pumping power required for carbon dioxide.

If, on the other hand, hydrogen were substituted for helium the existing blowers and motors could be used. Since the density of hydrogen is half that of helium for a given temperature and pressure, pumping hydrogen with the existing blowers at design flow and head would require only half the pumping power of helium, or 3000 hp. Table 6.3 shows the resulting conditions when operating with this flow rate of hydrogen at three different thermal outputs.

Operation with hydrogen at 700 Mw (T), at 300 psia, and full blower volumetric capacity would result in a fuel capsule surface temperature of only 980°F, well below the 1200°F limit. Further, because of the high heat capacity of hydrogen, the exit temperature would be only 842°F which gives a reduced thermal efficiency and consequently less gross electric power than for helium at 700 Mw (T). The resulting net electric power would also be less, even though less pumping power is required for hydrogen.

A preferable alternative would be to cut down the mass flow of hydrogen by reducing the system pressure to approximately 210 psia. This would allow the fuel capsule surface temperature to reach its 1200°F limit, at which point the coolant outlet temperature would thus be approximately 1020°F. Thermal efficiency would be maintained and pumping power would be further reduced giving a net electrical output of 234 Mw (E).

Full advantage of the properties of hydrogen could be obtained by raising the reactor power to 990 Mw (T) at a system pressure of 300 psia and full blower volumetric flow. The fuel capsule surface temperature would then be 1200°F. Net electric power would be 331 Mw (E), but additional heat exchanger equipment and generating capacity would have to be installed.

6.2 Heat Transfer Performance

The curves of Fig. 6.1 indicate the importance of minimizing the reactor inlet gas temperature. For a given exit gas temperature the mass flow of coolant required to remove a fixed quantity of heat will be reduced as the inlet temperature is lowered. In addition the mean gas density in the system is increased. Both effects decrease the linear velocity of coolant and decrease the pumping power requirement. Steam generator costs and thermodynamic cycle efficiency indicate an optimum reactor inlet gas temperature of ~ 450°F. This figure was later fixed at 460°F. For a total heat output of 700 Mw, the reactor output is 687 Mw.

The pumping power requirement also varies with the pressure level of the gas in the system for a given set of gas temperatures. For a given-system configuration, power level, and coolant temperatures the required mass flow of coolant is fixed; but the volumetric flow, and consequently the pumping power, will be reduced if the system pressure level is increased.

For the GCR-2, where size, and hence cost, depends principally on nuclear considerations, the coolant pressure level should be as high as current pressure vessel technology will permit, and the fuel capsule surface temperature should be as high as the capsule material will allow. The only remaining independent variables in optimizing the cooling system are the gross reactor power output and coolant temperatures.

If the heat transfer area and the capsule surface temperature are fixed, the gross reactor power output can be increased either by increasing the heat transfer coefficient or by decreasing the coolant temperature. The heat transfer coefficient can be controlled independent of the coolant mass flow rate by changing the channel diameter. If the channel diameter is decreased with the coolant mass flow held constant the heat transfer coefficient will increase.

Both the surface temperature of the fuel capsule and the power density vary along the axis of the channel with the maximum temperature occurring close to the outlet face of the reactor. Figure 6.2 shows the fuel capsule surface temperature as a function of distance from the reactor inlet for a series of channel diameters with fixed coolant temperatures and channel power output. Figure 6.3 summarizes the peak capsule temperatures obtained from a series of plots such as those in Fig. 6.2. It is apparent that as the channel diameter is decreased the coolant temperature or the power density could be allowed to increase without affecting the fuel element wall temperature. An increased coolant pressure drop along the channel will be necessary, however, to maintain the design mass flow. This results in an increased power requirement by the coolant circulating blowers which must be subtracted from the plant gross electrical output.

Figure 6.4 shows the trend of reactor thermal output, pumping power, net electrical power, power cost, and fuel capsule surface temperature with variation of mean coolant velocity in the channel for three different channel diameters. The mean system pressure and the coolant inlet and outlet temperatures are held constant.

The coolant temperature at any point in the channel is controlled by variation of the inlet temperature and the mass flow rate. If, for instance, the mass flow rate is increased the rate of temperature rise along the channel will be reduced resulting in a lower coolant temperature at any point in the channel and, of course, a lower discharge temperature. This will decrease steam temperatures giving lower thermodynamic cycle efficiencies and, ultimately, lower net electrical power output for the plant.

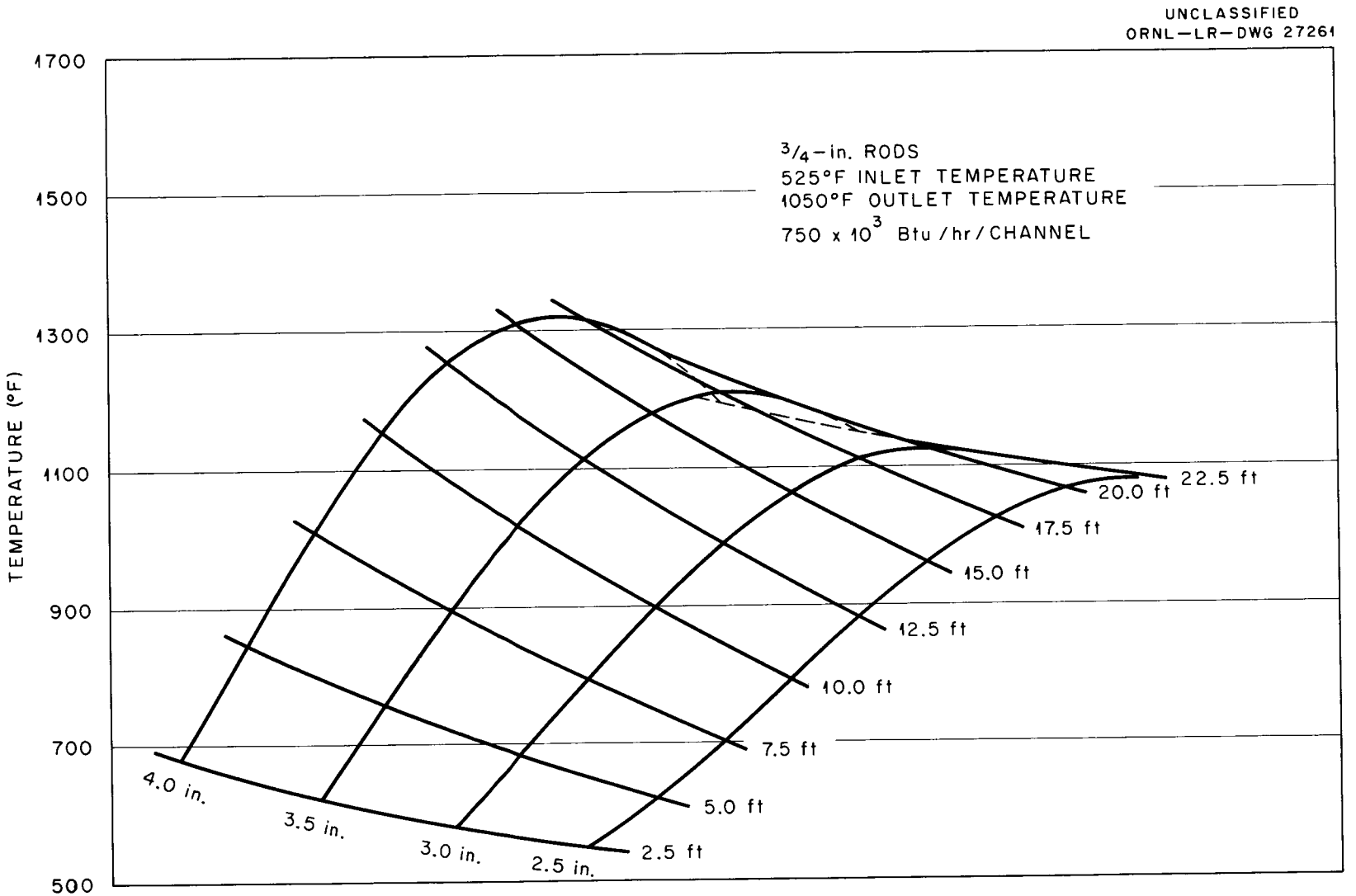

Fig. 6.2. Fuel Element Temperature as a Function of Channel Size and Distance from Inlet Face.

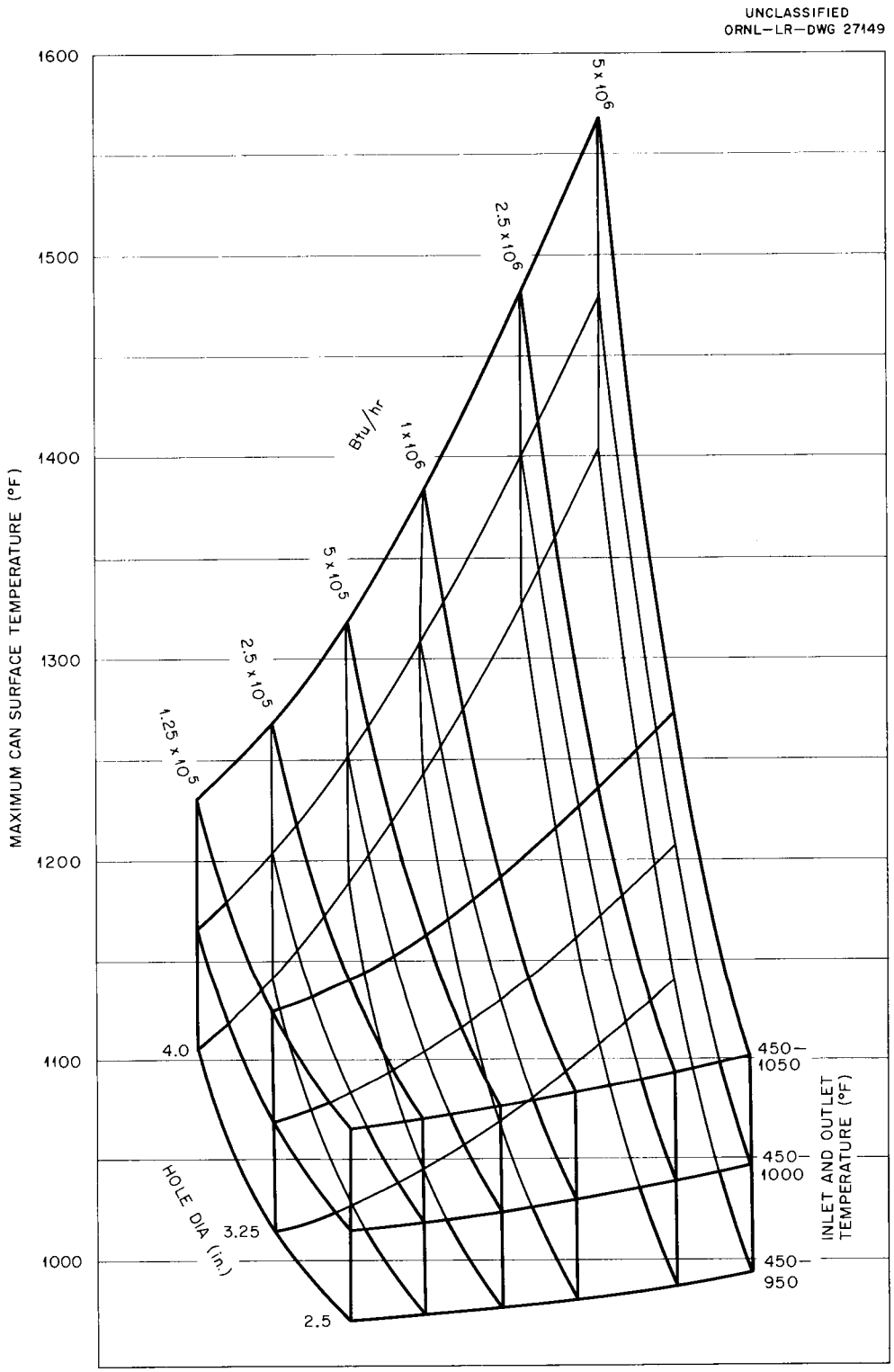

Fig. 6.3. Maximum Fuel Capsule Surface Temperature.

UNCLASSIFIED
ORNL-LR-DWG 27259

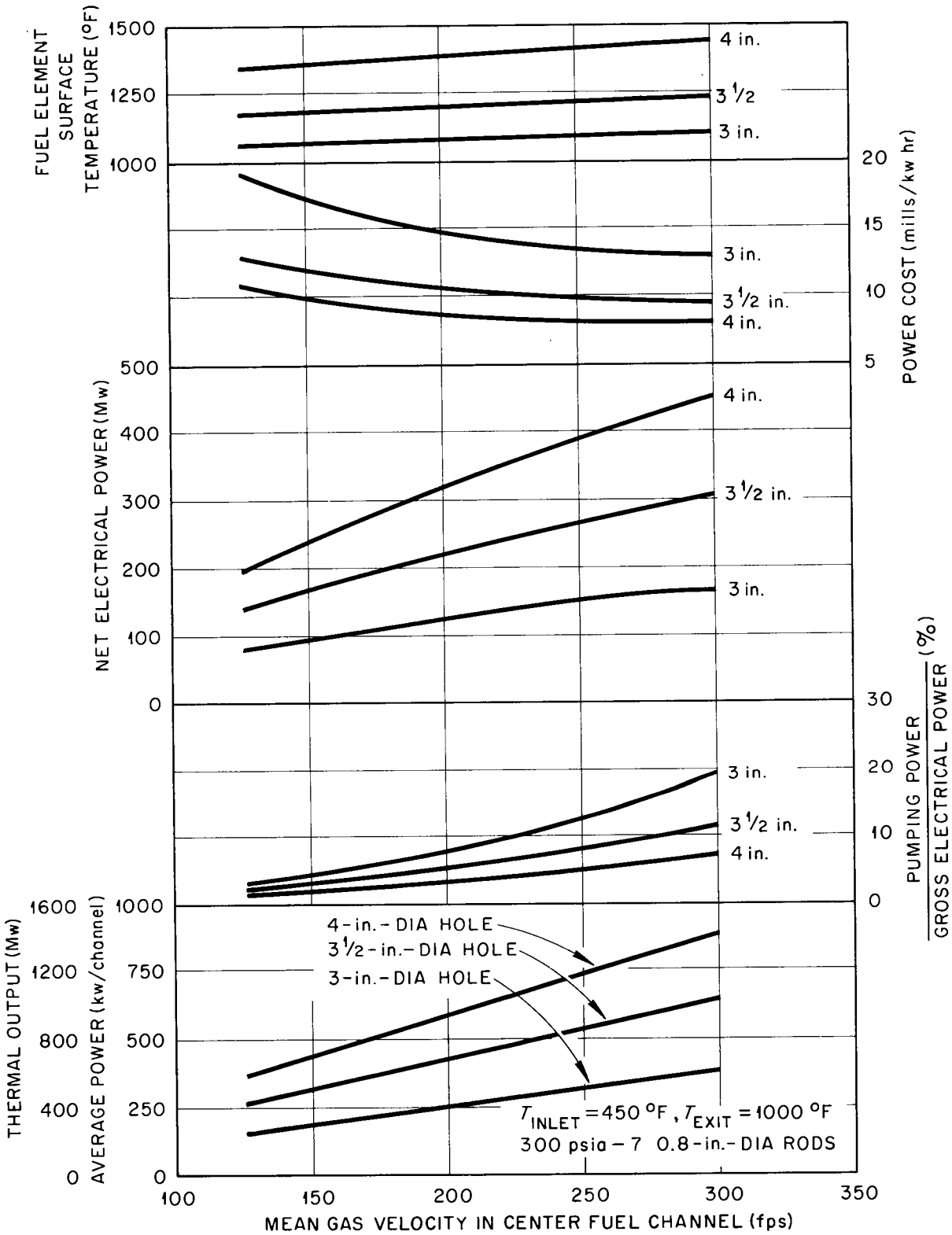

Fig. 6.4. Effects of Fuel Channel Size and Coolant Velocity on Reactor Performance.

Because of the several combinations of variables which were studied the pressure drop calculations were simplified by using incompressible flow formulae and mean coolant density conditions. For the case of compressible flow with both friction and heat addition actual pressure losses will be somewhat higher than those calculated for this study. For the range of conditions covered by these calculations the error would be between 2 and 5%. For a detailed reactor design more rigorous methods of calculating pressure loss in the core should be used.

The method of calculation of the optimum amount of power to be extracted from the reactor is described in detail in Appendix A. Results of the calculations are shown on Figs. 6.5 and 6.6. These show respectively power cost vs. gross reactor power output and net electrical output vs. exit temperature. In these calculations the actual cost charged to the pumping power is the cost of generating the power as shown in Fig. 6.5 which for 700 Mw (T) is 10.3 mills.

In an attempt to optimize the complete reactor it is necessary to make allowances for radial variations in power density. Maximum reactor output for a given pressure loss across the core is obtained when the capsule temperature in each channel is allowed to reach the maximum regardless of power density.

If one writes

$Q = hA\,(T_{cap} - T_{gas})$ = heat output per channel where the fuel capsule surface area, A, and temperature, T_{cap}, are fixed and assuming for the moment that h is constant it is apparent that as Q changes, the gas temperature must change inversely to maintain the equality. The optimized gas system will, therefore, have a radial variation in outlet temperature related inversely to the radial variation in power density. Actually the heat transfer coefficient is not constant; its variation tends to flatten the outlet temperature profile. This is taken into account in the detailed calculation.

Control of the coolant outlet temperature is accomplished by controlling the mass flow of gas through the channels. Since the pressure drop

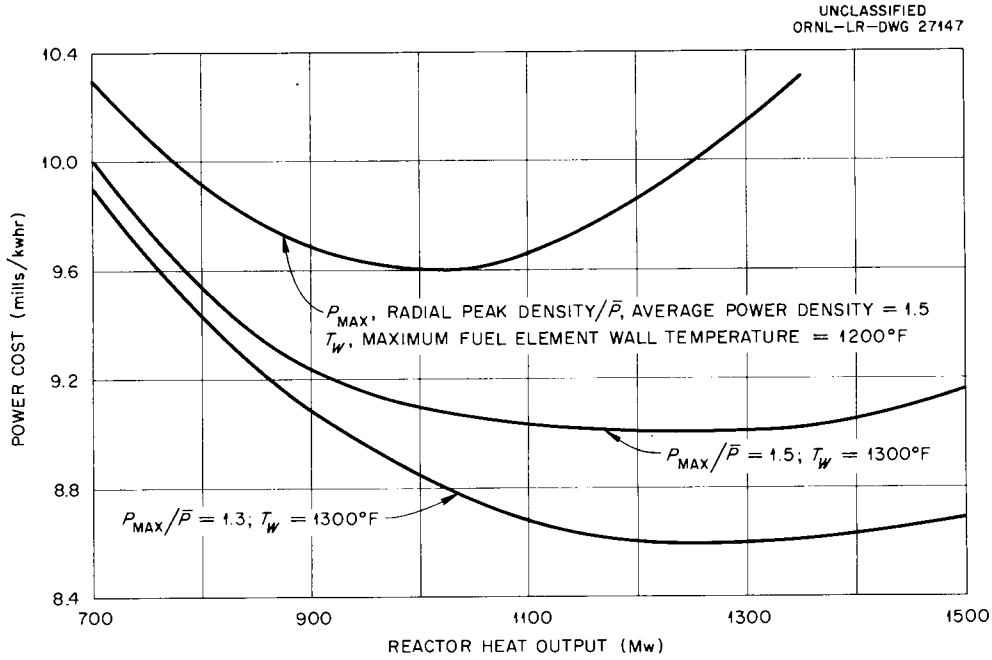

Fig. 6.5. Effects of Power Output on Power Cost as a Function of Gas Flow Rate.

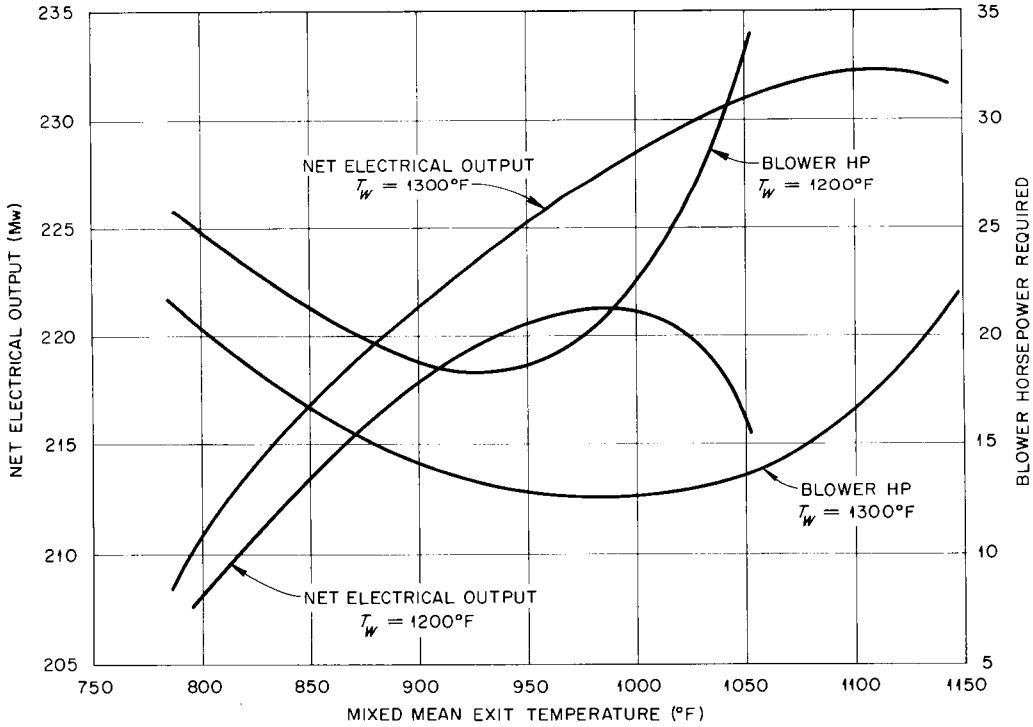

Fig. 6.6. Effects of Mixed Mean Exit Helium Temperature on Net Plant Electrical Output.

across the core is fixed, control is achieved by varying the resistance of the channels either by changing their diameters or by using orifice plugs. From curves given in Figs. 6.7 and 6.8 it is possible to select the proper channel diameter for the various power densities to be encountered. In order to limit the number of channel sizes the reactor is divided into annular regions of the same channel diameter with fine adjustment within the regions being obtained with orifice plugs. The effect of orificing and the number of regions of channel diameter on mixed-mean outlet temperature is shown on Figs. 6.9 and 6.10. The final design utilizes three-channel diameters, 3.45 in. for the central region out to a radius of 7 ft, 3.25 in. from 7 ft to 10.25 ft and 3.05 in.for the remaining annulus. Approximately five orifice plug sizes will be used to obtain a mixed mean outlet temperature of 1007°F at a maximum capsule temperature of 1200°F and a friction pressure loss within the core corresponding to 5700 ft/lb/lb as shown on Fig. 6.11.

It must be pointed out that the capsule temperatures referred to in the foregoing discussion are those calculated by heat and material balances along the channel and based on the assumption of constant heat transfer coefficient and wall temperature for every increment of capsule surface at a given axial position within a specific channel. These quantities are of course allowed to vary from channel to channel. The so called "maximum" capsule temperature is the highest value of the heat balance temperature reached in a given channel. If the channel and fuel element configurations had polar symmetry about all diameters and if the two were centered with respect to each other the temperature so calculated would be the actual capsule temperature. Unfortunately, the channel is made unsymmetrical by the axial slots used for hanging fuel elements. The seven-capsule cluster itself is unsymmetrical, and subject to misalignment. Finally, the fuel element support struts will produce wakes in which it is not possible to predict temperatures by analytical means. These factors work together to produce an unsymmetrical temperature profile in the coolant and a variation of the capsule temperature from point to point around the periphery of the seven capsules of the fuel element. At the writing of this report the combined effect

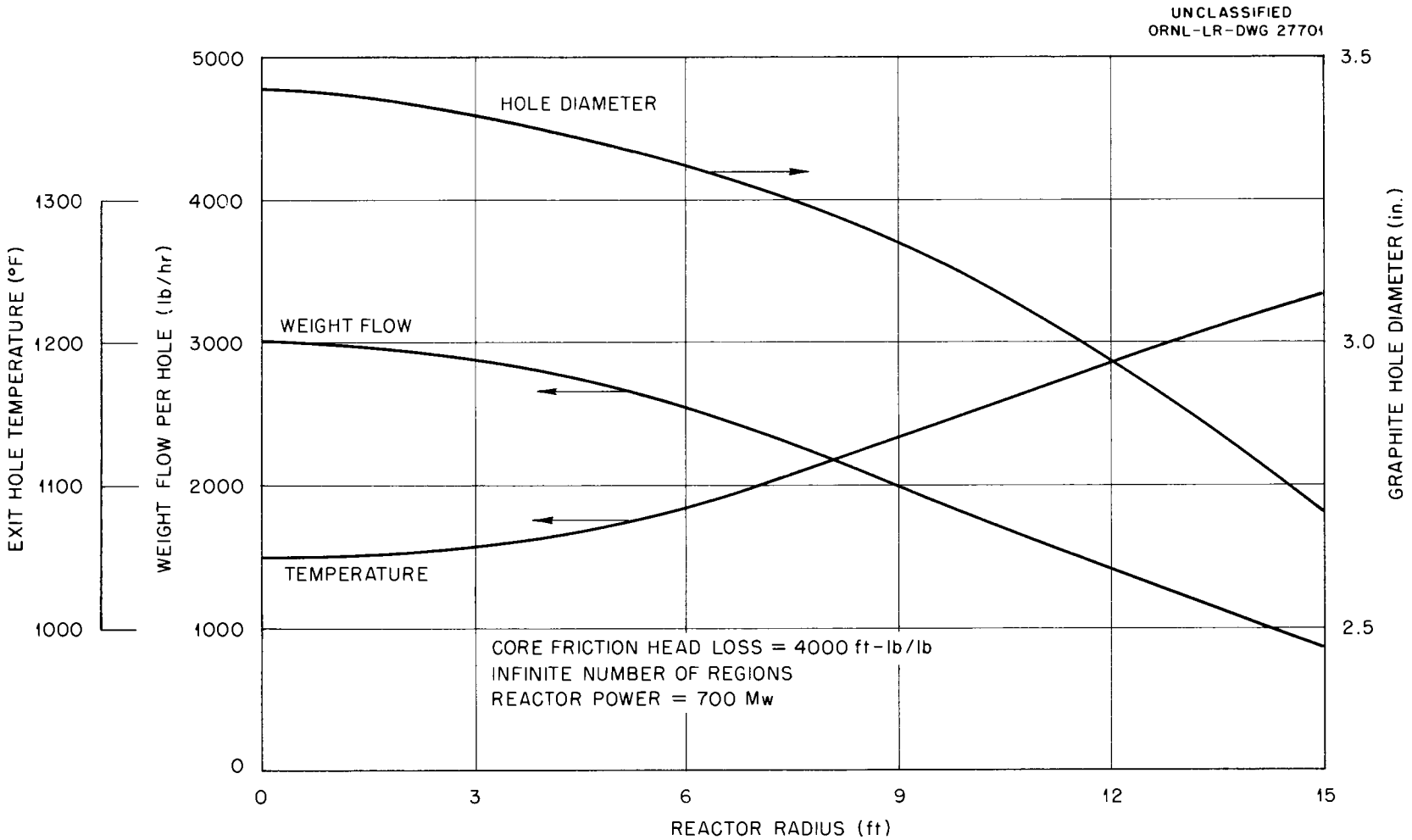

Fig. 6.7. Effects of Radial Power Distribution on Reactor Design.

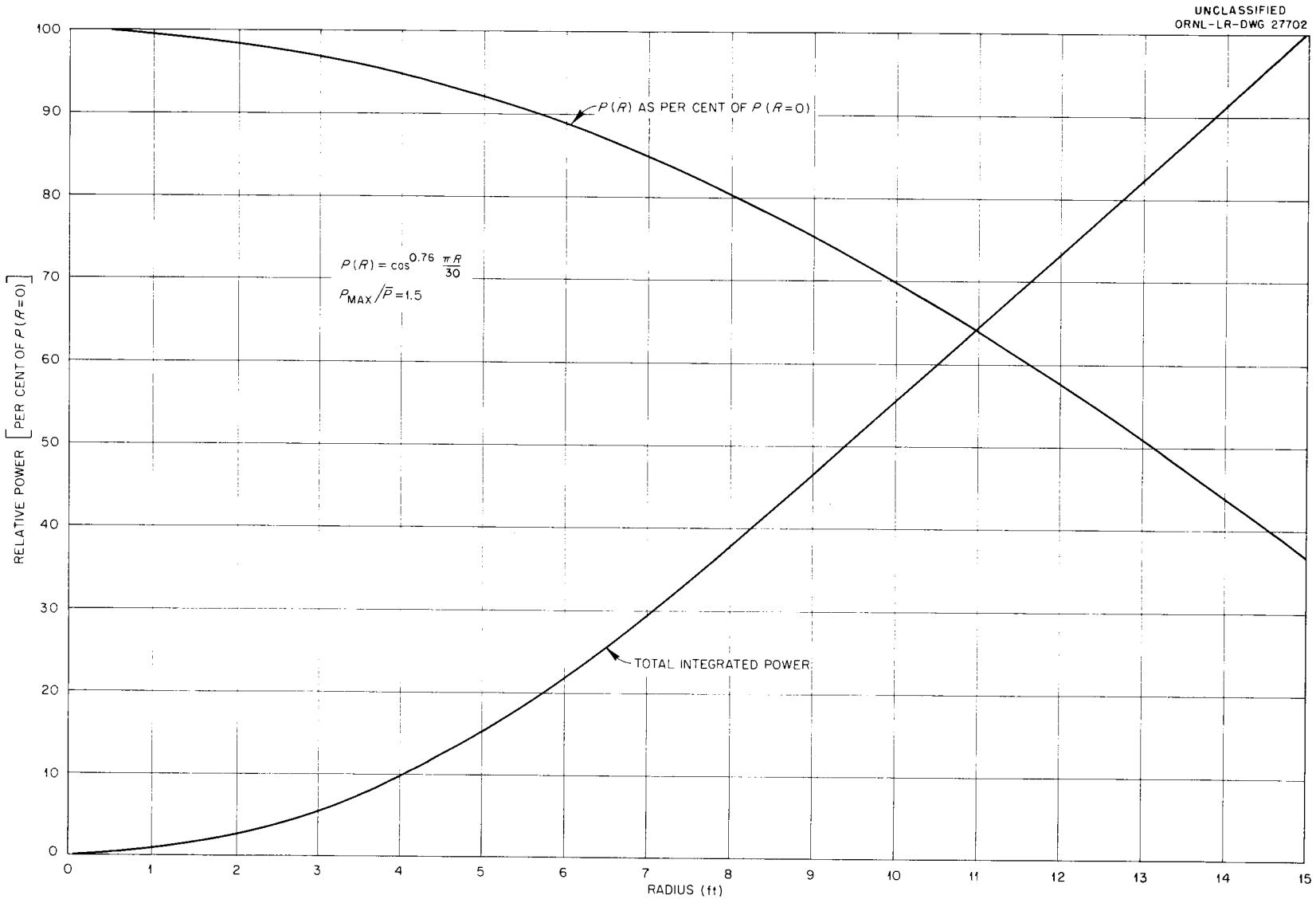

Fig. 6.8. Reactor Radial Power Distribution.

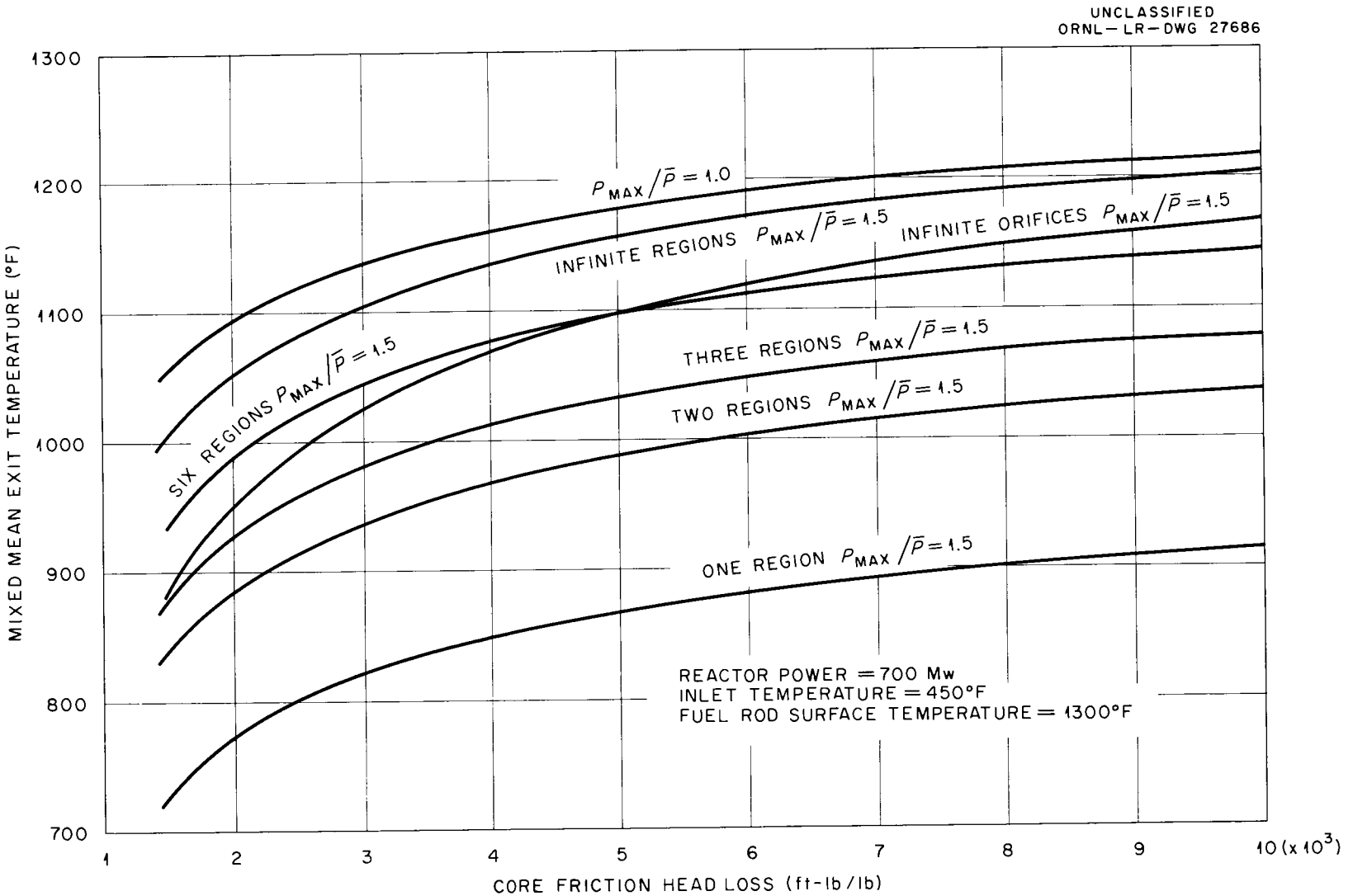

Fig. 6.9. Effect of Flow Orificing on Exit Gas Temperature (T_{max} = 1300°F).

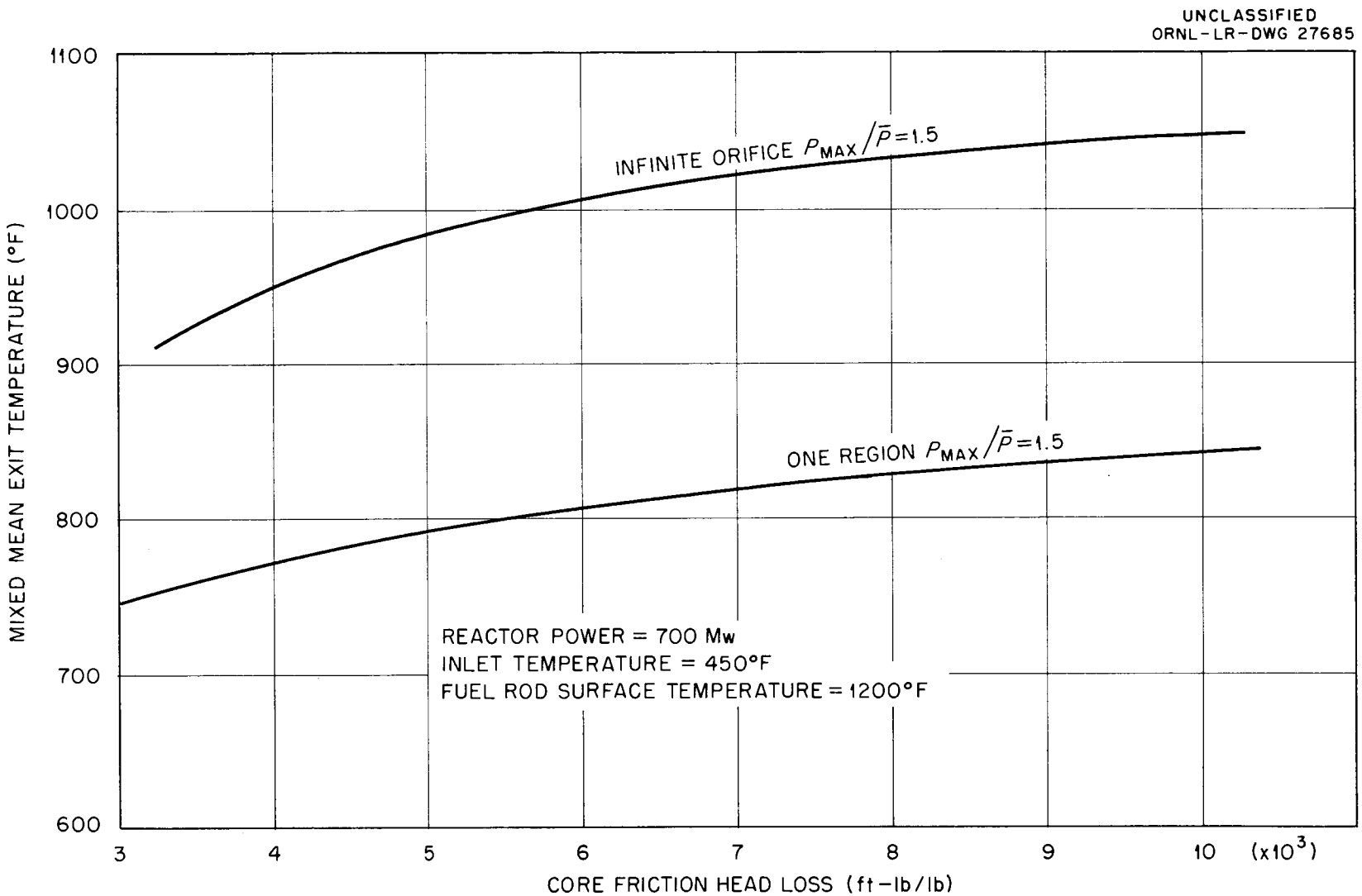

Fig. 6.10. Effect of Flow Orificing on Exit Gas Temperature (T_{max} = 1200°F).

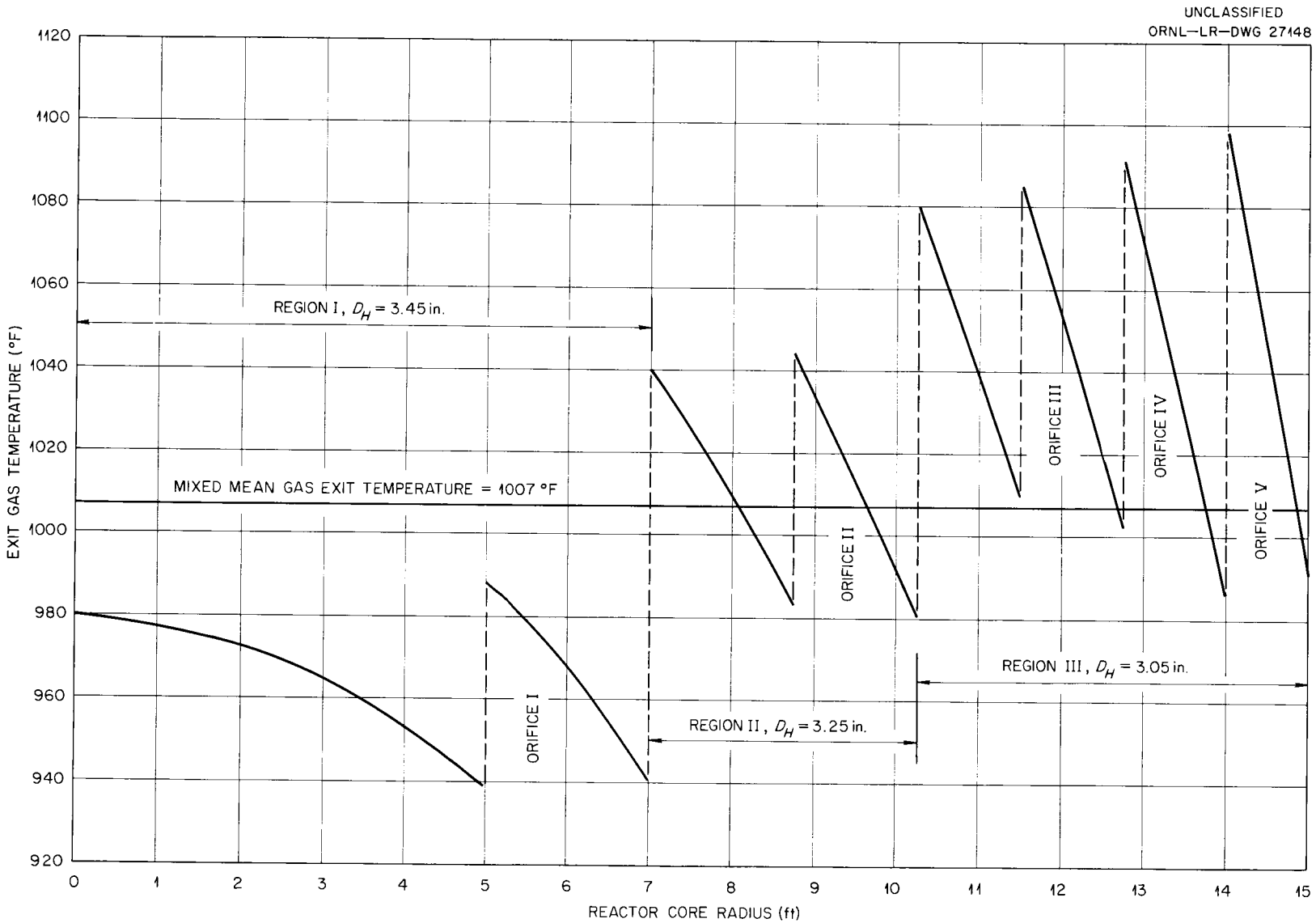

Fig. 6.11. Exit Gas Temperature Profile for Three Fuel Channel Diameters and Five Orifice Sizes.

of the above factors is taken into consideration by an arbitrary allowance of 300°F between the metallurgical limit of 1500°F maximum allowable hot-spot temperature and the "maximum" heat balance temperature. This factor of uncertainty is believed to be adequate. If it can be shown that a smaller allowance for hot spots would be sufficient the power density or outlet temperature could be increased. This would result in decreased capital costs, increased thermal output, or increased thermodynamic cycle efficiency.

It is possible to solve the differential equations for the equilibrium temperature profile in the seven-capsule fuel element by numerical relaxation methods. These calculations are currently being attempted and, if successful, will remove the uncertainty in the temperature allowance for asymmetry of the fuel element and reduce the uncertainty of the allowance for eccentricity between the fuel element and channel. An unknown quantity will remain in the effect of support strut wakes, but this can be minimized and perhaps eliminated by locating the fuel elements so that support struts are several diameters upstream of the point of maximum capsule temperature.

The remark was made in a previous paragraph that the fuel-element configuration was unsymmetrical and subject to misalignment. Further discussion of that statement is in order. It is doubtful that the thin-walled tubes which constitute the capsules will be perfectly straight throughout their 40-in. length. It is to be expected that manufacturing tolerances will allow the center of any individual rod to be as much as 5 mils from its ideal location. The combined effects may cause an error in positioning the mid point of an individual rod in an assembly by as much as 10 mils. In addition, because of the clearances necessary for moving the fuel elements in the channels, a fuel element assembly may be located eccentrically in a channel. Any asymmetry of the fuel element either within itself or with respect to the channel will result in a distortion of coolant flow and, consequently, the temperature profile.

It is not possible at this time to indicate the sensitivity of the temperature profile to fuel element asymmetries until results of the numerical calculations previously mentioned are available. The

approximate effect of an assumed temperature asymmetry can be predicted from the relationship,

$$y_{max} = \alpha \frac{1}{8} \frac{dt}{dr} L^2$$

where

y_{max} = maximum deflection, in.

α = thermal expansion coefficient

= $10 \times 10^{-6} \frac{1}{°F}$ for stainless steel at 1200°F

$\frac{dt}{dr}$ = transverse temperature gradient across a rod, °F/in. (assumed constant)

L = length of rod, in.

For the case of a 0.8-in.-dia rod 40 in. long having an assumed transverse temperature difference of 10°F the maximum deflection will be

$$\frac{10 \times 10^{-6}}{8} \times \frac{10}{0.8} \times 40^2 = 0.025 \text{ in.}$$

The greatest difficulty is expected from temperature conditions which tend to make adjacent rods move toward each other. When it is considered that two adjacent rods under such conditions would tend to bow toward each other and that the nominal clearance is approximately 0.260 in., it is conceivable that a temperature asymmetry of less than 50°F, initially, could cause adjacent rods to touch. It is anticipated that a situation in which a rod tends to deflect toward the channel wall would be less severe since the graphite is a good heat sink. There is the difficulty, however, that a rod might deflect toward the graphite to the extent that it touches and finally jams the fuel element in the channel.

It is expected that some modifications in design will be in order upon completion of further calculations and tests that have been planned to make the fuel element relatively insensitive to these difficulties. Simply shortening the fuel element would do much to improve it in this regard. The shorter length would be less subject to trouble from lack of straightness in the rods, and, since deflection is proportional to length squared,

the deflection due to a given temperature difference would be greatly reduced. Shortening the fuel element would reduce the distance from the last point where the temperature profile became disrupted by the spacers. This would decrease the distance over which an equilibrium temperature profile representing the maximum temperature variation could exist in the coolant. Other possibilities would be to change the fuel element design into something closer to polar symmetry about any axis and the use of turbulator devices to induce increased mixing in the coolant. These problems will be investigated in the heat transfer tests outlined later in this report.

6.3 Blowers

The primary coolant is circulated through the four steam generator circuits by four turbo blowers. The steady state operating point for each blower as determined by cooling requirements for the reactor core and pressure shell and the calculated system resistances is 243 lb helium/sec at a head of 10,000 ft lb/lb. At a mean-system pressure of 300 psia and blower inlet temperature of 450°F the suction volume of each blower will be approximately 122,000 cfm. An aerodynamic design study indicates that the above requirements can be met by a single centrifugal stage or two axial flow stages. The best design speed in either case is 3600 rpm. The required motor horsepower is approximately 6000.

The efficiency of axial and centrifugal blowers is comparable. The centrifugal blower has a slight advantage in ruggedness, but there is no reason to anticipate mechanical difficulties with axial blowers. Little difference is expected in the cost of the aerodynamic components of the two types provided that the stators do not constitute parts of the pressure shell. In either case the blower will be a special design although well within the current technology. On the basis of available cost information[3] for special turbo compressors of approximately the same

---

[3]Size 33 diffusion plant compressor prototype cost $265,000, production units cost $55,000 each. Unit was of light, low temperature construction. Data 5 yr old. Allis-Chalmers GDF compressor price quoted at $500,000 August 1957. Heavy multi-stage machine capable of operation at 200 psig and 450°F. In limited production.

dimensions the cost of either type is estimated as $500,000 for development and $150,000 for each unit for a 3600 rpm design which is mounted directly on the motor shaft.

The design of the coolant circulating blowers and the choice of their drive mechanism is intimately coupled with the over-all power plant control problem. Thermal stress considerations indicate the desirability of maintaining system temperatures essentially constant at all power levels from zero to full load. This requires the mass flow of coolant gas to be proportional to the reactor heat output.

Variation of coolant mass flow can be accomplished by changes in system pressure level, changes in volumetric flow, or by a combination of the two. The former is obtained by moving coolant inventory from the system to the storage vessel or vice versa. Although this is the most efficient way to change load it is a relatively slow process. The rate of load change which can be accommodated in this manner is limited by the capacity of the storage system compressor and is of the order of 10% per hr for this design.

More rapid changes in power level, for instance, a sudden loss of load, must be accommodated by changes in volumetric flow. This can be accomplished by changing blower speed or by using a bypass circuit. There are several mechanisms for obtaining variable speed. These include direct turbine drive, d-c electric motors, variable frequency a-c motors, and fixed speed induction or synchronous motors with fluid or magnetic couplings. The nature of turbo dynamic blowers demands that their speeds be matched when two or more are operated in parallel. Fixed speed electric motor drives of course insure matching of speeds at a single point. If it is necessary to match speeds over a substantial speed range the drive mechanism can be quite complicated. The Calder Hall reactors, for instance, use d-c drive motors with Ward-Leonard control.

The choice of drive mechanism is also influenced by problems which arise in sequence starting of parallel connected turbo blowers. Theoretically, if two or more blowers were started simultaneously and accelerated together to operating speed there would be no difference

from the case of a single blower. Actually, it is doubtful if simultaneous starting and acceleration could be achieved, and there will certainly be times when some blowers will have to be started while others are in operation.

Figure 6.12 shows a typical head vs. capacity characteristic for one blower and the composite characteristics for two and three identical blowers operating in parallel with a system characteristic curve superimposed.

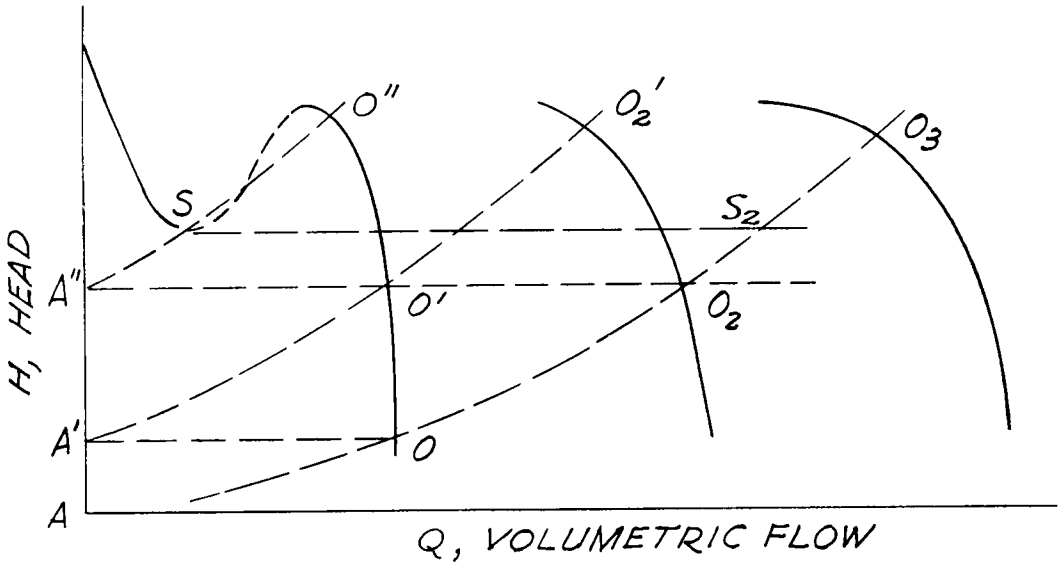

Fig. 6.12. Head as a Function of Capacity.

Suppose a single blower is operating at the point, O, and it is desired to start a second blower. If the system is provided with suitable valving to prevent back flow through circuits which are shut down, the head flow situation of the second blower at the instant the drive motor is energized is represented by the point, A. As the blower accelerates it cannot deliver any flow until its shut-off head reaches the same value as point O which is imposed by the operating blower. The operating point of the starting blower, therefore, moves vertically from A to A' and thence along a system characteristic to O'. The operating point of the running blower will simultaneously move from O to O', and the system will come to equilibrium at O_2.

Now, suppose it is desired to start a third blower. The third machine cannot deliver flow until it has reached a speed such that its shut-off head reaches A" which is imposed by the two blowers operating at O_2. From A" the third blower operating point moves along a system characteristic toward the desired operating point O". The operating point of the two running blowers moves simultaneously along the two blower composite curve from O_2 toward O'_2. However, the operating point of the third blower encounters the secondary stable portion of the characteristic curve at S and is unable to move on to O". The operating point of the three blowers will come to equilibrium at S_2, and the system is unable to reach the desired operating point O_3. The third blower will remain operating in a stalled but stable condition and will be in danger of overheating. It is obvious that the greater the number of blowers being operated in parallel, the greater will be the possibility that in sequence starting one or more of the later blowers cannot reach the desired operating point on the primary stable portion of the curve.

One possible method of avoiding such trouble is the use of blowers having relatively flat characteristic curves in which the head in the secondary stable region does not drop appreciably below the peak point of the primary stable region. Unfortunately this type of characteristic curve is most liable to lead to trouble due to load sharing between blowers.

The easiest solution to the starting problem is the use of a bypass line. By this means a blower can be brought up to an operating point on the primary stable portion of its curve while aerodynamically disconnected from the other machines. When such a point is reached it can be valved into the main system where it will come to equilibrium at the proper operating point provided the other system requirements have been properly considered in the design.

Table 6.4 summarizes some of the equipment arrangements suitable for the blower drive. It can be seen from the table that the squirrel-cage induction motor can be used in combination with either the hydraulic coupling or the bypass circuit and the steam turbine can be

TABLE 6.4. COST COMPARISON – BLOWER AND DRIVE ARRANGEMENTS

Arrangement	Installed Cost Per Loop ($)	20-Year Investment Cost Per Loop at 14% ($)	20-Year Power Cost Per Loop at 10 mills/kwhr and 85% Load ($)	20-Year Total Cost for Four Loops ($)	Advantages	Disadvantages
1. Constant-Speed Drive Contained Within Helium System, Controlled Bypass					Most simple arrangement; all equipment essentially standard and reliable; high efficiency at full volumetric flow; no helium shaft seal required	Poor maintenance access to motor; development necessary for motor lead entry into containment vessel
Blower (overhung from motor shaft)	250,000[a]					
Bypass piping (including valve and actuator)	25,000					
Containment vessel for blower and motor	50,000					
Motor, squirrel cage, 6000 hp, 3600 rpm	202,000[b]					
Total	527,000	1,476,000	7,018,000	36,080,000		
2. Constant-Speed Drive in Air with Shaft Seal, Controlled Bypass					Equipment other than shaft seal essentially standard and reliable; good maintenance access to motor; high efficiency at full volumetric flow	Helium shaft seal required (shaft seal maintenance costs not included in this table)
Blower (mounted on separate shaft)	280,000[a]					
Bypass piping (including valve and actuator)	25,000					
Containment vessel for blower	35,000					
Motor, squirrel cage, 6000 hp, 3600 rpm	152,000[c]					
Coupling, one required	1,000					
Helium shaft seal	32,000[d]		7,018,000			
Helium leakage through shaft seal			30,000[e]			
Total	525,000	1,470,000	7,048,000	36,170,000		
3. Variable-Speed Drive (Hydraulic Coupling) in Air with Shaft Seal					Equipment other than shaft seal essentially standard and reliable; good maintenance access to motor; more efficient at less-than-full volumetric flow than arrangements 1 and 2	Blower speeds may be difficult to synchronize; small increase in blower cost over arrangement 2; helium shaft seal required (shaft seal maintenance costs not included); approximately 3% efficiency loss at full load; difficulty may be encountered in sequence starting
Blower (mounted on separate shaft)	290,000[f]					
Hydraulic coupling (equipment cost $65,000)[g]	72,000					
Speed-control instrumentation	5,000					
Containment vessel for blower	35,000					
Motor, squirrel cage, 6000 hp, 3600 rpm	152,000[c]					
Couplings, two required	2,000					
Helium shaft seal	32,000[d]		7,228,000			
Helium leakage through shaft seal			30,000			
Total	588,000	1,646,000	7,258,000	37,970,000		
4. Variable-Speed Drive (Direct-Coupled Steam Turbine) with Shaft Seal					Equipment other than shaft seal essentially standard and reliable	Blower speeds may be difficult to synchronize; difficulty expected in sequence starting; helium shaft seal required (shaft seal maintenance costs not included)
Blower (same as arrangement 2)	280,000					
Containment vessel for blower	35,000					
Turbine (equipment cost $150,000)	173,000[h]					
Speed-control instrumentation	5,000					
Helium shaft seal	32,000[d]					
Coupling, one required	1,000					
Helium leakage through shaft seal			30,000			
Auxiliary steam plant (one-blower capacity) for startup[i] ($700,000 initial cost plus $1,960,000 20-year capital costs)						
Total	526,000	1,473,000	6,350,000[j]	36,060,000		
5. Variable-Speed Drive (Direct-Coupled D-C Motor with Motor-Generator Set and Ward-Leonard Control) with Shaft Seal	Cost is excessive; 20-year total cost for four loops approximately $7,000,000[c] above that for arrangement 1, 2, 3, or 4					Less reliable than any of the above; requires speed increaser between motor and blower for 3600 rpm
6. Variable-Speed Drive (Squirrel-Cage Motor with Magnetic Coupling) with Shaft Seal						Not available at required horsepower; would be similar in performance to hydraulic coupling
7. Constant-Speed Drive (Synchronous Motor) with Shaft Seal and Controlled Bypass	Cost is excessive; 20-year total cost for four loops approximately $4,000,000[c] above that for arrangement 1, 2, 3, or 4					Requires squirrel-cage starting motor

[a]Based on $500,000 development cost plus $150,000 per blower for five blowers. Blowers mounted on separate shaft cost $30,000 additional.

[b]Equipment costs from Westinghouse Electric Co. verbally; includes modification for enclosed operation and direct mounting of blower and also installation cost.

[c]Equipment costs from Westinghouse Electric Co. verbally; includes installation costs.

[d]Personal communication from W. F. Boudreau. Based on $150,000 development cost plus $2000 per seal for five units.

[e]Corresponds to 0.8-scfh leakage at $0.0227 per scf.

[f]Blower diameter increased to regain tip speed lost by coupling slip.

[g]Equipment cost from American Blower Corp. verbally.

[h]Equipment cost from Westinghouse Electric Co. catalog.

[i]Auxiliary steam plant will operate one blower only. Reactor must provide power for remaining blowers.

[j]90% of electric power costs.

used directly coupled. Other possible arrangements of equipment are eliminated either by the requirement that the drive possess high-speed capability or by high costs. In addition, reliability and maintenance of the equipment, parallel operation of turbo blowers, and helium loss through seals are important considerations in evaluating the above equipment. For reasons discussed previously it is believed that a by-pass circuit is desirable even where variable speed drive is used. The cost figures for variable speed drives given in Table 6.4 do not include costs of a bypass circuit.

In order to achieve minimum equipment costs and reliable operation, fixed-speed induction motors have been selected for use with a bypass circuit to obtain flow control. While bypassing does waste the power input to the bypassed stream large amounts of bypassing need be used only to handle short-term load changes. Extended operation at partial load can be obtained by reducing the coolant pressure level or by shutting down one or more of the four steam generator circuits.

It is desirable to avoid the problems associated with gears by coupling the blower directly to the drive motor. Further simplification can be obtained by mounting the blower rotor directly on the motor shaft thereby eliminating an extra set of bearings. Since the aerodynamic design study indicates a speed of 3600 rpm to be nearly optimum, gears can be eliminated by the use of a two-pole motor. It is, therefore, practical to "can" the complete blower-motor assembly in a cylindrical pressure vessel. Although cooling will have to be provided for the drive motor, canning will eliminate the shaft seal and the problems of pressure loads on the irregularly shaped blower volutes.

Details of the motor and blower installation are shown in Fig. 6.13. The motor which is located in a pressure vessel is isolated from the main helium stream by a heat barrier. Helium in the motor vessel is maintained at a maximum temperature of 40°C (104°F) by use of a water cooler. It is then passed through the motor windings by two parallel auxiliary blowers to keep the motor temperature within allowable limits. The motor would have Class B insulation suitable for a temperature rise of 60°C above a maximum ambient temperature of 40°C. The motor bearings would permit

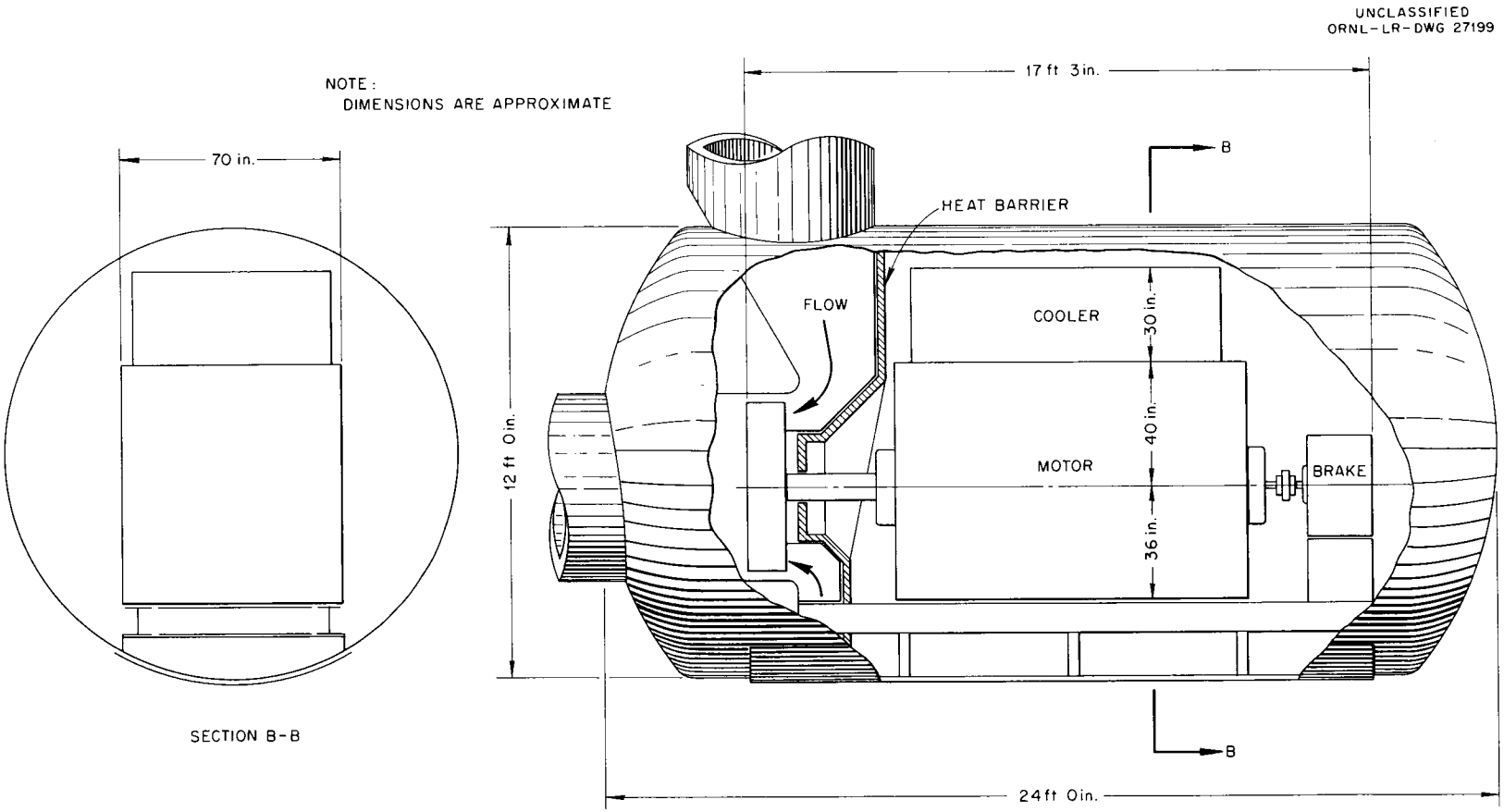

Fig. 6.13. Blower Drive Unit.

having the blower rotor mounted directly on the motor shaft thus allowing all bearings to be located within the cooled region. The bearing lubrication system would be of the pressure type, water cooled, and sealed to reduce helium contamination by oil vapors.

The canned motor arrangement essentially eliminates helium leakage at the blower since no shaft seal is required. The equipment is considered standard, although, 3600 rpm motors of the 6000 hp size have only been manufactured since 1957. The main point of concern is the ability to develop rotor end-rings to withstand the starting kva for high inertia loads. No difficulties are expected in the design of a motor suitable for a load inertia of 4000 lb ft^2 maximum. It appears that the blower inertia will be considerably below this figure. Although no particular difficulties are expected, development work would be required on a device to insulate and seal the high-voltage motor leads through the containment vessel wall.

Since performance reliability is an important factor, a study of failure experience was made which indicates squirrel-cage motors are comparatively reliable. Table 6.5 indicates failure experience for some motors of the large, high-speed, horizontal shaft type.

Data pertaining to the squirrel-cage motor is summarized in Table 6.6.

Another blower drive arrangement which was considered consists of a squirrel-cage motor located in air, with a shaft seal to prevent helium leakage, and a bypass piping arrangement to control the helium flow. However, a suitable shaft seal for 300 psia would have to be developed. It is standard practice to provide shaft seals for lower pressures of hydrogen-cooled generators. In addition, tests have been performed on oil type seals operating at 200 psia helium and the results indicate that a seal can probably be developed which will perform within the limits required. The maximum allowable leak rate based on hazards considerations for the four shaft seals would be approximately 1500 scfd.

The hydraulic coupling equipment is more expensive than the bypass circuit. The efficiency of the drive unit is improved during operation at reduced flow, however, the efficiency would be reduced by approximately

TABLE 6.5

SOME OPERATING EXPERIENCE OF LARGE HORSEPOWER MOTORS

Plant	Hp	Speed	Type* Service	No. of Motors	Accumulated Motor Years Service	Outages	Comments
Colbert, TVA	3000	3580	BFP	12	30	0	
	1500	591	I-D	8	20	0	
Gallatin, TVA	4000	3572	BFP	6	5	0	
	1250	592	I-D	6	5	0	
John Sevier, TVA	3000	3570	BFP	12	20	0	
	1750	593	I-D	8	14	0	
Johnsonville, TVA	1750	3585	BFP	18	100	1	Relays operated to trip motor because of stator winding failure. Failure believed to have been initiated by turn-to-turn fault. Duration of outage - 1 month.
	950	720	I-D	12	67	0	
Kingston (1-4), TVA	2000	3580	BFP	12	43	0	
	1400	590	I-D	8	29	1	Relays operated to trip motor because of stator winding failure. Cause of failure could not be determined. Duration of outage - 1 month.
Kingston (5-9), TVA	3000	3570	BFP	15	38	0	
	1750	593	I-D	10	25	0	
Shawnee, TVA	2000	3579	BFP	30	95	4	Motor removed from service because of intolerable vibration. Trouble resulted from loose rotor bars in slots. Duration of each outage - 3 days.
	1000	586	I-D	20	64	5	Relays operated to trip motor because of stator winding failure. Failure believed to have been initiated by effects of arcing between loose rotor bars and iron. Duration of outage - 3 weeks.

*BFP-Boiler Feed Pump
I-D-Induced Draft Fan
AFC-Axial Flow Compressor

TABLE 6.5 (cont'd.)

Plant	Hp	Speed	Type* Service	No. of Motors	Accumulated Motor Years Service	Accumulated Outages	Comments
Shawnee, TVA	1000	586	I-D	20	64	5	Relays operated to trip motor because of stator winding failure. Cause of failure could not be determined. Duration of two outages - 4 months each; duration of one outage - 1 week. Motor was removed from service because of intolerable vibration. Trouble caused by loose rotor bars in slots. Duration of outage - 10 days.
Widows Creek (1-4) TVA	1750	3560	BFP	12	62	3	Motor removed from service because of intolerable vibration. Trouble caused by loose rotor bars in slots, together with broken bars. Duration of 2 outages - 7 weeks each. Duration of 1 outage - 3 days,
	800	590	I-D	8	42	0	
Widows Creek (5,6) TVA	2000	3578	BFP	6	21	0	
	800	590	I-D	4	14	0	
Oak Ridge Gaseous Diffusion Plant, AEC	2000	1200	AFC	320	1066	22	8 motors - bearing failure (4 due to loss of common lube oil system. 7 motors - winding failure. 3 motors - winding end connection joint failure. 4 motors - winding failure from foreign objects.
Paducah Gaseous Diffusion Plant, AEC	950	1200	AFC	800	2366	39	Outages tabulated are due to winding failures. Other outages were relatively few and were not accumulated by operator. In addition, faulty end rings and bearing oil leakages were experienced, with motor replacements being accomplished during planned shutdowns.
	1750	1200	AFC	480	1800	24	
	2000	1200	AFC	480	1660	15	

TABLE 6.6

SQUIRREL-CAGE MOTOR DATA*

Cost - $175,000 each
Size - 6,000 hp
Speed - 3,580 rpm
Voltage - 4,160 V, 3-phase, 60 cycle
Efficiency - 92 - 93%
Enclosure - Top discharge, open type
Insulation - Class B
Ambient - 40°C Max.
Starting -
    Min. Terminal Voltage - 85% Nameplate
    Max. WR^2, (load) - 4,000 lb. ft.^{2}
    Min. Period Between Starts - 45 - 60 min.
    Acceleration Time - 30 sec.
Ambient Cooler - Water Type
Bearings - Sleeve Type
Lubrication - Pressurized, separate motor driven pumps
Cooling Water - 150 gpm, 78°F Max.
Non-Reverse Device - Brake
Motor Dimensions -
    Length - 207 in. (including shaft extension for blower and brake)
    Total Height - 106 in. (including cooler)
    Width - 70 in.
    Foot Height - 36 in. (Floor to shaft centerline)
    Rotor Diameter - 22-1/2 in.
Weight - 70,000 lbs
Min. Vessel Size:
    Diameter - 12 ft - 0 in.
    Length - 24 ft - 0 in. (from end of blower shaft extension to vessel head at center line)

---

* Westinghouse Electric Corporation to R. D. Stulting, Private Communications, January, 1958.

2% at full power operation due to the slip in the hydraulic coupling. The four blowers must operate in parallel resulting in a more critical problem of design and operation since unstable[4] performance can result from differences of speeds of the blowers.

[4]W. T. Furgerson UCNC Notes on Use of Turbo Blowers, ORNL-CF-57-12-24 (December 4, 1957).

A variable speed drive unit may be obtained by the use of a direct coupled steam turbine. Although the basic turbine is less expensive than the combination of a squirrel-cage motor and a bypass arrangement, the additional cost of an adequate steam supply for starting purposes must be considered, and as in the case of the hydraulic coupling, complications arise from starting and parallel operation of the blowers.

Other components commonly utilized in drive units are synchronous motors, d-c motors with motor-generator supply units and magnetic couplings. Application of these units for the blower drive was also considered. It was found that the starting torque that can be built into a synchronous motor is not sufficient to accelerate the blower. A separate motor rated at approximately 2000 hp would be required with a speed increaser to overcome the starting motor slip in order to accelerate the unit to a speed suitable for application of the exciting current to the field windings. The equipment is expensive and complicated. Cost prohibits the use of a variable speed d-c motor operating from a motor-generator unit (Ward-Leonard Control). Direct-current motors rated 6000 hp are not available for high-speed operation. A suitable arrangement would be a low-speed motor operating through a speed increaser to obtain 3600 rpm. The use of commutators, brushes, and the multiplicity of equipment would undoubtedly result in high maintenance costs. The magnetic-type coupling has general characteristics similar to the hydraulic coupling, but the largest standard unit manufactured is approximately 3000 hp, 1200 rpm. Since the hydraulic coupling is being manufactured at higher horsepower and speed ratings than required there appears to be no advantage in considering the magnetic type.

6.4 Piping

The primary purpose of the gas piping system is to transport the heat transfer medium between the reactor and the steam generators. Secondary but important functions are to provide cooling for the reactor pressure shell and to control the rate of heat removal from the reactor.

6.4.1 System Configuration: The gas piping system consists of four parallel circuits connecting the blowers, reactor vessel, and steam generators. Each circuit contains a by-pass line from the blower to the steam generator, a by-pass control valve, and a valve in the line between the blower and the reactor. The main helium and auxiliary system flow diagram is shown in Fig. 6.14.

It was necessary to establish the system layout early in the design study in order that other design studies could proceed. The study was based on two arbitrary decisions: (1) The piping system would be in one plane to minimize stress problems; (2) two right angle bends in each pipe circuit just inside the shield were provided to prevent streaming of radiation out through the pipes.

A limited comparison of a four-gas-circuit configuration to a two-gas-circuit configuration was made. The results as shown in Table 6.7 indicated that there is a slight economic advantage in the four-circuit configuration. This is due to the higher pumping power associated with the two-circuit configuration.

Immediately inside the reactor pressure shell the inlet coolant stream is split into two parts. The major part flows downward between the periphery of the graphite and the inside of the pressure shell cooling the latter regeneratively and finally entering the bottom of the core cooling channels. It is not practical to provide regenerative cooling of the upper part of the pressure shell in the region of the penetrations for fuel loading and coolant outlet pipes, but it is desired to keep the material temperature below 650°F. Cooling of these parts is accomplished by passing a stream of helium at inlet temperature between the pressure shell and the inner shell. This secondary coolant stream which amounts to approximately three per cent of the total coolant flow removes heat generated in the pressure shell by radiation and provides a temperature buffer between the pressure shell and the reactor discharge temperature. The secondary stream is finally mixed with the main stream through controlled leaks around the fuel loading tubes and the gas outlet pipes.

The pipe size was selected to give the lowest combination of capital and pumping power cost for the gas system. Costs are listed in Table 6.8

TABLE 6.7. HELIUM SYSTEM COST BREAKDOWN

	Length	Added Length to Account for Mitered Elbows	Total Length	Number of Expansion Joints	Length per Expansion Joint	Length of Purchased Piping	Number of Valves	Cost for Pipe ($) 4 Circuits			Cost for Pipe ($) 2 Circuits	
								48 in.	54 in.	60 in.	72 in.	78 in.
Hot Pipe	87	13	100	3	8	75	0	156,800	231,200	268,000	188,000	232,000
Cold Pipe	63	7	70	3	8	45	1	36,000	39,600	54,000	36,000	40,000
Bypass Pipe	25	0	25	1	8	17	1	9,600	9,600	12,000	6,800	6,800
(size as indicated)								36 in.	36 in.	42 in.	48 in.	48 in.
Total								202,400	280,400	334,000	230,800	278,800

	Expansion Joint Cost ($) 4 Circuits			Expansion Joint Cost ($) 2 Circuits		Valve Cost ($) 4 Circuits			Valve Cost ($) 2 Circuits	
	48 in.	54 in.	60 in.	72 in.	78 in.	48 in.	54 in.	60 in.	72 in.	78 in.
Hot Pipe	112,000	128,000	138,000	79,000	85,000	0	0	0	0	0
Cold Pipe	112,000	128,000	138,000	79,000	85,000	80,000	100,000	120,000	90,000	110,000
Bypass Pipe	28,000	28,000	34,500	19,400	19,400	44,000	44,000	60,000	40,000	40,000
(size as indicated)	36 in.	36 in.	42 in.	48 in.	48 in.	36 in.	36 in.	42 in.	48 in.	48 in.
Total	252,000	284,000	310,500	177,400	189,400	124,000	144,000	180,000	130,000	150,000

	Concrete Cost ($) 4 Circuits			Concrete Cost ($) 2 Circuits		Pumping Power Cost ($) 4 Circuits			Pumping Power Cost ($) 2 Circuits	
	48 in.	54 in.	60 in.	72 in.	78 in.	48 in.	54 in.	60 in.	72 in.	78 in.
Hot Pipe						2,844,000	1,700,000	1,076,000	2,092,000	1,412,000
Cold Pipe						654,000	393,000	250,000	455,000	326,000
Total	103,600	115,200	121,000	66,400	69,200	3,498,000	2,093,000	1,326,000	2,547,000	1,738,000

COST COMPARISON – 4 CIRCUITS

	48 in. System		54 in. System		60 in. System	
	Capital Costs	Power Costs	Capital Costs	Power Costs	Capital Costs	Power Costs
Pipe	202,000		280,000		334,000	
Expansion Joint	252,000		284,000		310,000	
Valves	124,000		144,000		180,000	
Concrete	103,000		115,000		121,000	
Total	681,000		823,000		945,000	
	× 2.8		× 2.8		× 2.8	
	1,906,000	3,498,000	2,304,000	2,093,000	2,646,000	1,326,000
Steam Generator* Charge × 2.8	9,456,000		9,456,000		9,456,000	
Total Cost Capital and Power	$14,860,000		$13,853,000		$13,428,000	

COST COMPARISON – 2 CIRCUITS

	72 in. System		78 in. System	
	Capital Costs	Power Costs	Capital Costs	Power Costs
Pipe	231,000		279,000	
Expansion Joint	177,000		189,000	
Valves	130,000		150,000	
Concrete	66,000		69,000	
Total	604,000		687,000	
	× 2.8		× 2.8	
	1,691,000	3,086,000	1,923,000	3,476,000
Steam Generator* Charge × 2.8	8,690,000		8,690,000	
Total Cost Capital and Power	$13,467,000		$14,089,000	

*Based upon 18 ft diameter steam generator for 4 circuit system and 20 ft diameter generator for 2 circuit system.

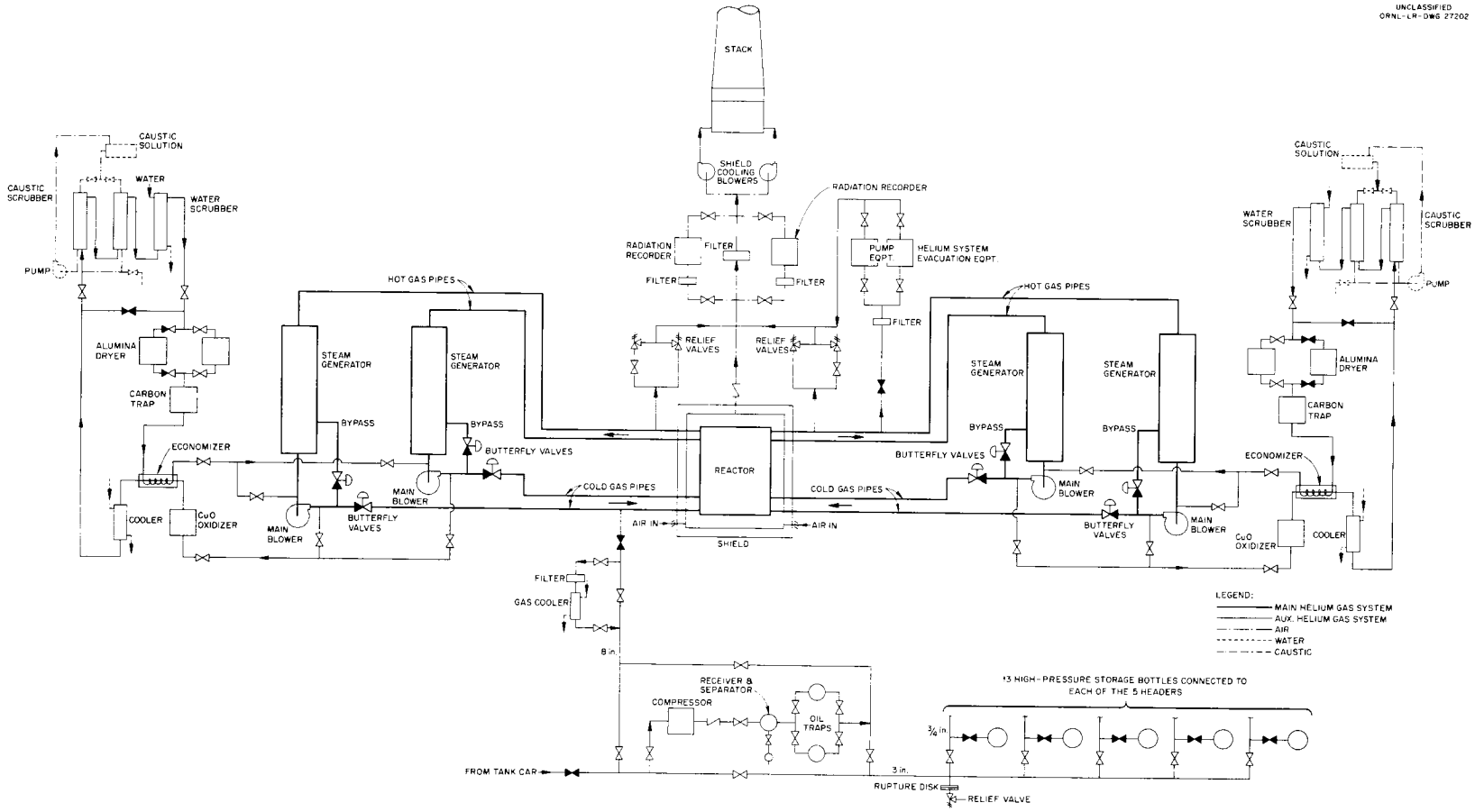

Fig. 6.14. Helium System Flow Diagram.

TABLE 6.8

GAS PIPING SYSTEM COSTS

Pipe Diameter	48 in.	60 in.	72 in.
Hot Piping	$ 39,200	$ 67,000	$ 94,000
Cold Piping	9,000	13,500	18,000
Expansion Joints	56,000	69,000	79,000
Valve	20,000	30,000	45,000
Total Cost Per Circuit	124,200	179,500	236,000
Total Cost	496,800	718,000	944,000
Capital Charges for 20 yr (Total x 20 x 14 per cent)	1,391,000	2,010,000	2,278,000
Pumping Power Cost for 20 yr (10 Mils/Kw-hr)	3,048,000	1,156,000	536,000
Grand Total	4,439,000	3,166,000	3,264,000

for 48; 60- and 72-in. pipes. Costs for the by-pass line and control valve are not included since the by-pass line is the same size for all three pipe sizes.

The pumping power required to make up the energy loss in the piping was calculated for each of the pipe sizes. The cost for this power was taken at 10 mils/kwh for 20 yr.

The total cost is plotted against pipe size in Fig. 6.15. The savings in pumping power is greater than the increase in capital cost up to about 63 in. after which the total cost begins to rise. A circular duct of 60-in. diameter was selected for the system.

Although cost data were incomplete it is felt that further optimization study would only have a small effect on the over-all cost. Table 6.7 indicates the helium system cost variation with the number of gas circuits and gas pipe size. As shown in Fig. 6.14 the helium gas system is comprised of four gas circuits each having a blower and steam generator. The hot and cold gas pipes are 60 in. in diameter. Costs used in this study are shown in Figs. 6.16, 6.17 and 6.18.

Vaned miter bends are used for compactness and to reduce head loss. A vaned miter bend is also provided where the coolant pipe enters the

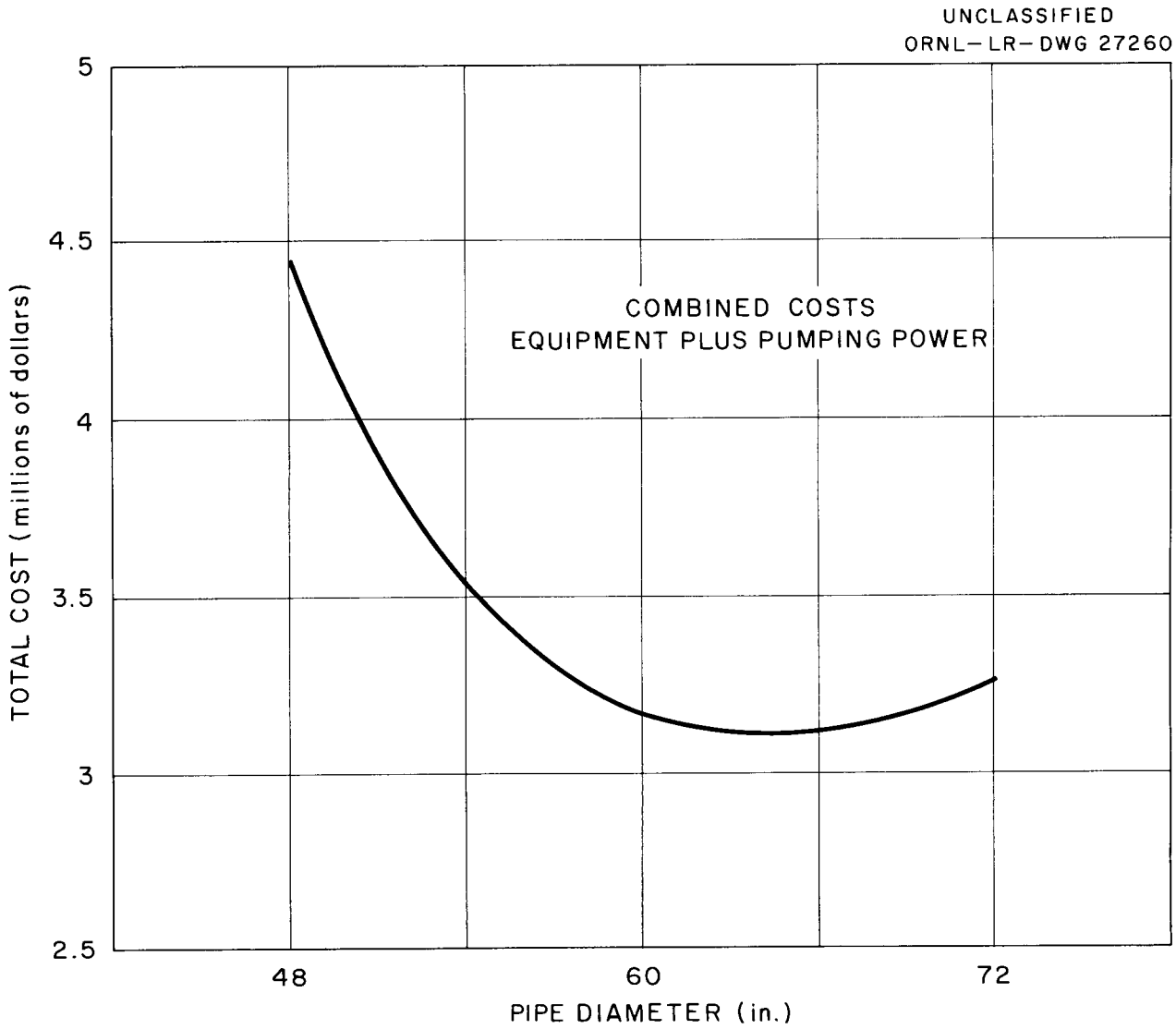

Fig. 6.15. Gas System Piping Costs vs Pipe Size.

UNCLASSIFIED
ORNL—LR—DWG 27190

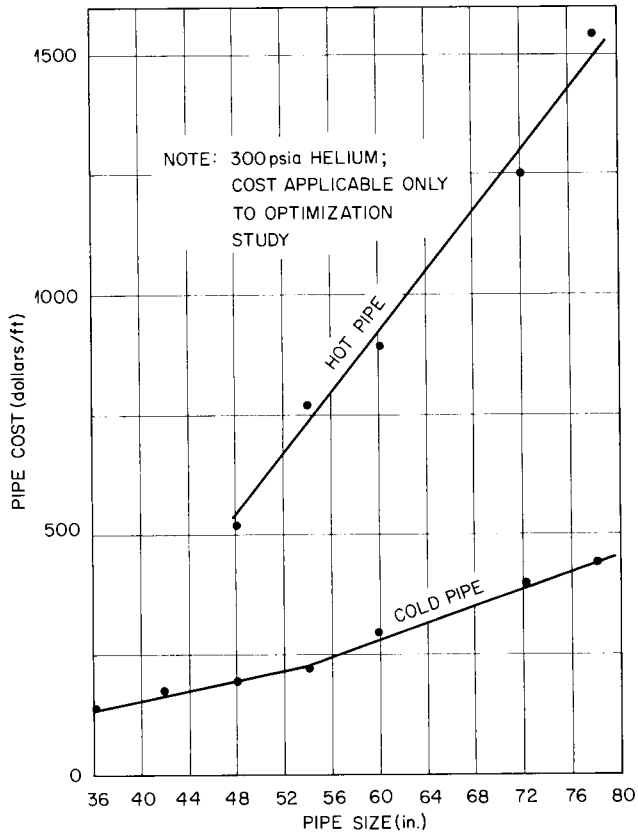

Fig. 6.16. Piping Costs.

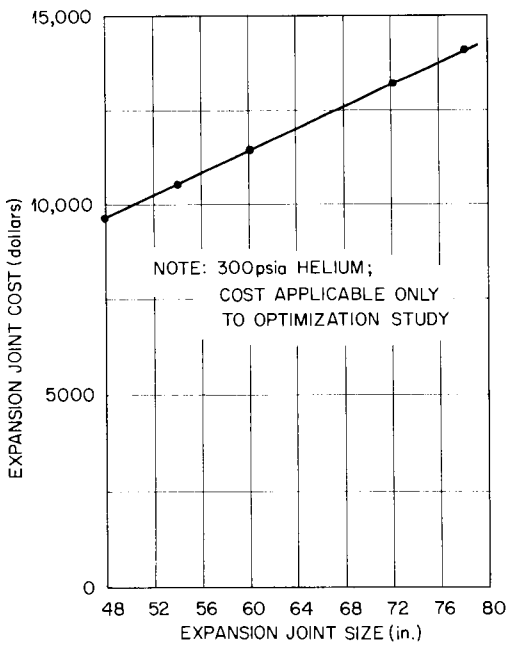

Fig. 6.17. Expansion Joint Costs.

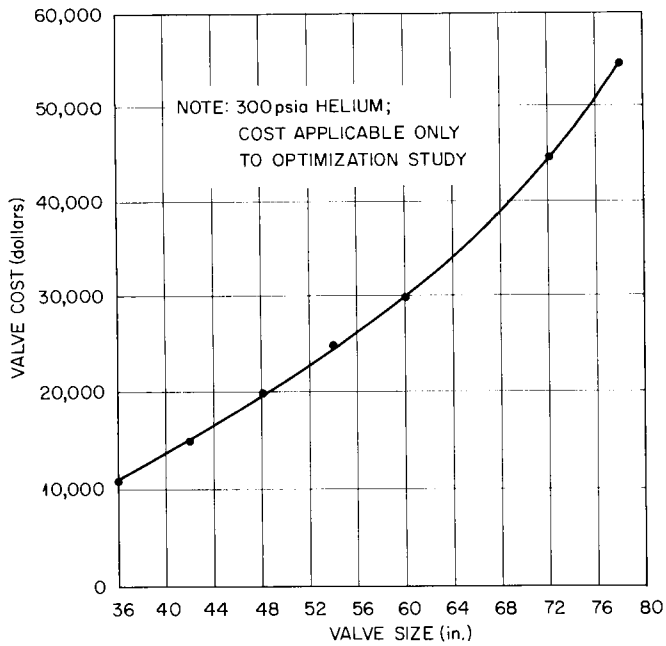

Fig. 6.18. Butterfly Valve Costs.

reactor to minimize entrance losses and to obtain a circumferential flow of coolant around the inside of the pressure shell. This feature is desired both to cool the pressure shell and to provide an even distribution of the coolant.

In order to provide short time flow adjustment and facilitate starting of blowers a 30-in. diameter by-pass pipe is provided which connects the blower discharge to an intermediate point in the steam generator. Butterfly type control valves are provided in the by-pass line and in the main blower discharge line downstream from the by-pass take-off point. These valves are to be actuated simultaneously and in inverse directions so that the blower operating point will remain essentially fixed for all flow arrangements.

The 30-in. pipe diameter was determined to be the size which would give the same system resistance through the by-pass circuit as for the main coolant circuit. The blower will, therefore, operate at the same point for 0 or 100% bypass. Where it will operate between these two valve settings depends on the control valve characteristics which must be determined for detailed design of the cooling system.

6.4.2 Material Selection: A number of iron-base metals were evaluated for use in the piping system. As discussed in detail in Section 3 the low-carbon steels are easy to fabricate while the high-alloy materials have the greatest high-temperature strength. In between these two extremes are the low-alloy steels.

There are two sets of temperature conditions involved: (1) Between the reactor exit and the steam generator the temperature is 1000°F, and (2) between the exit and the reactor inlet the gas temperature is 460°F. In the latter case the material choice is an easy one. The low-carbon SA-212B steel has adequate strength and has, therefore, been selected.

The 1000°F piping is more difficult to evaluate. Type 347 stainless steel and SA-387B low-alloy (1 Cr 1/2 Mo) steel are both possible candidates. When cost studies were carried out the costs of the two were about the same on a lineal foot basis and in the first analysis, the type 347 stainless steel looked best because its wall thickness would be only 3/4 in. as opposed to 1-3/8 in. for the type SA-387B material. It was pointed

out by the vessel fabricators, however, that the joining of high-nickel alloys such as type 347 stainless to carbon steel was sometimes accompanied by brittle conditions and occasional cracking in the weld regions, whereas similar joints using types SA-387B low-alloy steel are almost trouble free. Types SA-387B which can readily be welded to the SA-212B steel of the reactor pressure vessel as well as the SA-387B steel of the steam generator shell was selected.

6.4.3 Fabrication Methods: The large pipe sizes required for the GCR-2 result in fabrication problems more nearly akin to pressure vessel fabrication than to ordinary piping systems. It has been decided that piping fabrication requirements should adhere as closely as possible to the ASME Unfired Pressure Vessel Code where it is applicable.

Piping subassemblies are small enough so that fabrication could be done in off-site fabrication shops and shipped to the site for installation. These pieces could be stress relieved, pretested and cleaned before shipment. Such pieces as elbows which would be fabricated by welding together mitered sections of pipe could thus be made up where there was access to suitable fixtures and forming tools. Turning vanes in pipe bends could also be shop installed.

This would not eliminate the need for on-site shops, but it would greatly reduce the quantity of work to be performed there. On-site facilities would be needed for welding subassemblies, grit blasting and chemical cleaning of pipe to eliminate objectionable contaminants.

All major subassemblies as well as the final assembly would have to be leak tested. Pipe stress relieving would be done on-site by electrical-resistance heater methods.

In establishing fabrication methods and costs, a number of fabricators[5] were consulted. Cost data for pipe fabricated from types SA-387B and SA-212B steel are shown in Section 11 as a function of pressure and size for the 1000°F and 450°F conditions respectively.

---

[5]Midwest Piping Company, Alco Products Division, American Locomotive Company, Grinnell Company.

6.4.4 Valves: The selection of valves for GCR-2 is dependent on the design philosophy of the gas system. Information obtained from U. S. manufacturers as well as the comments of British engineers experienced in the design of gas-cooled reactors indicates that design of a tight shutoff valve is a very difficult engineering problem for the large sizes required. Gate valves cannot be fabricated to maintain sufficient tightness to contain the coolant gas at operating pressure levels. The gate valves in the Calder Hall plant are inadequate in this respect. In addition valves in the hot gas system require heavy structures to avoid metal creep problems. M. L. Bayard and Company has suggested that the problem might be solved with rotary valves but only at very high cost.

In reviewing the problem it was concluded that the valves had two useful functions:

1. Control gas flow through the steam generator.
2. Isolate the steam generator for repairs in case of a leak.

Since it seemed to be impractical to maintain a valve tightness which would permit servicing a steam generator while the gas system was under pressure this latter function seemed impractical for GCR-2. In the event of a steam leak no valve could be actuated fast enough to prevent steam flow into the gas system. Protection against such leakage could best be obtained by cutting off the water supply to the generator, thus, the use of valves as isolation devices is not sound practice.

Gas flow can be controlled as well by butterfly valves as by any other type. Butterfly valves in the size required can be designed for gas flow control without necessitating heavy body structures. A number of manufacturers[6] have been contacted, of which two furnished cost information. The Henry W. Pratt Co. states that a butterfly valve can be designed which will limit flow to a few hundred cubic feet per hour when closed. This is more than adequate for the service requirements.

---

[6] Crane Co., M. L. Bayard and Co., Newport News Ship Building and Drydock Corp., Henry W. Pratt Co., Black, Sivalls and Bryson, Inc. The last two furnished cost estimates.

Stem leakage is, of course, a problem to be considered. Stem packing such as is used in the Calder Hall gate valves is of questionable merit as a seal for 300 psi helium service. Such a seal would require, at the very least, considerable development work. A straightforward solution to the problem is a bellows-sealed stem which actuates the butterfly through a linkage arrangement. Such a valve has been built in sizes up to 24 in. for gaseous diffusion plants and appears practical for this application in larger sizes.

The valves are designed for location in the 460°F piping and can, therefore, be fabricated from low-alloy steel which will reduce construction problems.

A number of drive devices for the valve have been considered. The design recommended utilized pneumatic motors but electric and hydraulic drive units could also be applicable and would have little influence on the over-all valve cost.

With the limited amount of design time available it was impossible to obtain cost estimates from a detailed design. Valve costs as a function of size are indicated in Fig. 6.18. These costs were calculated using somewhat pessimistic assumptions. An actual estimate of the valve costs by one valve supplier are somewhat lower than anticipated. Since this would be a shop fabricated device the comments regarding site conditions do not apply in the same manner as for the piping.

6.4.5 Expansion Joints: The expansion joints appear to be the weakest link in the piping system. Zallea Brothers, a large supplier of such joints, was consulted on their recommendations and hinge type joints, Fig. 6.19, were specified for maximum reliability.

In a piping system using such joints the bellows act solely as flexible sealing members at the pivot points. Every means is used to prevent the bellows from assuming system loads. The back-up rings prevent bellows collapse under pressure, distribute the flexural deformation equally between corrugations and serve as limit stops on total hinge rotation. The heavy structural items, tension bars and reinforcing rings welded to the pipe, transmit axial pressure forces across the bellows and maintain mechanical continuity of the piping.

UNCLASSIFIED
ORNL-LR-DWG 27282

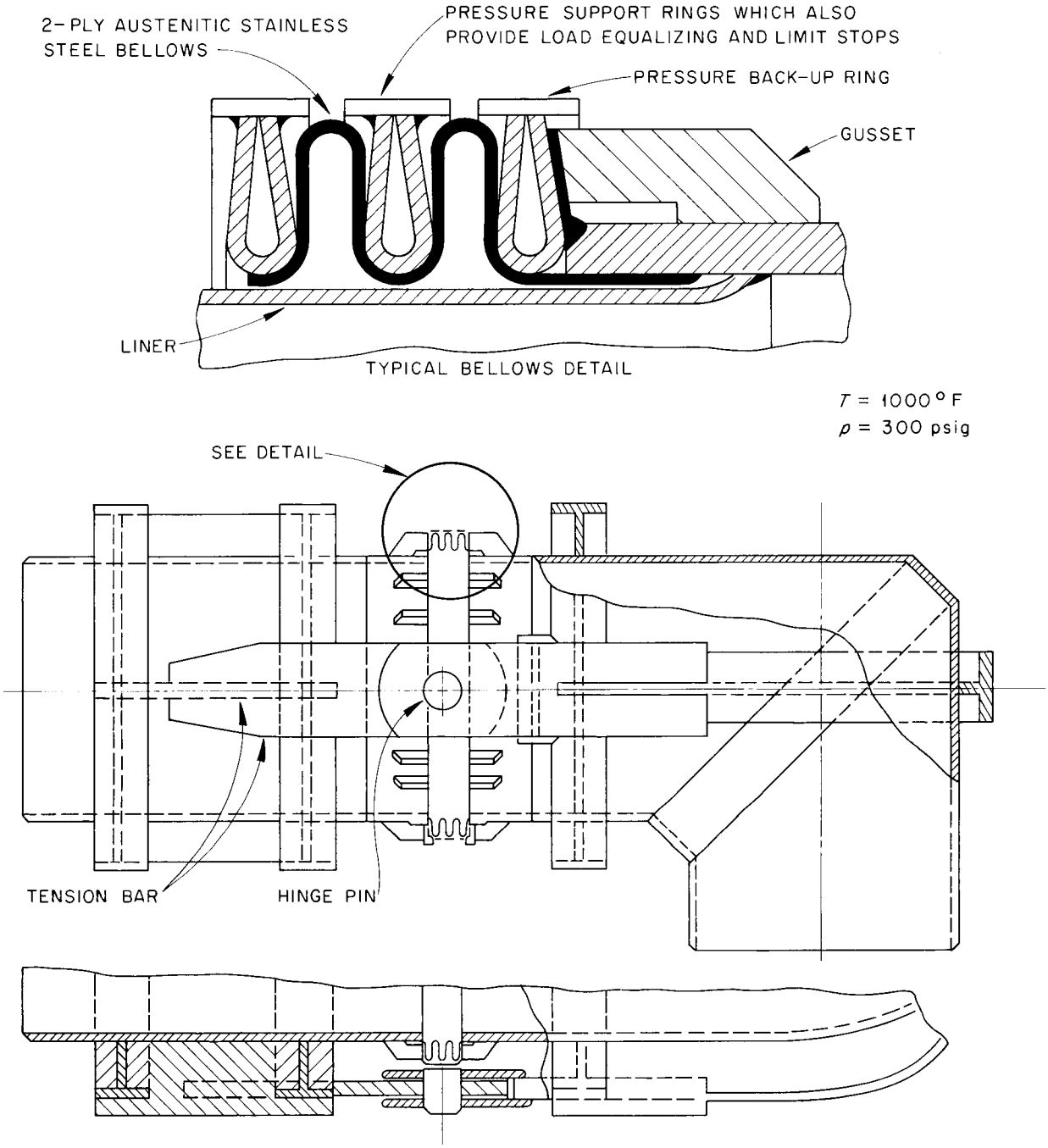

Fig. 6.19. Typical Expansion Joint.

The two-ply bellows which are the critical elements are fabricated from austenitic stainless steel with a minimum of welding.

Complete and careful inspection of expansion joints is required. It is recommended that any purchasing specification include an extra hot-side joint to be tested under conditions of pressure, temperature, bellows deformation and a number of cycles calculated to simulate service.

6.4.6 Leak Tightness: The problem of limiting helium losses is important from the viewpoint of operating cost, possible hazard and capital investment for storage capacity. The cost of helium delivered at Oak Ridge is quoted at 2.27¢/SCF[7]. The total free volume of this reactor gas system is 105,000 ft^3. At an operating pressure of 300 psia and an average temperature of 725°F the helium inventory for this design is

System Volume x Temp. Correction x Pressure Correction =
Helium Inventory Volume at S.T.P.

$$105{,}000 \times \frac{520°R}{1185°R} \times \frac{300.0}{14.7} = 940{,}000 \text{ SCF}$$

This volume would cost $21,300.

A pessimistic view of the tightness problem would be to assume that the losses might amount to 1% of this volume per day which would permit a total leakage loss 3.65 times the helium inventory each year at a cost of $78,000 per year. On this basis the helium cost per kwh would be

$$\left[\begin{array}{l} \dfrac{\text{Helium Cost in Mills}}{\text{Output Capacity in kw x Plant Factor x hr/yr}} = \text{Helium Cost/kwh} \\[2ex] \dfrac{78{,}000 \times 1{,}000}{210{,}000 \times 0.80 \times 365 \times 24} = 0.05 \text{ mills/kwh} \end{array}\right]$$

[7] U. S. Air Force and Bureau of Mines, Private Communication.

As a practical matter to achieve even a 1%/day leakage rate it is necessary that fabrication methods be adapted to rigid tightness requirements. All joints would be welded, all flanged connections would be sealed by metallic "O" ring gaskets or by soft solder. Valves could have bellows-sealed stems. To avoid losses at the blower shaft the entire installation of blower and motor would be placed inside the 300 psia gas system. Finally the whole system would be leak tested using high-vacuum methods.

For those who are unfamiliar with high-vacuum fabrication and testing techniques the question of obtaining a tight system frequently raises serious doubts. The success of the AEC gaseous diffusion plants at Oak Ridge, Paducah and Portsmouth is an example of the type performance which can be expected. In these plants miles of pipe, thousands of tanks and heat exchangers, and tens of thousands of valves were installed in systems and tested to leak rates of 2 μ/hr which in a volume equivalent to the GCR-2 represents a leak rate of only 0.03% per day. To cite some equipment of unclassified nature in these installations equivalent to the GCR-2 which were tested the following are noted:

At Paducah, Ky. - 2 - 30-ft dia spheres

At Oak Ridge, Tenn. - Tank systems containing 1,500,000 ft^3 and 2,800,000 ft^2 of surface area

At Oak Ridge National Laboratory - 24-ft dia x 36 ft high x 2 in. thick pressure vessel

In many cases these systems included gasketed joints and boundary valves.

There is no dispute with the fact that such tightness is not obtained without additional cost, but this cost is not a major factor in capital costs. Opinions on this matter were obtained from two major fabricators experienced in fabrication of high-vacuum equipment.[8] Both companies stated that the quality of fabrication work necessary was no greater than that required by the ASME Unfired Pressure Vessel Code and that the testing requirements imposed only a minor increase in cost. Alco Products

---

[8] Alco Products Division of American Locomotive Company, Dunkirk, New York and A. O. Smith Company, Milwaukee, Wisconsin.

stated that testing requirements would not increase costs by more than 5%. A. O. Smith stated that the costs would not be greater than that for x-ray examination of welds. A supplemental investigation[9] of the cost of test installations shows that $50,000 would pay for any single test setup either in the field or at the fabricator's shop. In cost studies carried out for this report, allowances were made for test labor and setup costs.

The Chicago Bridge and Iron Company was consulted about field fabrication. It has fabricated two large vessels to mass spectrometer test specifications in the field. No difficulty was experienced in either instance and Chicago Bridge and Iron stated that no fabrication cost extras had resulted from this requirement.

The time spent for testing is an important consideration. To avoid an undue time loss in erection it is desirable that pipe subassemblies, steam generator tube bundles, valves, and expansion joints be pretested before installation so that likely leak sources will be limited to field welds. Consultation with gaseous diffusion plant personnel at Oak Ridge indicates that a system of this design and complexity would require an elapsed time of two weeks for the final field test. A pessimistic estimate thus would be an extra two months for leak testing and repair which would still represent only a minor cost penalty.

There are side effects from the testing that are extremely beneficial to the reactor. Vacuum testing assures that the reactor system will be clean of oil, water and other volatile contaminants. It guarantees that there will be no inherent steam leaks into the gas system from the steam generator. Both of these considerations are important in any gas-cooled reactor system and the vacuum test requirement establishes a form of insurance that would be desirable under any circumstances. The importance of these considerations is discussed in the sections on hazards and steam system design. Finally, it should be remembered that leak tightness is not a problem peculiar to helium cooled reactors. The Calder Hall type

---

[9] Cost data obtained from AEC Gaseous Diffusion Plant Installation at Oak Ridge.

reactors required a vacuum-leak test for the steam generators.

With regard to design there are some important considerations to be remembered when dealing with a vacuum-tight system. These are:

1. Avoid gasketed joints where possible and use seal welds wherever practicable as back up.
2. Use good quality plate. Inspect for and avoid laminations.
3. Where possible use butt welded joints and full penetration welds.
4. Pretest as much of the system as possible in subassembly form.
5. Install adequate vacuum pumping capacity for testing purposes.
6. Insure that all equipment is clean and dry when installed.
7. Avoid crevices, trapped volumes, and porous materials.

One final note on the test problem is worth mentioning. Though most of the system can be pretested before the graphite is installed, the graphite will make conventional testing of the final closure welds difficult because gas trapped in its void volume necessitates long pump-down periods. Exterior test connections have been devised for comparable systems to leak test the closure welds and could be used here or as an alternative a halide leak detector can be used. This latter instrument has adequate sensitivity for the location of a significant leak.

Retesting after the helium has been added to the system may also be done by the halide leak detector method or with a mass spectrometer using a helium "sniffer" on the outside of the system.

6.4.7 Stress Analysis: A preliminary stress analysis was undertaken to determine whether it was practical to consider a fixed- or pin-ended piping system for the main helium pipes. The piping diagram shown in Fig. 6.20 was used for this purpose. The study revealed that the forces and moments at the vessels and the maximum bending stresses within the pipe were excessive for a single 60-in. line. This situation could be markedly improved, however, by utilizing a bundle of smaller pipes in place of a single large pipe. Although the loads at the vessels could be reduced in this way, it was decided that this approach would not yield a practical solution in view of the increased number of pressure vessel penetrations required for these configurations.

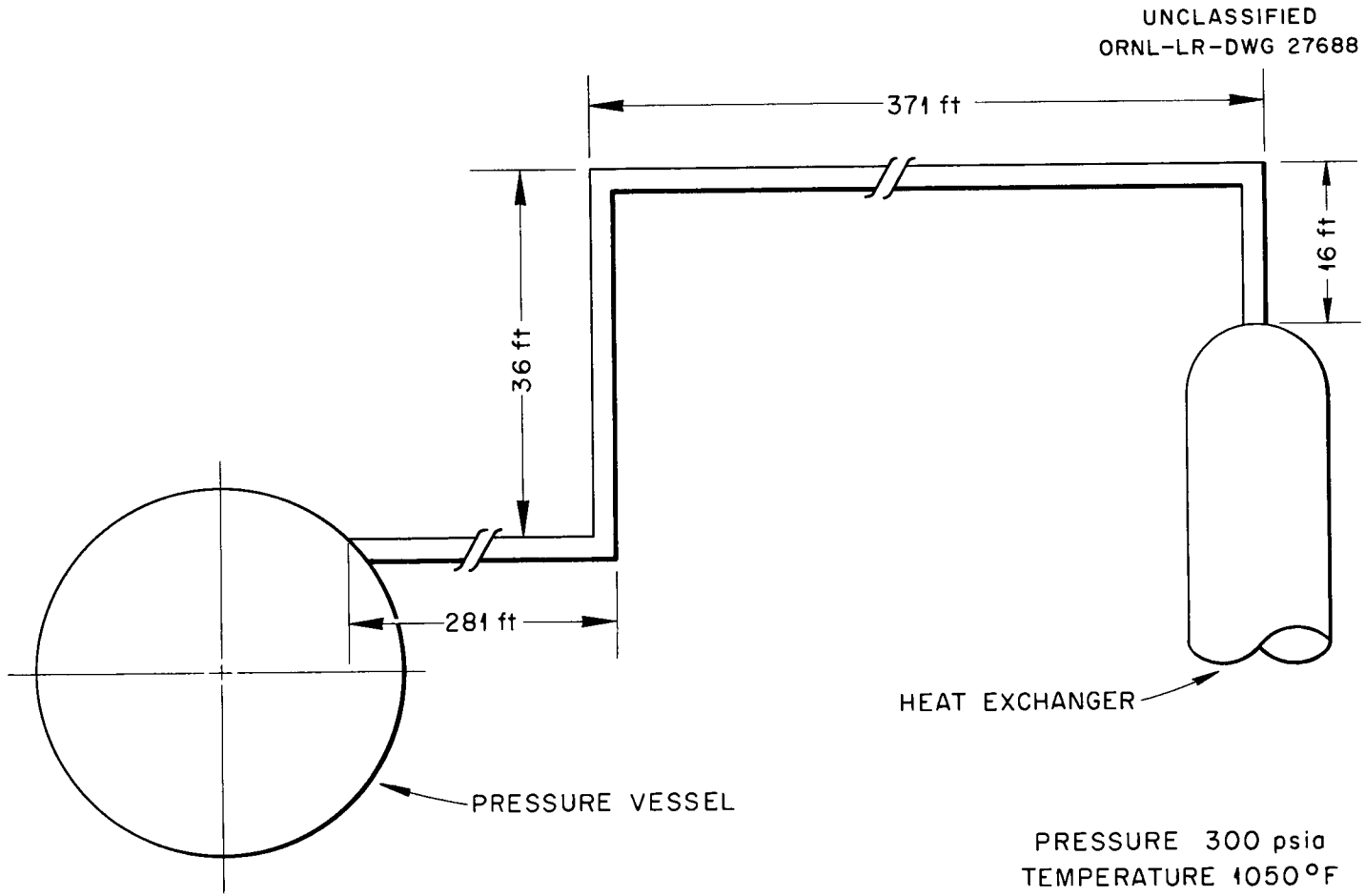

Fig. 6.20. Helium Piping Diagram.

On this basis the decision was made to use single 60-in. pipes with expansion joints to accommodate the relative thermal growth in the structure.

6.5 Storage System

A study of the helium storage system indicated that it is desirable to provide for 1,000,000 SCF of He in 2000 psig storage bottles with compressors for transfering the gas to and from the reactor system. The equipment is sized to permit venting and recharging the system in 4 hr. The capital cost of the storage system is estimated to be $500,000.

A schematic of the system is found on the gas flow diagram, Fig. 6.14. The system contains the following:

65 Bottles (Military Specification M.1-C-7127 air)
1 500 hp compressor
100 ft. 8 in. Sch.-40 pipe
300 ft. 3 in. Sch.-80 pipe
1 Activated Alumina oil and water trap
1 Filter
1 Gas Cooler
1 Gas receiver and oil separator

6.6 Helium Purification System

The proposed chemical purification scheme as described in detail in the materials section of this report includes (1) an oxidizer for conversion of H_2 (T_2) and CO to H_2O and CO_2, (2) a cooler and economizer to bring the gas temperature to 80°F and to reheat the treated gas before re-entry into the system, (3) a caustic scrubber for removal of the CO_2, (4) an activated alumina drier for removal of H_2O introduced by the scrubber.and (5) an activated carbon trap for removal of heavy hydrocarbon vapors. A simple schematic diagram of the system is shown in Fig. 6.21.

The use of cyclone separators and/or particulate filters to remove carbon dust and iron oxide particles from the circulating gas stream was considered. Allowing for differences in temperature, CO_2 concentration and cycle times the GCR-2 system is expected to transfer about $\frac{1}{30}$ the amount of graphite of the Calder Hall system assuming the $CO_2 + C \rightleftarrows CO$ reaction goes to equilibrium in each case. Since the operation of the

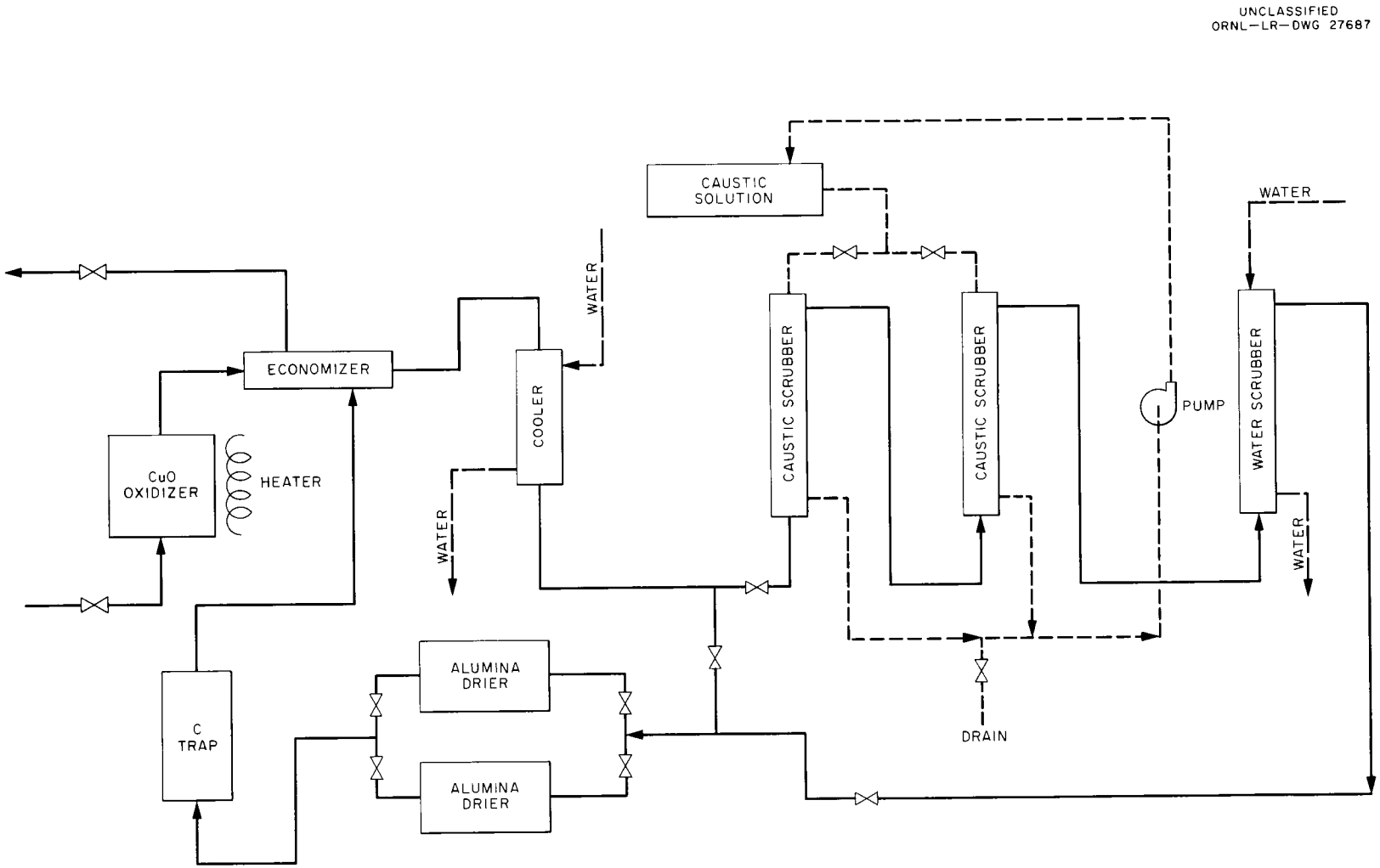

Fig. 6.21. Helium Purification System.

Calder Hall Plant has demonstrated that separators and filters are not necessary, they are not provided in the design of GCR-2. The helium purification system of GCR-2 cannot handle appreciable quantities of such material.

The oxidizer is a tower packed with pellets of copper oxide with provision for maintaining the temperature of the bed and gas at 900-1000°F. Oxidation of H_2 and CO by CuO should be rapid under these conditions; it seems expedient, however, to allow ~ one minute residence time for the gas in the bed. Accordingly, a tower volume of 80 ft^3 containing about 10,000 lb of CuO is suggested. Such an oxidant bed would ultimately need regeneration, which should be possible by treatment with air or O_2 at high temperature. Such regeneration would presumably not be necessary more than once per year.

For effective drying of the gas stream and for absorption of CO_2 it is essential to cool the gas stream of the purification system. In addition it is desirable, if not essential, to minimize thermal stresses in the reactor system by heating the purified gas to 450°F for re-entry to the main stream. Accordingly, the 1000°F gas from the oxidizer should be cooled to 550°F in an economizer by heating the purified gas stream to 450°F. The entering gas should then be cooled to 60°F in a water-cooled heat exchanger.

The CO_2 is removed by absorption in an aqueous 2.5 N NaOH solution. For this purpose two towers, 1 ft diameter and 10 ft high packed with 1 in. beryl saddles, should suffice to remove CO_2 to less than 10 ppm. The capacity of the towers is 2000 ft^3 (200 lb) of He/hr; 250 gal/hr caustic is sprayed into the top of each tower. Since the system operates under 300 psia, canned-rotor pumps are recommended for the caustic. The removal efficiency of the system should remain high so long as less than 15% of the NaOH is converted to carbonate and bicarbonate. Accordingly, if the storage capacity for each system were 500 gal, some 60 lb of CO_2 could be removed in the first tower before replenishment was needed. However, since (especially at startup) the caustic will be diluted with water from the system it will probably be more convenient to provide a continuous bleed of radioactive solution from the system and addition of

fresh solution.

The caustic towers will in addition remove T_2O from the system and should be at least moderately effective in scrubbing some of the fission products and corrosion products from the stream. The system will as a consequence need to be shielded and remotely controlled.

It is likely that a third tower using water will be necessary to remove entrained caustic as a protection to the drying system.

The gas leaving the caustic towers will be saturated with water vapor at 80°F; this places a load on the dryer of less than one pound H_2O per hour.

The drying system should be capable of producing He under 300 psia having a dew point of -21°F (-45°F at 1 atmosphere) at a minimum rate of 200 lb/hr. A system with two parallel towers, 5 ft in diameter by 6 ft high, each containing some 8000 pounds of alumina should be adequate. Breakthrough of water in such a system should occur after absorption of some 400 lb of H_2O. Accordingly, regeneration of the system would be required every two to three weeks during normal operation but during start-up it may be necessary to regenerate once or twice during the first week.

Gases will be adsorbed in an activated charcoal bed. Since a vapor residence time of one minute is adequate, a tower volume of some 80 ft^3 containing about 4000 lb of good gas absorbent charcoal is required.

SECTION 7

INSTRUMENTATION AND CONTROLS

7. INSTRUMENTATION AND CONTROLS

Contents

7.1 Introduction..... 7.1

7.2 Coupling of Reactor and Load..... 7.2

7.3 Control Rod Speeds..... 7.12

7.4 Nuclear Instrumentation..... 7.15

7.5 Defective Fuel Element Detection..... 7.16

7.5.1 Detection of Gamma Activity..... 7.18

7.5.2 Detection of Delayed Neutrons..... 7.21

7.5.3 Detection of Beta Particles from Daughters of Xenon and Krypton..... 7.21

7.5.4 Detection System..... 7.25

7. INSTRUMENTATION AND CONTROLS

7.1 Introduction

The fundamental objective of the instrumentation and control system is to provide for the safe operation of the reactor within the framework of the design. The reactor operation must be safe for the operating personnel and should be conducive to achieving the longest possible life of the reactor components. To a great extent, freedom from hazards and long component life are complementary.

Since the contamination of the gas system with fission products represents an operating hazard, particularly from the standpoint of maintenance, the detection of capsule failures is very important. In order to reduce the probability of a capsule gas leak developing, the thermal cycling associated with load changes should be eliminated as far as possible. The helium temperatures in the inlet and outlet reactor pipes will be measured continuously. The control system has been designed to maintain these temperatures irrespective of reactor power under normal operating conditions. The gas temperature in the outlet pipes is controlled by varying the positions of the control rods. The inlet temperature is controlled by varying the gas flow through the reactor with a by-pass system as has been discussed in Section 6. A steam load increase will cool the gas being returned to the reactor below the design operating temperature. The reduced temperature will cause the gas by-pass controller to direct a greater gas flow through the reactor. The cooler gas entering the reactor will tend to reduce the outlet temperature which will cause the control rods to be withdrawn to the extent needed to bring the outlet temperature back to normal. The reactor power will then have increased to match the steam load and the gas system temperatures will have returned to the design levels. Since the temperature rise of the gas flowing through the reactor will be kept constant, the gas flow through the reactor will always be directly proportional to the heat production rate.

Changes in load on the steam system are limited to 2% of full power output per minute in order to avoid objectionable transient thermal stresses in the steam system. This means that, as the plant is being brought up to power, a minimum time interval of 50 min would be required to take the

electrical load from zero to full power. In practice, a much longer time interval will be taken. Therefore, the reactions of the control system to load changes need not be fast.

Instrumentation must be provided to indicate the reactor power from zero power to somewhat above the full power. In order to have sufficient thermal flux at the power measuring chambers, the shutdown power must be of the order of 7 w. Antimony-beryllium sources will be provided to produce this power with a shutdown value of k_{eff} of approximately 0.93. These sources have adequately long lives and are regenerative. Conventional nuclear instrumentation is to be employed with fission chambers for low power levels, compensated chambers for logarithmic and period indication over the intermediate to full power range, a compensated chamber for linear flux indication, and uncompensated chambers for high flux alarm during power operation.

In addition to the helium temperatures and neutron flux, many other quantities must be measured to provide an adequate picture of the behavior of the reactor. For example, the flow of helium through the pipes, the temperature of the graphite at several locations within the reactor, and the position of each rod are to be measured as indicated in Fig. 7.1. The steam flow diagram, including instrumentation, is shown in Fig. 7.2.

The controls for the three main divisions of the power plant are grouped into a single control room, Fig. 7.3. There are three sets of control boards, Reactor System, Fig. 7.4, Steam System, Fig. 7.5, and Electrical System, Fig. 7.6. The cost of the reactor instrumentation and control excluding the control rods and the defective fuel element sensing system is $827,000. When the cost of the equipment for detecting defective fuel elements (see Section 7.5) is included in this estimate, the total cost becomes $1,827,000.

7.2 Coupling of Reactor and Load

The temperatures of the helium entering and leaving the reactor are to be maintained at 460°F and 1000°F, respectively, while the flow is to be varied to enable the reactor heat production rate to match the heat removal rate of the steam system.

The temperature of the gas returning to the reactor after being cooled in the steam generator controls the positions of the valves controlling the gas by-pass flow rate. This temperature is measured immediately downstream of the

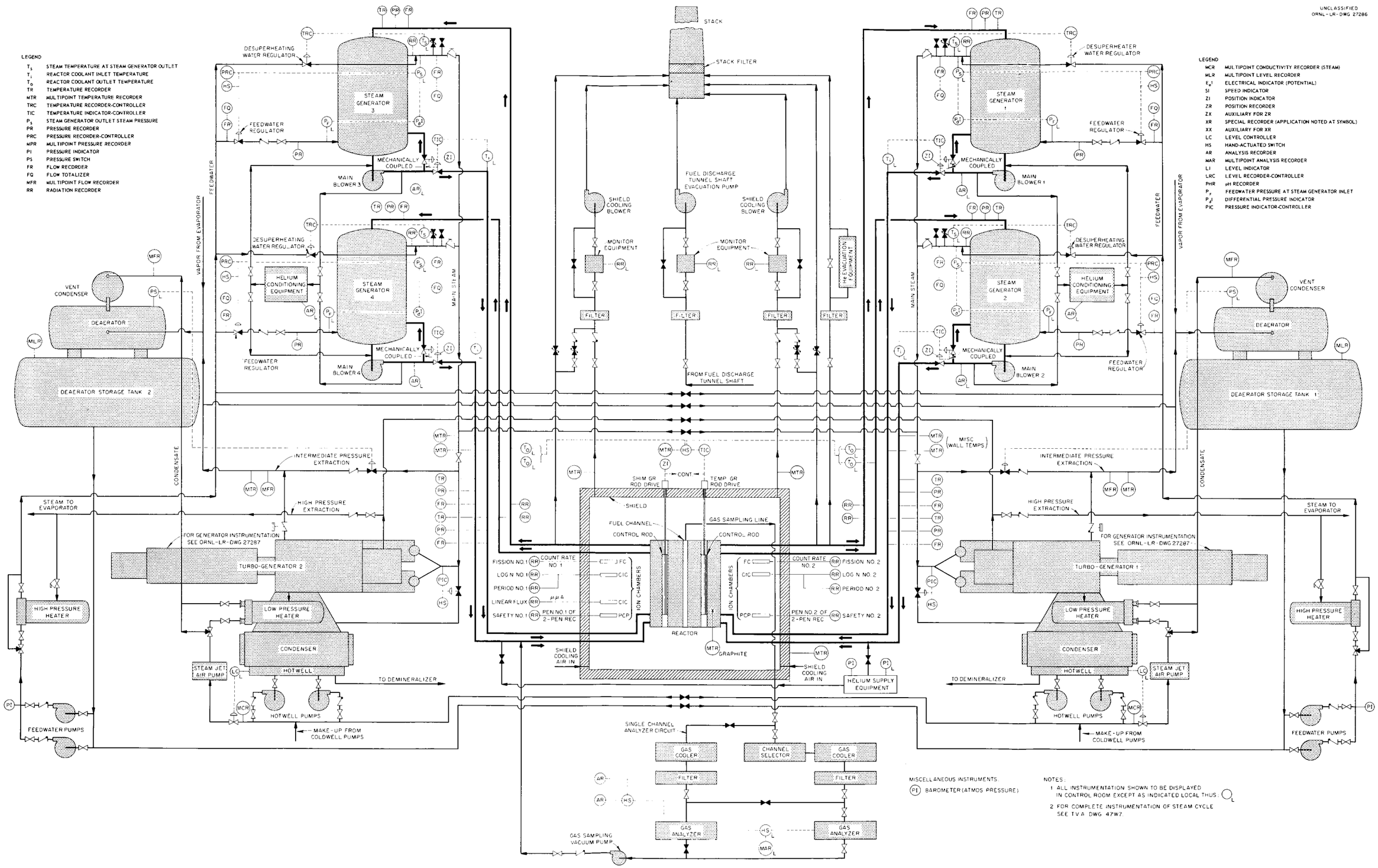

Fig. 7.1. Instrumentation and Controls Flowsheet.

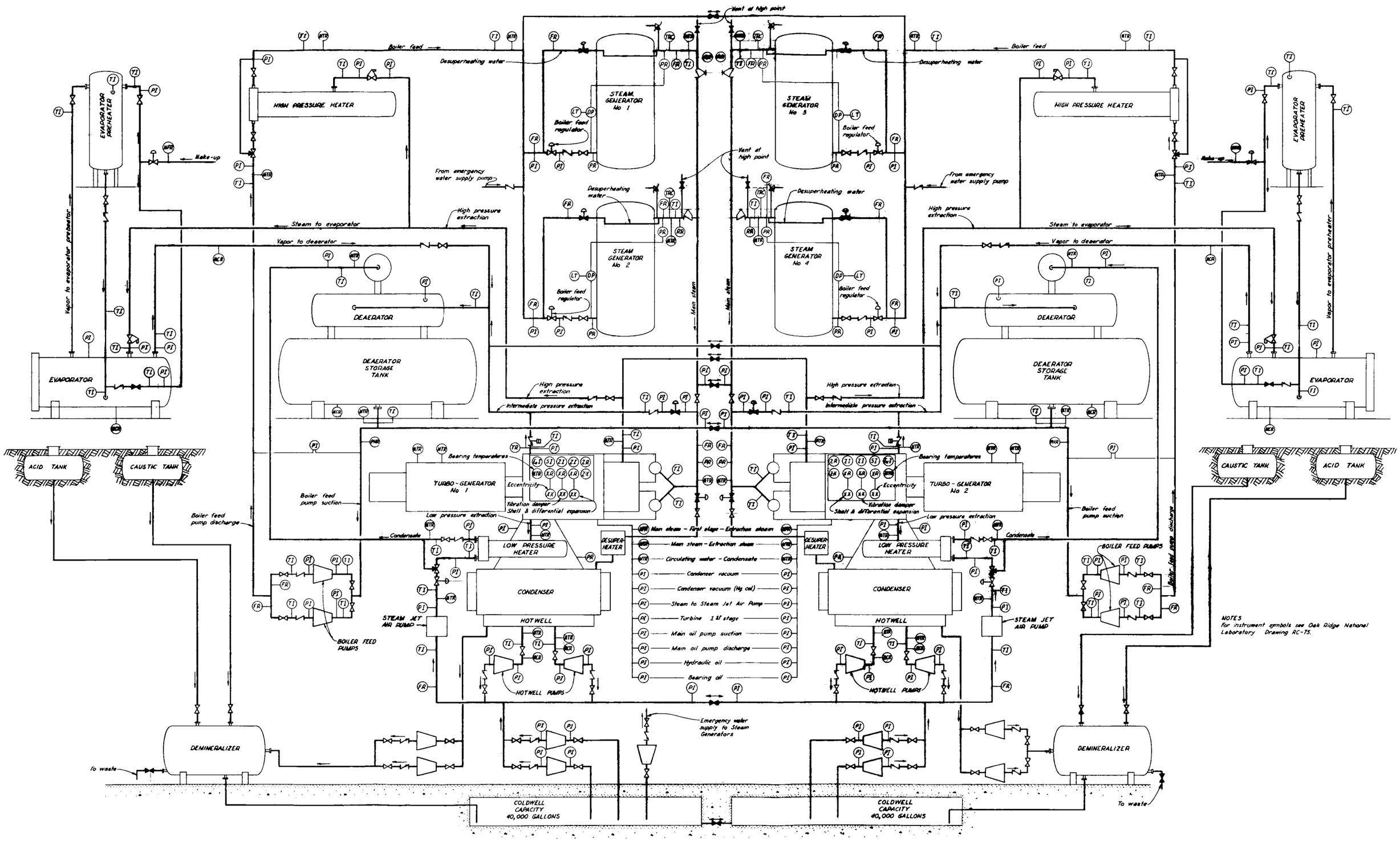

Fig. 7.2. Flow Diagram Principal Piping System.

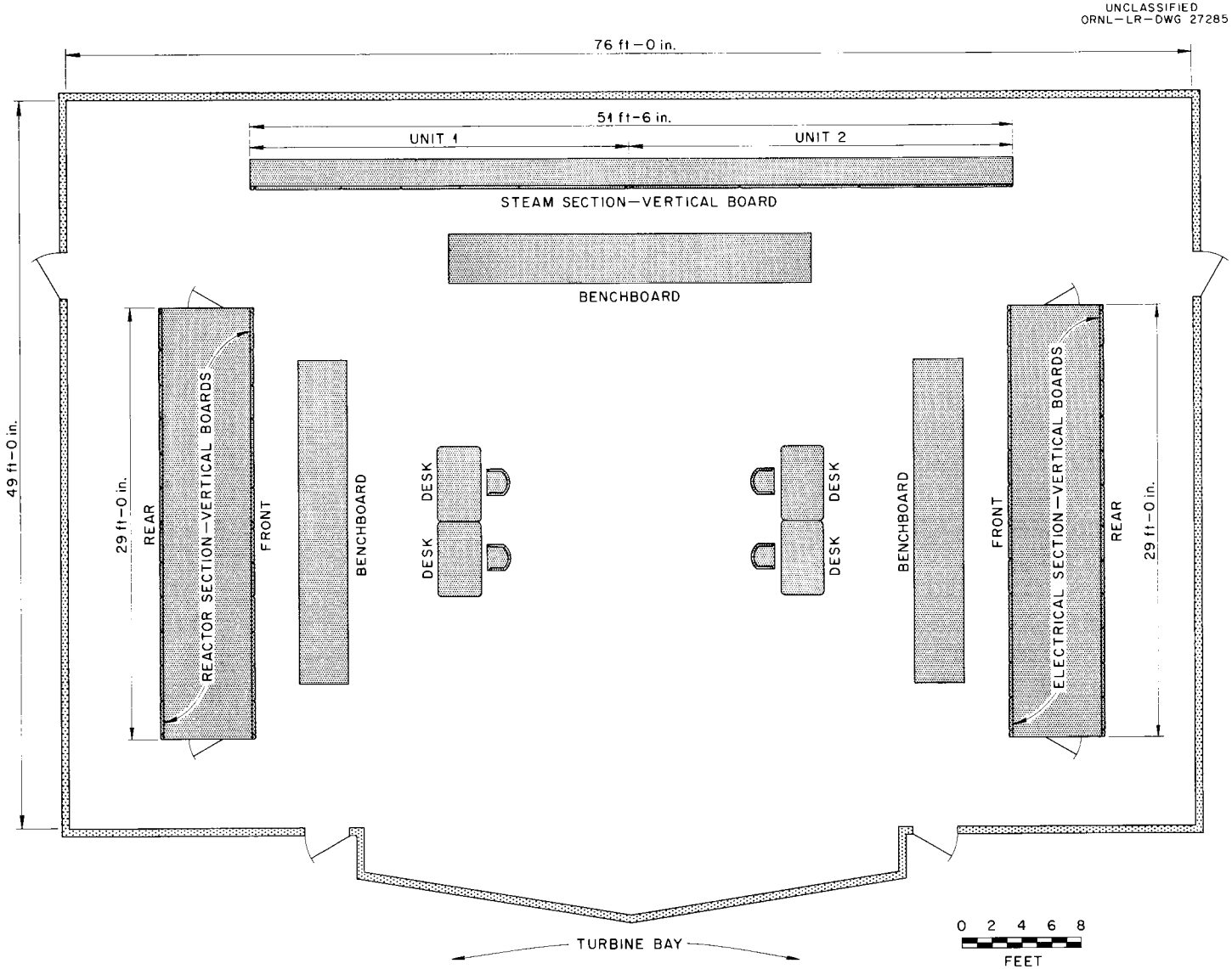

Fig. 7.3. Control Room Floor Plan.

INSTR NO.	DESCRIPTION	SERVICE
RV-1	Radiation recorder	Defective fuel element detection
RV-2	Radiation recorder	
RV-3	Radiation recorder	Steam generator 1 activity
RV-4	Radiation recorder	Steam generator 2 activity
RV-5	Radiation recorder	Steam generator 3 activity
RV-6	Radiation recorder	Steam generator 4 activity
RV-7	Radiation recorder	Main gas duct 1 activity (out of reactor)
RV-8	Radiation recorder	Main gas duct 2 activity (out of reactor)
RV-9	Radiation recorder	Main gas duct 3 activity (out of reactor)
RV-10	Radiation recorder	Main gas duct 4 activity (out of reactor)
RV-11	Temperature recorder (2-pen)	Main gas 1 temperatures (in and out of reactor)
RV-12	Temperature recorder (2-pen)	Main gas 2 temperatures (in and out of reactor)
RV-13	Temperature recorder (2-pen)	Main gas 3 temperatures (in and out of reactor)
RV-14	Temperature recorder (2-pen)	Main gas 4 temperatures (in and out of reactor)
RV-15	Pressure recorder (2-pen)	Main gas 1 pressures (in and out of reactor)
RV-16	Pressure recorder (2-pen)	Main gas 2 pressures (in and out of reactor)
RV-17	Pressure recorder (2-pen)	Main gas 3 pressures (in and out of reactor)
RV-18	Pressure recorder (2-pen)	Main gas 4 pressures (in and out of reactor)
RV-19	Flow recorder (2-pen)	Main gas 1 flows (in and out of reactor)
RV-20	Flow recorder (2-pen)	Main gas 2 flows (in and out of reactor)
RV-21	Flow recorder (2-pen)	Main gas 3 flows (in and out of reactor)
RV-22	Flow recorder (2-pen)	Main gas 4 flows (in and out of reactor)
RV-23	Temperature indicator-controller	Main gas 1 temperature to reactor
RV-24	Temperature indicator-controller	Main gas 2 temperature to reactor
RV-25	Temperature indicator-controller	Main gas 3 temperature to reactor
RV-26	Temperature indicator-controller	Main gas 4 temperature to reactor
RV-27	Radiation recorder	Fission 1
RV-28	Radiation recorder	Fission 2
RV-29	Radiation recorder	Log N 1
RV-30	Radiation recorder	Log N 2
RV-31	Radiation recorder	Period 1
RV-32	Radiation recorder	Period 2
RV-33	Radiation recorder	Linear flux ($\mu\mu a$)
RV-34	Radiation recorder (2-pen)	Safety 1 and 2
RV-35	Multipoint temperature recorder	Coolant maximum temperatures
RV-36	Temperature indicator-controller	Coolant maximum temperature control (rod position)
RV-37	Selector switch	Use with RV-35 and RV-36
RV-38	Clock	
RV-39	Pressure gage	Helium supply
RV-40	Position indicators (69 total)	Control rods positions
RB-1	Oval-handle switch	Defective fuel element recorder selector switch
RB-2	Pistol-grip switch	Shield cooling blower 1 control
RB-3	Pistol-grip switch	Shield cooling blower 2 control
RB-4	Synchro receiver with indicator lights	Main gas 1 bypass valve position indicator
RB-5	Synchro receiver with indicator lights	Main gas 2 bypass valve position indicator
RB-6	Synchro receiver with indicator lights	Main gas 3 bypass valve position indicator
RB-7	Synchro receiver with indicator lights	Main gas 4 bypass valve position indicator
RB-8	Pistol-grip switch	Main gas 1 bypass valve manual positioner
RB-9	Pistol-grip switch	Main gas 2 bypass valve manual positioner
RB-10	Pistol-grip switch	Main gas 3 bypass valve manual positioner
RB-11	Pistol-grip switch	Main gas 4 bypass valve manual positioner
RB-12	Pistol-grip switch	Main gas blower 1 on-off switch
RB-13	Pistol-grip switch	Main gas blower 2 on-off switch
RB-14	Pistol-grip switch	Main gas blower 3 on-off switch
RB-15	Pistol-grip switch	Main gas blower 4 on-off switch
RB-16	Indicating light	Feedwater pump 1 "on" indication
RB-17	Indicating light	Feedwater pump 2 "on" indication
RB-18	Indicating light	Feedwater pump 3 "on" indication
RB-19	Indicating light	Feedwater pump 4 "on" indication
RB-20	Indicating light	Main gas backflow damper 1 position
RB-21	Indicating light	Main gas backflow damper 2 position
RB-22	Indicating light	Main gas backflow damper 3 position
RB-23	Indicating light	Main gas backflow damper 4 position
RB-24	Synchro receiver with indicator lights	Fission chamber 1 position indicator
RB-25	Synchro receiver with indicator lights	Fission chamber 2 position indicator
RB-26	Pistol-grip switch	Fission chamber 1 drive control
RB-27	Pistol-grip switch	Fission chamber 2 drive control
RB-28	Oval-handle switch	$\mu\mu a$ range selector switch
RB-29	Toggle switch (69 total)	Individual control rod drive control
RB-30	Oval-handle switch	Individual control rod permissive switch
RB-31	Oval-handle switch	Individual control rod permissive switch
RB-32	Oval-handle switch	Individual control rod permissive switch
RB-33	Pistol-grip switch	Control rod group 1 group drive
RB-34	Pistol-grip switch	Control rod group 2 group drive
RB-35	Pistol-grip switch	Control rod group 3 group drive
RB-36	Oval-handle switch	Servo-manual selector
RB-37	Pistol-grip switch	Fast insert all rods
RB-38	Pistol-grip switch	All rods drive control
RB-39	Indicating lights	Auxiliary reactor boards power indicator
RB-40	Oval-handle switch	Main gas 1 bypass volve manual-automatic switch
RB-41	Oval-handle switch	Main gas 2 bypass valve manual-automatic switch
RB-42	Oval-handle switch	Main gas 3 byposs valve manual-automatic switch
RB-43	Oval-handle switch	Main gas 4 bypass valve manual-automatic switch
RB-44	Indicating lights	Control power indication
RB-45	Push-button switch	Annunciator test
RB-46	Push-button switch	Annunciator reset

UNCLASSIFIED
ORNL-LR-DWG 27289

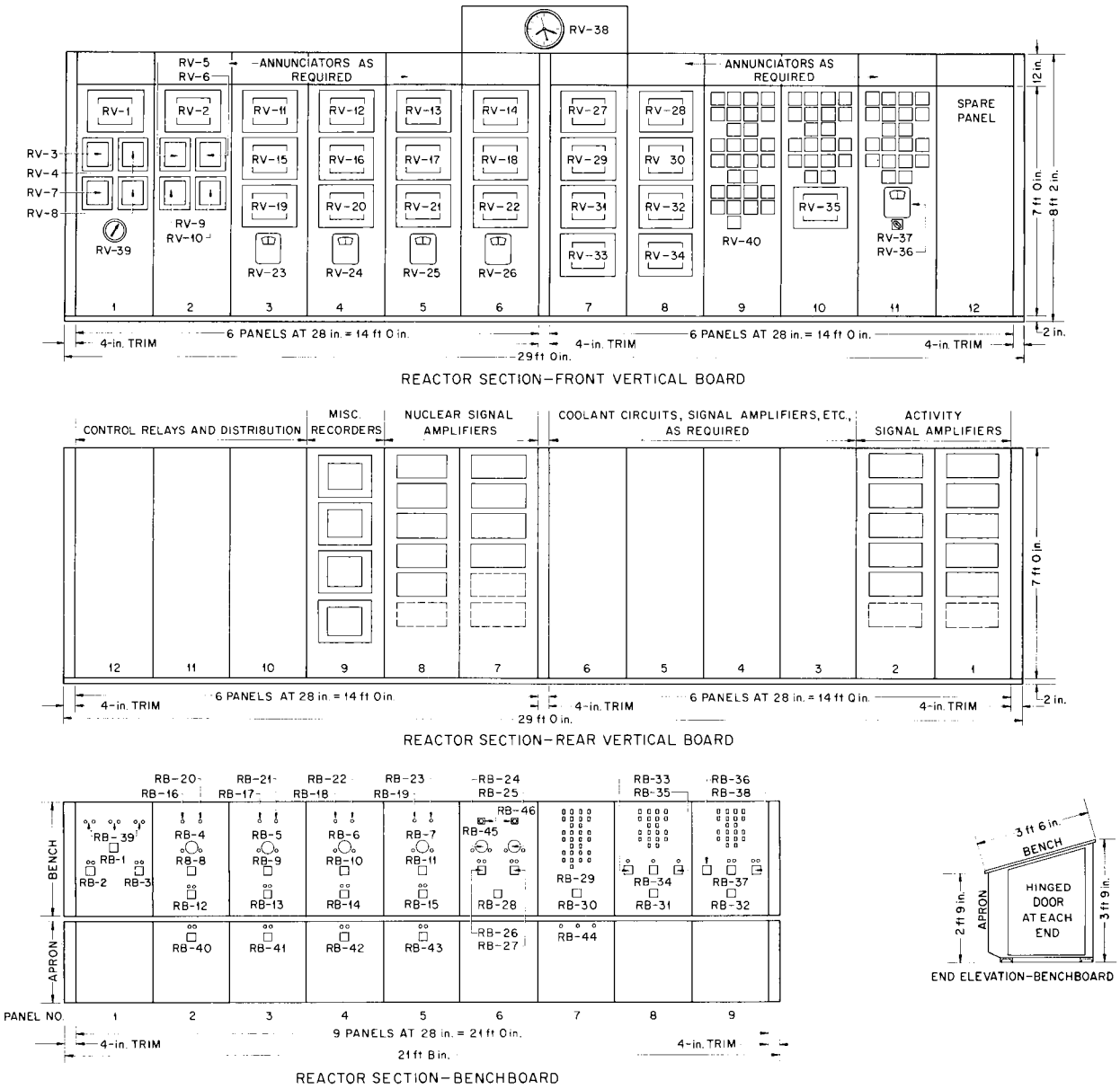

Fig. 7.4. Panel Layout for Reactor System.

INSTR NO.	DESCRIPTION	SERVICE
SV-1	Pressure recorder-controller	Main steam 1 and feedwater 1
SV-2	Pressure recorder-controller	Main steam 2 and feedwater 2
SV-3	Flow recorder	Main steam 1
SV-4	Flow recorder	Main steam 2
SV-5	Temperature recorder-controller	Main steam 1 (desuperheater controller)
SV-6	Temperature recorder-controller	Main steam 2 (desuperheater controller)
SV-7	Multipoint flow recorder	Feedwater 1 and desuperheater 1 flows
SV-8	Multipoint flow recorder	Feedwater 2 and desuperheater 2 flows
SV-9	Pressure gage	Feedwater header pressure
SV-10	Megawatt meter	Generator load
SV-11	Pressure gage	Bearing oil pressure
SV-12	Pressure gage	Main oil pump discharge pressure
SV-13	Pressure gage	Main oil pump suction pressure
SV-14	Pressure gage	Hydraulic oil pressure
SV-15	Multipoint temperature recorder	Condenser and circulating water temperatures
SV-16	Multipoint temperature recorder	Hydrogen and air temperatures
SV-17	Strip chart recorder (6-pen)	3 flows and 3 levels
SV-18	Pressure gage	Steam to steam jet air pump
SV-19	Pressure gage	Condenser vacuum
SV-20	Pressure gage	Main steam at stop valve
SV-21	Pressure gage	Main steam – first stage
SV-22	Governor position indicator	Turbine governor
SV-23	Voltmeter	Generator voltage
SV-24	Tachometer	Turbogenerator speed
SV-25	Turbine supervisory instrumentation	Shell and differential expansion
SV-26	Turbine supervisory instrumentation	Use with SV-25
SV-27	Turbine supervisory instrumentation	Vibration amplitude
SV-28	Turbine supervisory instrumentation	Use with SV-27
SV-29	Turbine supervisory instrumentation	Speed and camshaft position
SV-30	Turbine supervisory instrumentation	Use with SV-29
SV-31	Turbine supervisory instrumentation	Eccentricity recorder
SV-32	Turbine supervisory instrumentotion	Use with SV-31
SV-33	Turbine seal and hydrogen board	Turbine seal and hydrogen control (see Note 1)
SV-34	Flow integrators (4/unit)	Feedwater and steam flows
SV-35	Pressure recorder-controller	Deaerator pressure control
SV-36	Multipoint temperature recorder	Main steam and extraction temperatures
SV-37	Pressure recorder (2-pen)	Main steam and first-stage pressure
SV-38	Conductivity recorder	Conductivity of condensate and evaporator vapor
SV-39	Temperature scanner	Bearing temperatures
SV-40	Switch cabinet	Use with SV-39
SV-41	Indicating lights	Automatic load control indication
SV-42	Differential pressure indicator (2/unit)	Steam generator startup
SB-1	Ammeter	Feedwater pump 1 current
SB-2	Ammeter	Feedwater pump 2 current
SB-3	Pistol-grip switch	Feedwater pump 1 on-off control
SB-4	Pistol-grip switch	Feedwater pump 2 on-off control
SB-5	Pistol-grip switch	Coldwell pump 1 on-off control
SB-6	Push-button switch	Annunciator test
SB-7	Push-button switch	Annunciator reset
SB-8	Pistol-grip switch	Hotwell pump 1 on-off control
SB-9	Pistol-grip switch	Hotwell pump 2 on-off control
SB-10	Pistol-grip switch	Hotwell selector valve
SB-11	Pistol-grip switch	Coldwell pump 2 on-off control
SB-12	Pistol-grip switch	A-C turning gear oil pump
SB-13	Pistal-grip switch	D-C turning gear oil pump
SB-14	Pistol-grip switch	Auxiliary oil pump
SB-15	Pistol-grip switch	A-C oil pump test switch
SB-16	Pistol-grip switch	Auxiliary oil pump test switch
SB-17	Indicating lights	Turning gear engagement indication
SB-18	Pistol-grip switch	Field breaker emergency trip
SB-19	Pistol-grip switch	Turbogenerator emergency trip
SB-20	Pistol-grip switch	Automatic load control emergency cutout
SB-21	Pistol-grip switch	Governor load-limit control
SB-22	Pistol-grip switch	Vapor extraction valve control
SB-23	Indicating lights	Steam stop valve 1 position
SB-24	Indicating lights	Steam stop valve 2 position
SB-25	Pistol-grip switch	Instrument air compressor-control
SB-26	Pistol-grip switch	Distilled water pump control
SB-27	Pistol-grip switch	Motor-operated valve water to hydrogen cooler
SB-28	Pistol-grip switch	Motor-operated valve water to oil cooler
SB-29	Indicating lights (2/unit)	Main blower "on" indication
SB-30	Oval-handle switch (2/unit)	Steam generator differential pressure indicator cutout switch

UNCLASSIFIED
ORNL-LR-DWG 27288

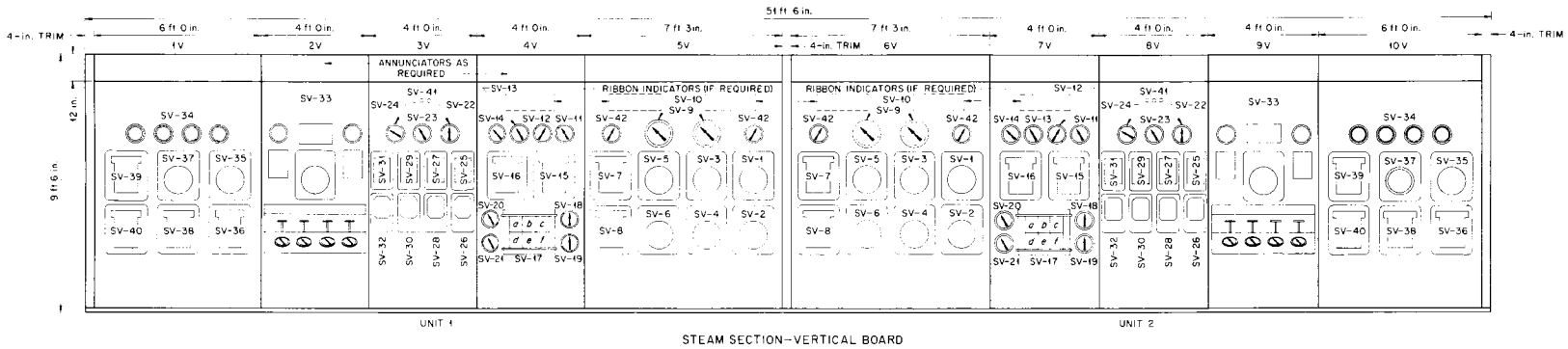

STEAM SECTION—VERTICAL BOARD

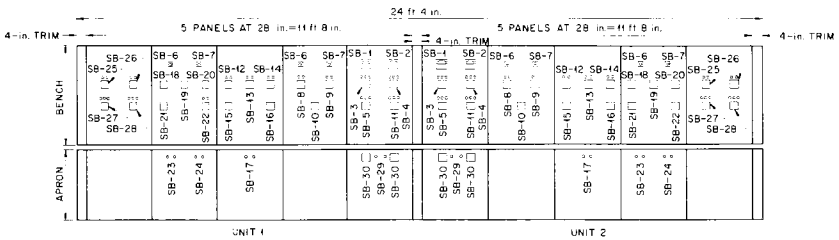

STEAM SECTION—BENCHBOARD

1V AUXILIARY INSTR. BOARD 1
2V TURBINE SEAL AND HYDR. CONTROL BOARD 1 (SEE NOTE 1)
3V SUPERVISORY INSTR. BOARD 1
4V TURBINE BOARD 1
5V STEAM GENERATOR BOARD 1
6V STEAM GENERATOR BOARD 2
7V TURBINE BOARD 2
8V SUPERVISORY INSTR. BOARD 2
9V TURBINE SEAL AND HYDR. CONTROL BOARD 2 (SEE NOTE 1)
10V AUXILIARY INSTR. BOARD 2

NOTES

1. TURBINE GLAND SEAL AND HYDROGEN CONTROL PANEL LAYOUT DETERMINED BY TURBINE MANUFACTURER AND SHOWN ON THIS DWG AS 4-ft 0-in. FOR ESTIMATING PURPOSES ONLY.
2. PRESSURE INDICATORS FOR ATMOSPHERIC PRESSURE AND CONDENSER VACUUM TO BE MOUNTED ON CONTROL ROOM WALL.

Fig. 7.5. Panel Layout for Steam System.

INSTR NO.	DESCRIPTION	SERVICE
EV-1	Ammeter (3 total)	Generator 1 current
EV-2	Speed indicator	Generator 1 speed
EV-3	Voltmeter	Generator 1 voltage
EV-4	Voltmeter	Generator 1 neutral voltage
EV-5	Wattmeter	Generator 1 wattage
EV-6	Reactive volt-ammeter	Generator 1 reactive volt-amperage
EV-7	Voltmeter	Generator 1 exciter voltage
EV-8	Ammeter	Generator 1 exciter current
EV-9	Voltmeter	Generator 1 pilot exciter voltage
EV-10	Ammeter	Generotor 1 pilot exciter current
EV-11	Indicating lights	Voltage regulator 1 normal response indication
EV-12	Indicating lights	Voltage regulator 1 quick response indication
EV-13	Voltage regulator	Generator 1 voltage regulotion
EV-14	Push-button switch	Generator 1 neutral voltage push button
EV-15	Watthour meter	Generator 1 watthour metering
EV-16	Pistol-grip switch	Main transformer 1 sprinkler system test
EV-17	Pistol-grip switch	Main transformer 1 coolant system test
EV-18	Ammeter (2 total)	Unit 1 station service current
EV-19	Ammeter (2 total)	Unit 2 station service current
EV-20	Voltmeter	Unit 1 station service voltage
EV-21	Voltmeter	Unit 2 station service voltage
EV-23	Synchronizing panel	Synchronize generators with system (V – voltmeter, F – frequency meter, S – synchroscope)
EV-24	Ammeter (3 total)	Line 1 current
EV-25	Wattmeter	Line 1 wattage
EV-26	Reactive volt-ammeter	Line 1 reactive volt-amperage
EV-27	Ammeter	Line 1 carrier current
EV-28	Push-button switch	Line 1 telemetering reset push button
EV-29	Pistol-grip switch	Line 1 carrier current test
EV-32	Temperature recorder	Generator 1 field temperature
EV-33	Load recorder	Generator 1 load
EV-34	Temperature recorder	Generator 1 and transformer 1 temperatures
EV-35	Ammeter	Battery charger m-g set 1 current
EV-36	Ammeter	Battery charger m-g set 2 current
EV-37	Ammeter	Battery charger m-g set 3 current
EV-38	Voltmeter	Battery 1 voltage
EV-39	Voltmeter	Battery 2 voltage
EV-40	Voltmeter (2 total)	D-C bus 1 and 2 voltage
EV-41	Ammeter	Battery 1 current
EV-42	Ammeter	Battery 2 current
EV-43	Ground-indicating voltmeter	D-C bus 1
EV-44	Ground-indicating voltmeter	D-C bus 2
EV-45	Frequency meter	115-v a-c m-g set frequency
EV-46	Voltmeter	115-v a-c m-g set voltage
EV-47	Voltage regulotor	115-v a-c m-g set voltage regulation
EV-48	Speed regulator	115-v a-c m-g set speed regulation
EV-49	Protective relay	115-v a-c m-g set overvoltage protection
EV-50	Protective relay	115-v a-c m-g set undervoltage protection
EV-51	Auxiliary relay	Use with EV-50
EV-52	Indicating light	Normal power feed indication
EV-53	Indicating light	Emergency power feed indication
EV-54	Clock	
EV-55	Generator and transformer relay panel	Generator and transformer protection (differential, overcurrent, overvoltage, field failure, and auxiliary relays; various trip cutout switches and test blocks)
EV-56	Station service transformer relay panel	Station service transformer protection (differential, overcurrent, and auxiliary relays; various trip cutout switches and test blocks)
EV-57	Tronsmission line relay panel	Line protection (impedance, ground, timing, reclosing, undervoltage, synchronizing check, and auxiliary relays; various trip cutout switches and test blocks)
EV-58	161-kv bus relay panel	Bus protection (ground, breakup, differential, and auxiliary relays; various trip cutout switches and test blocks)
EB-1	Pistol-grip switch	161-kv oil circuit breaker control
EB-2	Pistol-grip switch	Synchronizing control
EB-3	Pistol-grip switch	Synchronizing control
EB-4	Pistol-grip switch	161-kv oil circuit breaker control
EB-5	Pistol-grip switch	Generator oil circuit breaker control
EB-6	Pistol-grip switch	Synchronizing control
EB-7	Pistol-grip switch	Main exciter field rheostat control
EB-8	Pistol-grip switch	Voltage regulator transfer control
EB-9	Pistol-grip switch	Motor-operated disconnect control
EB-10	Pistol-grip switch	Governor control
EB-11	Rheostat	Generator voltage adjustment
EB-12	Pistol-grip switch	Generator voltmeter switch
EB-13	Jack	Telephone
EB-14	Pistol-grip switch (3 total)	4.16-kv unit board air circuit breaker control
EB-15	Pistol-grip switch (3 total)	4.16-kv reactor board air circuit breaker control
EB-16	Pistol-grip switch (3 total)	4.16-kv common board air circuit breaker control
EB-17	Pistol-grip switch	Line 1 oil circuit breaker control switch
EB-18	Pistol-grip switch	Line 1 synchronizing switch
EB-19	Pistol-grip switch	Line 1 motor-operated disconnect interlock switch
EB-20	Pistol-grip switch	Line 1 motor-operated disconnect control switch
EB-21	Pistol-grip switch	Battery charger m-g set 1 control switch
EB-22	Pistol-grip switch	Battery charger m-g set 2 control switch
EB-23	Pistol-grip switch	Battery charger m-g set 3 control switch
EB-24	Pistol-grip switch	D-C bus voltmeter switch
EB-25	Rheostat	Battery charger m-g set 1 voltage regulator
EB-26	Rheostat	Battery charger m-g set 2 voltage regulator
EB-27	Rheostat	Battery charger m-g set 3 voltage regulator
EB-28	Pistol-grip switch	115-v a-c m-g set voltage regulator switch
EB-29	Pistol-grip switch	115-v a-c m-g set speed control switch
EB-30	Pistol-grip switch	115-v a-c m-g set voltmeter switch
EB-31	Pistol-grip switch	115-v a-c m-g set test switch
EB-32	Rheostat	115-v a-c m-g set d-c motor field control
EB-33	Rheostat	115-v a-c m-g set a-c generator field control
EB-34	Push-button switch	Annunciator test
EB-35	Push-button switch	Annunciator reset

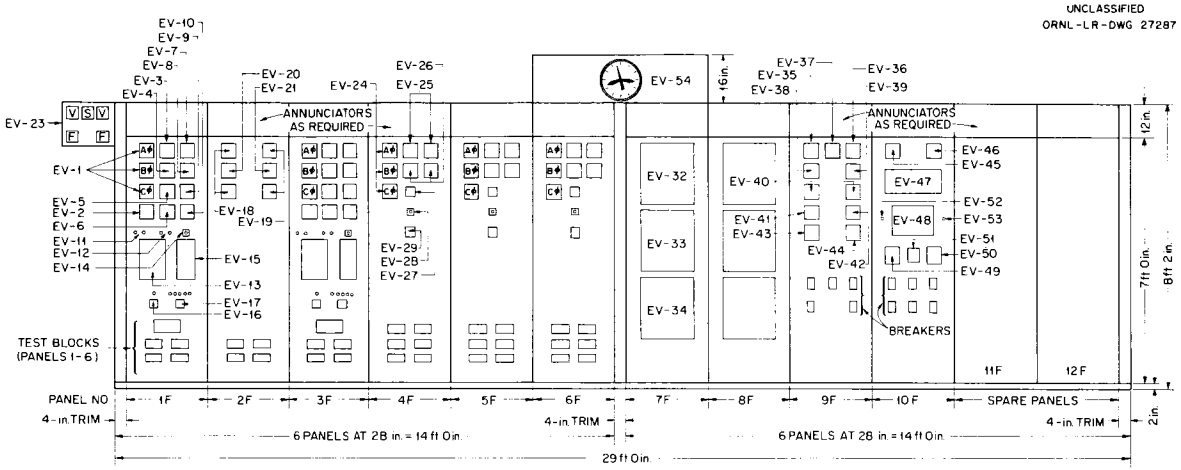

ELECTRICAL SECTION-FRONT VERTICAL BOARD

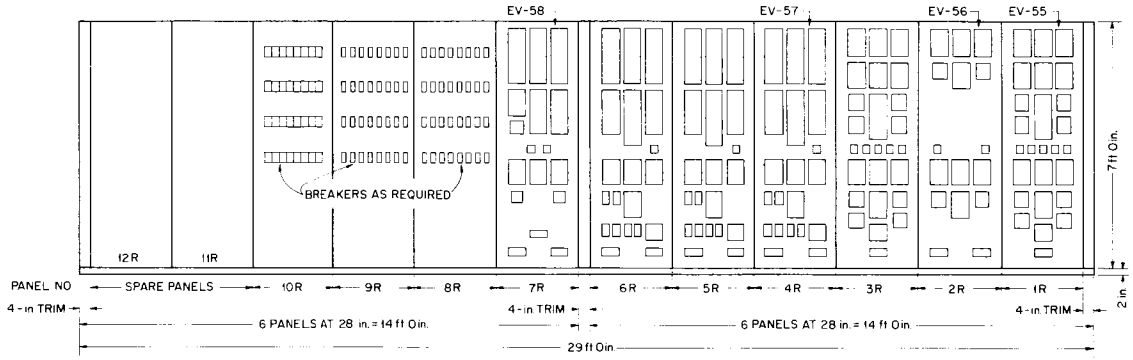

ELECTRICAL SECTION-REAR VERTICAL BOARD

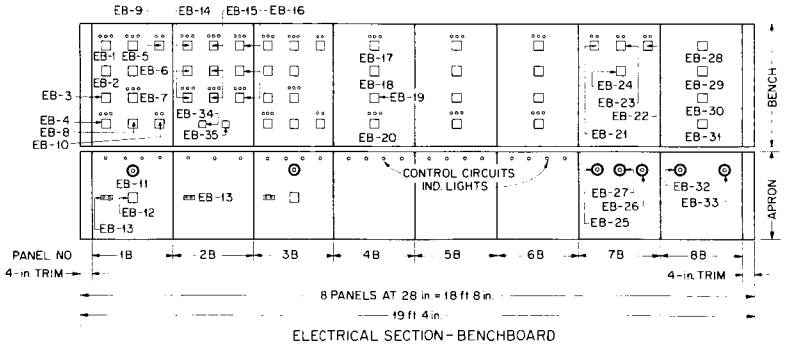

ELECTRICAL SECTION-BENCHBOARD

KEY

1F GEN. 1 AND TR. 1	10R 250 v dc DISTR.
2F UNIT S.S. TRANSFORMERS	9R 48 v dc DISTR.
3F GEN. 2 AND TR. 2 SAME AS PNL. 1	8R 115 v dc DISTR.
4F LINE 1	7R BUS RELAYS
5F LINE 2 SAME AS PNL. 4	6R LINE 3 RELAYS SAME AS PNL. 4
6F LINE 3 SAME AS PNL. 4	5R LINE 2 RELAYS SAME AS PNL. 4
7F GEN. 1 RECORDERS	4R LINE 1 RELAYS
8F GEN. 2 RECORDERS SAME AS PNL. 7	3R GEN. 2 AND TR. 2 SAME AS PNL. 1
9F BATT. CHARGER M-G SETS	2R UNIT S.S. TR. 1 AND 2 RELAYS
10F 115 v dc M-G SET	1R GEN. 1 AND TR. 1 RELAYS

1B GEN. 1 AND TR. 1
2B 4.16 kv UNIT BD. REACTOR AND COMMON BDS. ACB. CONTROL
3B GEN. 2 AND TR. 2 SAME AS PNL. 1
4B LINE 1
5B LINE 2 SAME AS PNL. 4
6B LINE 3 SAME AS PNL. 4
7B BATTERY CHARGER M-G SETS
8B 115 v dc M-G SET

Fig. 7.6. Panel Layout for Electrical System.

blower in the reactor inlet pipe in order that the temperature change caused by a change in the positions of the by-pass valves will be sensed as quickly as possible. Likewise, the temperature of the gas in one reactor outlet pipe is used to regulate a number of the control rod actuators; this temperature is measured as close to the reactor outlet as practical. Since there are four outlet pipes each containing gas at the same temperature, the operator may select manually any one duct for this control.

The response of the system to change is sluggish, primarily because of the low ratio of power density to heat capacity in the system, as indicated in Table 7.1. Further, the long system transit times, 100 sec for the water and steam flowing through the steam generator and 10 sec for the helium circuit, contribute to this sluggishness. Thus, it can readily be seen that this reactor is not tightly coupled to its load.

Variations introduced by control actuators must be slow to prevent excessive overshoots and undershoots in the parameters being controlled. In fact, the full stroke of the by-pass valves should require on the order of 180 sec, and the rate of reactivity change for the control rods regulating the helium outlet temperature should be of the order of 5×10^{-6}/sec which will require no more than 4 rods. (See 7.3 below) In view of the sluggishness of the system, the temperature of the steam from the steam generator is not to be regulated by means of the control rods but rather will be controlled by the desuperheater.

The gas temperatures in the pipes will be measured by thermocouples which are shielded from the radiant heat from the pipe inside surface. This arrangement will virtually eliminate the effects of the pipe temperature, which will lag behind the changes in gas temperature.

7.3 Control Rod Speeds

The control rod drive mechanism has already been described in Section 5. The full rod stroke is 20 ft, the lower limit being the position where the top of the neutron absorbing silver section is level with the top of the core. All of the rods are to be at approximately equal heights at all times. During start-up, all of the rods are manually withdrawn simultaneously by means of a master switch. The operator can manually insert all of the rods simultaneously at the normal insert speed at any time. The operator can also

TABLE 7.1

HEAT CAPACITIES OF VARIOUS COMPONENTS IN THE GCR-2 HELIUM SYSTEM

Component	Material	Wt	c, Btu/lb-°F	Q, (Btu)/°F
Fuel	UO_2	1.78×10^8 g or 3.92×10^5 lb	0.056	2.195×10^4
Fuel Capsule	304 Stainless steel	1.11×10^7 g or 2.45×10^4 lb	0.12	2.94×10^3
Moderator	Graphite	2×10^6 lb	0.35	7×10^5
Pressure Vessel	Steel	1.8×10^6 lb	0.11	1.98×10^5
Steam generator tubes		8×10^5 lb	0.12	9.6×10^4
Steam generator tubes		1.7×10^6 lb	0.12	2.04×10^5
Pipes	Stainless steel	1.9×10^5 lb	0.12	2.28×10^4
	Carbon steel	1.2×10^5 lb	0.11	1.32×10^4
Primary Coolant	Helium	9720 lb	1.24	1.205×10^4
Secondary Coolant	Water	2.10^5 lb	1	2×10^5

initiate the emergency insertion of all rods at any time. The manual withdrawal or insertion at normal speed can be stopped at any time; however, the fast emergency insertion will continue to the lower limit when once initiated in order to relieve the operator of further attention to rod insertion during an emergency.

Although channels for 69 control rods are available, 8 of these channels on the periphery of the core will not be used. Therefore, 61 control rods are to be employed, their total worth being approximately 0.17 Δk. The normal rod withdrawal speed is chosen to produce an average rate of change in k_{eff} of 10^{-4}/sec, requiring 1700 sec to withdraw the rods 20 ft, provided the withdrawal is continuous. This corresponds to a rod speed of 8.48 in./min.

The emergency insert speed produces an average rate of change in k_{eff} of 10^{-3}/sec, ten times that of the normal withdrawal rate. This rate, then, corresponds to an insert speed of 84.8 in./min.

The emergency insert speed is produced by a pneumatic motor operating from a high-pressure helium supply. Whenever the emergency insertion is initiated, the electric power to the normal drive motor is removed through the operation of a circuit breaker on each individual rod drive.

The normal withdrawal rate together with the emergency insert speed were selected to keep the power within safe limits in case of a start-up accident while at the same time providing an acceptable start-up time for the reactor. An extremely slow withdrawal rate will produce a relatively long reactor period at a given power level during start-up, but the start-up would take an excessively long time. Should the rods be withdrawn continously from their lower limits, starting with the reactor at a source level of 7 w, the fast insert speed will immediately reduce the power level with very little overshoot in power. In case the fuel cooling rate were reduced instantaneously from 600 Mw to 6 Mw, an analog computer study has shown that the fuel mean temperature would rise only 100°F after a rod insert rate of 1.2×10^{-3}/sec in Δk has been initiated. Thus, a fast insert rate of 10^{-3}/sec should be sufficient to limit the fuel temperature rise to a safe value in case of a sudden loss in cooling.

The normal insert speed is chosen identical to the normal withdrawal speed to allow the use of a reversible 3-phase motor to drive the rod actuator.

During the start-up of the reactor, at power levels between 700 w and 10 Mw, periods shorter than 5 sec will automatically initiate an emergency insert.

At power levels above 10 Mw, the reactor will be delivering power to the steam system, and temperature indications will become the most important control consideration. The automatic fast insert will be deactivated at 10 Mw so that a fast insert will require action by the operator when the reactor is at power.

The temperature coefficient of reactivity will vary during the lifetime of the reactor (see Section 2). An average value of the negative temperature coefficient of the fuel is approximately $3 \times 10^{-5}/°F$. An upper limit of 10°F/min has been taken for rates of change of temperature. Three rods moving continuously at the normal speed should be able to produce this rate of change. Consequently, the servo controlling the helium exit temperature is expected to require the action of only 4 rods.

Whenever the rod positions differ by more than 6 in., the operator is expected to synchronize their positions manually by individual control of each rod drive.

7.4 Nuclear Instrumentation

The nuclear instruments are designed to indicate the reactor power from the shut-down source level to above 700 Mw. In order to have the neutron detecting chambers in a low-temperature, low-pressure region where they are readily available for inspection and replacement, it was decided to locate them outside the reactor pressure vessel. In order to provide the chambers with the greatest possible thermal flux and to allow the determination of any asymmetry in the spatial flux distribution, the channels are placed in two graphite thermal columns located on opposite sides of the pressure vessel at the midplane of the reactor.

At a reactor power of 700 Mw, it is estimated that there will be a thermal flux of approximately 10^9 n/cm^2·sec, with a gamma dose level of 3.6×10^5 R/hr at the chamber locations. It will be necessary to provide a window in the boron curtain surrounding the reactor. The compensated chambers should be able to cover a range of 10^6 down from the design point

value by the use of 4-in. lead shields, surrounding these chambers. This thickness of lead should reduce the gamma flux by a factor of approximately 100 and the neutron flux by about one-third.[1] The lower flux limit at the chamber positions is approximately 10 $n/cm^2 \cdot sec$ when the reactor is shut down with all the control rods fully inserted.

From source level to approximately 70 kw, fission chambers and counting instruments will supply power level information. These chambers will be retracted into shielded positions at higher reactor powers in order to prolong chamber life and provide continuous indication throughout the operating range. Compensated ion chambers will cover the range from 700 w to 700 Mw, providing the signal current for logarithmic power level, reactor period, and linear power level indication. Parallel circular plate chambers will sense the flux over a 2-decade range at high power and provide a high-flux warning.

7.5 Defective Fuel Element Detection

Any defect in the fuel capsule results in the leakage of fission products into the circulating gas stream. It is important to locate a defective fuel element so that it may be replaced as soon as possible. The process of locating this defective fuel element should be as simple as possible consistent with the requirement that the sensitivity of the equipment permits the unique detection of the defective element in the required time.

It is proposed to determine the location of a defective fuel element by sampling the gas from each channel. Sampling tubes carry the gas from each channel or group of channels to a point where the activity can be measured. Since activity can result from several types of radioactive decay, the sensitivity of detection for each mode must be examined separately.

In the subsequent analysis the following general relationships are useful:

The concentration of an isotope in the gas due to surface contamination can be expressed by

$$N_1 = \frac{P_1 \; 3.1 \times 10^{10} \gamma_n}{2\lambda_n V} \qquad (7.1)$$

---

[1] R. J. Cox and K. R. Sandiford, "Reactor Control and Instrumentation," J. Brit. Nucl. Energy Conf., 2, No. 2, 205 (April, 1957).

where,

N_1 = concentration in atoms/cm^3 in gas (at equilibrium)

P_1 = watts generated by surface contamination

γ_n = fractional yield of isotope n

λ_n = decay constant of isotope n in sec^{-1}

V = system volume in cm^3

(It is assumed that only one-half of the fission recoils enter the gas).

The concentration of an isotope in a leaking channel due to the leak in that channel can be written

$$N_2 = \frac{P_2 \; 3.1 \times 10^{10} \gamma_n \; \nu_n}{\lambda_n F} \tag{7.2}$$

where,

N_2 = concentration in atoms/cm^3 in gas leaving leaking channel

P_2 = watts generated in a single fuel rod

ν_n = escape constant of isotope n in sec^{-1}

F = flow rate through leaking channel, cm^3/sec

For the GCR-2 with a surface contamination of 10^{-9} g/cc,

$P_1 = 0.5$,

$P_2 = 1.25 \times 10^4$,

$V = 1.76 \times 10^9$ cm^3, and

$F = 2.2 \times 10^5$ cm^3/sec

Therefore,

$$\frac{N_1}{N_2} = \frac{2.5 \times 10^{-9}}{\nu_n} \tag{7.3}$$

The concentration of an isotope in the gas due to the equilibrium build-up of activity is

$$N_3 = \frac{P_2 \times 3.1 \times 10^{10} \gamma_n \; \nu_n}{\lambda_n^2 \; V} \tag{7.4}$$

where,

N_3 = concentration in atoms/cm^3 in system due to leak.

Other constants are as previously defined.

Employing the values given above, we find

$$\frac{N_2}{N_3} = 8 \times 10^3 \lambda_n \tag{7.5}$$

Thus, if $\lambda_n >> 1.25 \times 10^{-4}$, the concentration of the isotope in the leaking channel will exceed the general background concentration in the gas and identification of the leaking channel may be possible.

The above relationship which assumes equilibrium concentrations neglects the decay of an isotope during the helium transit time, which becomes significant for half lives much shorter than 10 sec.

7.5.1 Detection of Gamma Activity: It is of interest to calculate, (1) the activity per cm^3 in the leaking channel due to the activity issuing from the leak, (2) the activity due to the build-up of fission products in the system because of the leak, and (3) that due to activity in the gas without the leak.

Employing the escape constants computed in Section 13 and a gas flow rate per channel of 2.2×10^5 cm^3/sec, the number of decays per cm^3·sec in the leaking channel due to the leak may be determined. This number for all decay processes[2] which yield a gamma greater than 0.1 mev is 36 d/cm^3·sec Twenty minutes after the onset of the leak, the system concentration is 3.9 d/cm^3·sec which increases to a value of 390 d/cm^3·sec at equilibrium as indicated in Table 7.2. Thus, if these were the only activities involved, the leak would have to be detected in less than 1/2 hr, otherwise, the build-up of the fission product background activity would mask the contribution of the leak.

There is, in addition, a significant background activity in the system due to radioactive recoils and to surface contamination of the fuel capsules. The recoil activity[2] amounts to 420 d/cm^3·sec, which is principally Mn^{56}, while the activity from the assumed surface contamination of 10^{-9} g/cm^2 may be calculated for each isotope from the relationship:

$$\frac{N_1}{N_2} = \frac{2.5 \times 10^{-9}}{\nu_n} \tag{7.6}$$

[2] See Section 13

TABLE 7.2

ACTIVITY PER $CM^3 \cdot Sec$ IN LEAKING CHANNEL (FROM GAMMA EMITTERS ONLY)

	No. of atoms per sec escaping from a leak* νN_0	No. of atoms per cm^3 ensuing from leaking channel+ N_1	No. of decays per $cm^3 \cdot sec$ in leaking channel λN_L
Te^{125m}	9×10^{13}	1.3×10^{3}	1×10^{-3}
Te^{129m}	3.9×10^{12}	3.2×10^{2}	5.1×10^{-2}
Te^{131m}	4.2×10^{12}	3.4×10^{2}	2.2×10^{-2}
Te^{131}	3.9×10^{12}	3.2×10^{2}	1.5×10^{-1}
Te^{132}	1.1×10^{15}	9×10^{4}	2.3×10^{-1}
Te^{133m}	1.6×10^{13}	1.3×10^{3}	2.3×10^{0}
Te^{133}	6.3×10^{11}	5.1×10^{1}	3.0×10^{-1}
I^{131}	2.6×10^{16}	2.1×10^{6}	2.1×10^{0}
I^{132}	4.8×10^{14}	3.9×10^{4}	3.1×10^{0}
I^{133}	5.6×10^{15}	4.6×10^{5}	4.3×10^{0}
I^{135}	1.6×10^{14}	1.3×10^{4}	3.8×10^{-1}
I^{136}	3.2×10^{12}	2.6×10^{2}	2.1×10^{0}
Xe^{121m}	6.6×10^{14}	5.4×10^{4}	3.6×10^{-2}
Xe^{133m}	7.0×10^{14}	5.7×10^{4}	2.0×10^{-1}
Xe^{133}	7.0×10^{14}	5.7×10^{4}	8.5×10^{-2}
Xe^{135m}	3.6×10^{13}	2.9×10^{3}	2.1×10^{0}
Cs^{136}	2.2×10^{11}	1.8×10^{1}	1.1×10^{-5}
Cs^{138}	3.6×10^{11}	2.9×10^{1}	1.0×10^{-2}
Ba^{139m}	1.9×10^{11}	1.5×10^{1}	6.6×10^{-2}
Ba^{139}	5.6×10^{12}	4.6×10^{2}	6.4×10^{-2}
Ba^{140}	1.3×10^{12}	1.1×10^{2}	6.9×10^{-2}
La^{140}	2.7×10^{12}	2.2×10^{2}	1.1×10^{-3}
La^{141}	1.9×10^{11}	1.5×10^{1}	7.6×10^{-4}
Ce^{141}	5.0×10^{13}	4.1×10^{3}	1.0×10^{-3}
Ce^{143}	2.2×10^{12}	1.8×10^{2}	1.1×10^{-3}
Ce^{144}	4.3×10^{14}	3.5×10^{4}	1.0×10^{-3}
Ce^{146}	8.5×10^{9}	6.9×10^{-1}	5.7×10^{-4}
Pr^{146}	1.5×10^{10}	1.2×10^{0}	5.6×10^{-4}
Nd^{147}	3.1×10^{14}	2.5×10^{4}	1.8×10^{-2}
Nd^{151}	4.8×10^{9}	3.9×10^{-1}	3.0×10^{-4}
	3.636×10^{16}		17.69

Table 7.2 (continued)

Se^{83}	2.7×10^{11}	2.2×10^{1}	1.0×10^{-2}
Br^{84}	2.8×10^{12}	2.2×10^{2}	9×10^{-2}
Br^{87}	2.6×10^{11}	2.1×10^{1}	2.7×10^{-1}
Kr^{95m}	4.1×10^{13}	3.3×10^{3}	1.5×10^{-1}
Kr^{87}	3.8×10^{14}	3.1×10^{4}	4.6×10^{0}
Kr^{88}	1.1×10^{15}	9×10^{4}	6.3×10^{0}
Rb^{88}	1.2×10^{14}	1.0×10^{4}	6.5×10^{0}
Sr^{91}	4.5×10^{12}	3.6×10^{2}	7.2×10^{-3}
Y^{91m}	4.6×10^{9}	3.7×10^{-1}	8.5×10^{-4}
Y^{93}	1.5×10^{10}	1.2×10^{0}	2.3×10^{-5}
Y^{94}	2.1×10^{8}	1.7×10^{-2}	1.2×10^{-5}
Zr^{95}	1.2×10^{13}	1.0×10^{3}	1.2×10^{-4}
Nb^{95m}	2.8×10^{11}	2.3×10^{1}	4.8×10^{-5}
Nb^{95}	2.5×10^{14}	2.0×10^{4}	4.6×10^{-3}
Nb^{97m}	4.8×10^{9}	3.9×10^{-1}	4.7×10^{-3}
Nb^{97}	3.5×10^{11}	2.8×10^{1}	4.5×10^{-3}
Mo^{99}	1.8×10^{13}	1.5×10^{13}	4.4×10^{-2}
	1.93×10^{15}		17.96

TOTAL 35.65 d/cm^3 per sec from leaking channel

$3.64 \times 10^{16} \times 1.015 \times 10^{-14} = 3.7 \times 10^{2} = 370$ d/cm^3 per sec Xe in total system

$1.93 \times 10^{15} \times 1.015 \times 10^{-14} = 2.0 \times 10^{1} = 20$ d/cm^3 per sec Kr in total system

390 d/cm^3 per Xe + Kr in total system

*The data in this column was taken from Section 13. N_0 is the equilibrium concentration of an isotope in the fuel, $(P \times 3.1 \times 10^{10} \times \gamma)$, and ν is the escape coefficient.

+N_L is νN_0 divided by the flow rate (2.2×10^{5} cm^3/sec) and the number of fuel elements (5.6×10^{4}).

Since the values of ν for the iodine, xenon and krypton isotopes, which are controlling, are 4×10^{-8}, 7×10^{-8} and 1×10^{-7}, respectively, $N_1 \cong 0.1\ N_2$. Thus, a surface contamination of the level assumed, (10^{-9} g/cm^2) would permit identification of the leaking channel if the recoil activity were not present.

The gamma radiation from the 2.5 hr Mn^{56} will mask any small leak and prevent detection by this means. In addition, the build-up of background from the leak alone will prevent identification of the leaking channel after an elapse of something like 10 to 20 hr.

7.5.2 Detection of Delayed Neutrons: Since the background gamma activity is too high to permit the detection of a leaking fuel element by gamma activity from the leaking channel, the use of delayed neutrons is suggested since such neutrons would not be present in the gas from recoil processes. There would, however, be some background due to surface contamination and diffusion through the capsule wall. Furthermore, the concentrations may be so low as to make their detection impracticable, if not impossible.

The escape constants for I^{137} and Br^{87}, the two known delayed neutron emitters, are 4×10^{-8} and 6×10^{-9}, respectively, so that it may be possible to separate the activity from the leak and that from the surface contamination.

The delayed neutron emission rate in the gas from the leaking channel is approximately 5 delayed neutrons/cm^3·sec which is too low to be used as a satisfactory leak monitoring technique.

7.5.3 Detection of Beta Particles from Daughters of Xenon and Krypton: The detection of leaks by means of the beta activity from the daughters of the noble gases offers greater sensitivity over the previously discussed techniques in that the measurement is made on relatively short lived activities (so that the background does not build up to such high levels that the leak is masked), and a convenient means exist to concentrate the activity for counting purposes. The surface contamination and cladding diffusion will determine the sensitivity of such a leak detection system.

The principle of operation is to sample and filter a portion of the gas passing through a particular channel. The filter removes almost all solid fission product atoms, and passes the gaseous krypton and xenon fission products.

The gaseous isotopes, which decay to rubidium and cesium, respectively, are ionized and deposited on a central wire. The beta particles emitted during the subsequent decay of these two groups of isotopes provide the signal which indicates a fuel element leak. The system parameters have been reported in detail.[3]

It is important to know the relative magnitude of the activity from background contamination to that from the leak. Table 7.3 summarizes the relative activity in $d/cm^3 \cdot sec$ in gas leaving the channel of all xenon and krypton isotopes whose first daughter has a significant beta activity based upon data listed in Table 7.4. Fortunately, all of the isotopes involved decay to isotopes of Cs or Rb with half lives of 32 min or less and emit betas of 0.9 mev or greater with very few gammas.

As may be seen from Table 7.3, the ratio of the activity from the leak to the background activity is between 30 and 40 for each isotope, except for the very short lived gases (i.e., < 2 sec). Since the transient time of the sampling device will be at least 10 sec, the contribution of the short lived isotopes to the activity to be counted may be neglected.

While the effect of diffusion through the capsule wall is uncertain (since the relevant diffusion constants are not known) extrapolation of existing data suggests that it could be significant for temperatures of 1300°F and above. However, since xenon and krypton are not produced within the capsule wall, they will not diffuse through it and the diffusion process does not affect this method of leak detection.

Of the three methods of leak detection considered, gammas, neutrons, and betas, only the beta detection seems favorable. The use of betas is made practical by the concentration technique which has been developed.

The signal-to-noise ratio determines the number of channels which may be ganged to a single leak detector. Since the assumed values for the ratio of leakage activity to surface contamination gave only a value of 30 for the signal-to-noise ratio of a single channel, it is concluded that each channel should be individually sampled in order to assure positive identification of a leak. If experimental evidence should indicate that the surface contamination

---

[3] R. J. Cox and K. R. Sandiford, op. cit., p. 7.16.

TABLE 7.3

SPECIFIC ACTIVITY FROM NOBLE GASES
($d/cm^3 \cdot sec$)

Isotope	Half Life	Activity from Leak at Channel Exit	Background from Leak	Background from Surface	Remarks
Xe-131m	12.0 d	omit			Xe-131 stable
Xe-133m	2.3 d	omit			Cs-133 stable
Xe-133	5.27 d	omit			Cs-133 stable
Xe-135	9.13 hr	omit			Cs-135 long T, low β mev
Xe-137	3.9 m	omit			Cs-137 long T, low β mev
Xe-138	17 m	7.5	1.4	0.3	
Xe-139	41 s	7.7	0.0	0.3	
Xe-140	16 s	7.3	0.0	0.3	
Xe-141	1.7 s	5.3	< 0.01	0.4	
Xe-143	1 s	4.4	< 0.01	0.6	
Xe-144	1 s	6.9	< 0.01	0.9	
Kr-83m	114 m	omit			Kr-83 stable
Kr-85m	4.36 hr	omit			Rb-85 stable
Kr-85	10.27 yr	omit			Rb-85 stable
Kr-87	78 m	omit			Rb long T, low β mev
Kr-88	2.77 hr	6.3	11	0.2	
Kr-89	3.18 m	7.6	0.3	0.2	
Kr-90	33 s	11	0.06	0.3	
Kr-91	9.8 s	11	< 0.01	0.3	
Kr-92	3.0 s	12	< 0.01	0.3	
Kr-93	2.0 s	12	< 0.01	0.8	
Kr-94	1.4 s	12	< 0.01	1.2	
Kr-95	~ 1 s	11	< 0.01	1.6	
Kr-97	~ 1 s	11	< 0.01	1.6	

TABLE 7.4. ACTIVITY FROM NOBLE GASES

	T	λ	Yield	Particles γ % Mev	Particles β % Mev	ν_n (1)	$f\gamma$ (2)	$N_0 = \frac{f\gamma}{\lambda}$	νN_0 (3)	$N_L = \frac{\nu N_0}{F}$ (4)	Activity Ensuing From Leaking Channel First Cycle λN_L (5)	Equil. Sys. Contam. From Leak $\frac{\nu N_0}{V}$ (6)	Activity From Surface Contamination d/cm³·sec
Xe^{131m}	12.0 d	6.7×10^{-7}	0.0003	100 0.16		7×10^{-8}	1.1×10^{11}	1.6×10^{17}	1.1×10^{10}	5.0×10^{4}	3.4×10^{-2}		
Xe^{133m}	2.3 d	3.5×10^{-6}	0.0016	100 0.23		7×10^{-8}	6×10^{11}	1.7×10^{17}	1.2×10^{10}	5.5×10^{4}	1.9×10^{-1}		
Xe^{133}	5.27 d	1.5×10^{-6}	0.066	100 0.1	100 0.1	7×10^{-8}	2.5×10^{13}	1.7×10^{19}	1.2×10^{12}	5.5×10^{6}	8.3×10^{0}		
Xe^{135m}	15.6 min	7.4×10^{-4}	0.017	100 0.52		7×10^{-8}	6.4×10^{12}	8.7×10^{15}	6.1×10^{8}	2.8×10^{3}	2.1×10^{0}		
Xe^{135}	9.13 hr	2.1×10^{-5}	0.066		100 0.3	7×10^{-8}	2.5×10^{13}	1.2×10^{18}	8.4×10^{10}	3.8×10^{5}	8.0×10^{0}		
Xe^{137}	3.9 min	3.0×10^{-3}	0.062		100 1.33	7×10^{-8}	2.3×10^{13}	7.7×10^{15}	5.4×10^{8}	2.4×10^{3}	7.2×10^{0}		
Xe^{138}	17 min	6.8×10^{-4}	0.061		100 1.0	7×10^{-8}	2.3×10^{13}	3.4×10^{16}	2.4×10^{9}	1.1×10^{4}	7.5×10^{0}	1.4	0.27 (7)
Xe^{139}	41 sec	1.7×10^{-2}	0.063		100 1.7	7×10^{-8}	2.4×10^{13}	1.4×10^{15}	1.0×10^{8}	4.5×10^{2}	7.7×10^{0}	0.06	0.28 (7)
Xe^{140}	16 sec	4.3×10^{-2}	0.061		100 1.3	7×10^{-8}	2.3×10^{13}	5.3×10^{14}	3.7×10^{7}	1.7×10^{2}	7.3×10^{0}	0.02	0.27 (7)
Xe^{141}	1.7 sec	4.1×10^{-1}	0.046		100 2.0	7×10^{-8}	1.7×10^{13}	4.2×10^{13}	2.9×10^{6}	1.3×10^{1}	5.3×10^{0}	<0.01	0.42 (8)
Xe^{143}	1 sec	6.9×10^{-1}	0.038		100 2.3	7×10^{-8}	1.4×10^{13}	2.0×10^{13}	1.4×10^{6}	6.4×10^{0}	4.4×10^{0}	<0.01	0.58 (8)
Xe^{144}	1 sec	6.9×10^{-1}	0.058		100 1.9	7×10^{-8}	2.2×10^{13}	3.2×10^{13}	2.2×10^{6}	1.0×10^{1}	6.9×10^{0}	<0.01	0.88 (8)
											64.92		
Kr^{83m}	114 min	1.0×10^{-4}	0.005	100 0.04		1×10^{-7}	1.9×10^{12}	1.9×10^{16}	1.9×10^{9}	8.6×10^{3}	8.6×10^{-1}		
Kr^{85m}	4.36 hr	4.4×10^{-5}	0.0085	20 0.3	85 0.2	1×10^{-7}	3.2×10^{12}	7.3×10^{16}	7.3×10^{9}	3.3×10^{4}	1.5×10^{0}		
Kr^{85}	10.3 yr	2.14×10^{-9}	0.0038		100 0.23	1×10^{-7}	1.4×10^{12}	6.5×10^{20}	6.5×10^{13}	2.9×10^{8}	6.2×10^{-1}		
Kr^{87}	78 min	1.5×10^{-4}	0.027		100 1.0	1×10^{-7}	1.0×10^{13}	6.7×10^{16}	6.7×10^{9}	3.0×10^{4}	4.5×10^{0}		
Kr^{88}	2.77 hr	6.95×10^{-5}	0.0378	68 ?	100 0.3	1×10^{-7}	1.4×10^{13}	2.0×10^{17}	2.0×10^{10}	9.1×10^{4}	6.3×10^{0}	11	0.17 (7)
Kr^{89}	3.18 min	3.6×10^{-3}	0.046		100 1.3	1×10^{-7}	1.7×10^{13}	4.7×10^{15}	4.7×10^{8}	2.1×10^{3}	7.6×10^{0}	0.3	0.20 (7)
Kr^{90}	33 sec	2.1×10^{-2}	0.061		100 1.0	1×10^{-7}	2.3×10^{13}	1.1×10^{15}	1.1×10^{8}	5.0×10^{2}	1.1×10^{1}	0.06	0.25 (7)
Kr^{91}	9.8 sec	7.1×10^{-2}	0.062		100 1.2	1×10^{-7}	2.3×10^{13}	3.2×10^{14}	3.2×10^{7}	1.5×10^{2}	1.1×10^{1}	<0.01	0.30 (8)
Kr^{92}	3.0 sec	0.23	0.065		100 1.7	1×10^{-7}	2.4×10^{13}	1.1×10^{14}	1.1×10^{7}	5.0×10^{1}	1.2×10^{1}	<0.01	0.34 (8)
Kr^{93}	2.0 sec	0.35	0.069		100 2.7	1×10^{-7}	2.6×10^{13}	7.2×10^{13}	7.2×10^{6}	3.3×10^{1}	1.2×10^{1}	<0.01	0.82 (8)
Kr^{94}	1.4 sec	0.5	0.069		100 2.1	1×10^{-7}	2.6×10^{13}	5.2×10^{13}	5.2×10^{6}	2.4×10^{1}	1.2×10^{1}	<0.01	1.17 (8)
Kr^{95}	~1 sec	0.69	0.068		100 3.1	1×10^{-7}	2.5×10^{13}	3.6×10^{13}	3.6×10^{6}	1.6×10^{1}	1.1×10^{1}	<0.01	1.60 (8)
Kr^{97}	~1 sec	0.69	0.066		100 3.5	1×10^{-7}	2.5×10^{13}	3.6×10^{13}	3.6×10^{6}	1.6×10^{1}	1.1×10^{1}	<0.01	1.60 (8)
											101.38		

166.2 d/cm³·sec of Kr and Xe from leaking channel

(1) Assuming same value of ν applies to all isotopes of an element.
(2) For 700 Mw and 1 fuel capsule $2.1 \times 10^{19}\ \gamma / 5.6 \times 10^{4} = 3.74 \times 10^{14}\ \gamma$.
(3) Number per sec leaking into system $\nu N_0 \equiv \lambda N_g$.
(4) Number per cm³ ensuing from leaking channel where F is flow rate of He through channel, 2.2×10^{5} cm³/sec.
(5) d/cm³·sec of Kr and Xe from leaking channel.
(6) Equilibrium system contamination from leak where V is the system volume, 6.3×10^{4} ft³.
(7) Calculated from equilibrium activity by dividing by system volume.
(8) Calculated activity leaving channel the first time.

of the fuel is an order of magnitude lower than the assumed value of 10^{-9} g/cm^2, the background will be lower and a matrix system of sampling could be employed. The sampling manifold would be arranged to establish a grid with one set of manifolding tubes extending in the x direction and the other set in the y direction. The channel containing the leaking fuel element could be identified by comparing the indications from the x-set to those from the y-set. Thus, the number of pressure vessel penetrations would be reduced.

7.5.4 Detection System: The coolant gas flowing out of each fuel channel is sampled by means of individual sampling tubes which are terminated in the gas sampling room. Several sampling systems must be in operation simultaneously in order to provide a reasonable time interval in which to examine all of the fuel channels. Groups of gas sampling lines are connected to a channel selector valve; the gas from this valve is cooled, filtered, and piped into the gas analyzing unit. A vacuum pump, common to all analyzers, assures adequate flow, and returns the gas to one of the main coolant return ducts. The signal information from each analyzer is exhibited on separate multipoint recorders located in the gas sampling room. The occurrence of high activity in a channel is annunciated in the main control room. The faulty channel may then be connected to the spare analyzer for continuous observation, and its signal recorded on either one of two recorders in the main control room. A spare analyzer is available in the event of failure of a gas analyzer.

SECTION 8

OPERATING PROCEDURES

8. OPERATING PROCEDURES

Contents

8.1 Introduction..... 8.1

8.2 Design Load Operation..... 8.3

8.2.1 Sequence of Automatic Control Actions Following a Decrease in Load..... 8.4

8.2.2 Sequence of Automatic Control Actions Following an Increase in Load..... 8.4

8.3 Part Load Operation..... 8.5

8.3.1 Removing One Heat Exchanger Loop From Operation..... 8.5

8.3.2 Placing Stand-by Heat Exchanger Loop in Operation..... 8.7

8.4 Normal Start-up..... 8.8

8.5 Initial Start-up..... 8.12

8.6 Normal Shutdown..... 8.14

8.7 Emergency Shutdown..... 8.16

8.8 Inspection and Maintenance..... 8.17

8.8.1 Annual Shutdown..... 8.17

8.8.2 Remote Inspection of the Reactor..... 8.18

8.9 Personnel..... 8.19

8. OPERATING PROCEDURES

8.1 Introduction

A brief summary of plant operating procedures has been prepared to permit an appraisal of the operational feasibility of the proposed power plant. Many procedural details, particularly those associated with the steam plant operation, have not been included at this time, as they would not affect the general procedures outlined here. It should not be presumed that there are not acceptable means of operation other than by the procedures outlined herein, but only that these procedures represent a consistent and satisfactory operating procedure.

The procedure proposed for this plant is predicated on taking every reasonable effort to minimize unnecessary transients and excessive temperatures in the belief that system life will thus be improved. While it is possible to avoid fast transients during start-up and normal load changes, the abrupt loss of an appreciable fraction of the load will cause the most severe transient to which the system will be exposed.

Control of the plant involves balancing the heat production of the reactor with the heat extraction capabilities of the steam system at the proper flow, temperatures, and pressures in both the helium and the steam systems. The system is so large physically that its thermal capacity tends to minimize the amplitude of temperature excursions (see Table 7.1). In order to take full advantage of this thermal inertia the system blowers must be operating so as to couple the heat source (the reactor) closely to the heat sinks (the steam generators). It has been pointed out in Section 7 that if the reactor were operating at a power of 6 Mw with the blowers off, and if it is assumed that all the heat produced goes into the fuel, the fuel temperature would rise at the rate of 10°F/min. With the blowers and steam generators operating the additional heat capacity will reduce the above heating rate by a factor of 6.

It is evident that this system will be sluggish, particularly at low powers. No unique demands are imposed upon the control system under full load, but because of the increase in response times as the power level decreases, the automatic control system will probably not function well

below 20 to 40% of full load. Hence in the following procedures, manual operation is planned for powers below this range. This is considered to be quite practical, particularly in view of the sluggishness of the system as long as the helium blowers are operating. Boiler water level indication is obtained from the pressure difference between the water entering and the steam leaving the unit. This does not give an accurate indication of the water level, but will be of value when the operator is manually controlling the water flow below one-half design flow.

There are several operating conditions of general interest including start-up, design point operation and shutdown, as well as such related operating conditions as initial start-up, off-design operation, inspection and maintenance, etc. Each of these unique conditions is discussed under a separate heading. Since an appreciation of the full-load operation of the plant is helpful in understanding the objectives and constraints of the other phases, this is discussed first.

8.2 Design Load Operation

There are a number of automatic controls on the steam and gas systems which are designed to maintain the temperature of the helium and the temperature and pressure of the steam at design values during high power operation. The principal factors changing with load are the flows in the steam and helium systems. The sequence of operations for the more important controls (see Fig. 7.1) is as follows:

1. The fraction of the gas flow diverted from the reactor is controlled by the reactor inlet gas temperature: a temperature increase causes the by-pass flow to increase; a temperature decrease causes the by-pass flow to decrease. The valves in the main pipe and the bypass are linked so that when one opens the other closes.
2. The position of 4 rods is controlled by the reactor outlet gas temperature: a temperature increase causes the rods to insert; a temperature decrease causes the rods to withdraw.
3. The steam flow is controlled by the turbine load: a load increase (which tends to cause the turbine to slow down) opens the throttle valves in the steam supply to the turbines; a load decrease closes the throttle valves.

4. The boiler feed-water flow is controlled by the steam pressure: an increase in steam pressure will decrease the feed-water flow; a decrease in pressure will increase the feed-water flow.
5. A small percentage of the water flow is diverted around the boiler for desuperheating. This flow is controlled by the steam temperature at the turbine inlet: an increase in steam temperature will increase the desuperheating water flow; a decrease in steam temperature will decrease the desuperheating water flow.

With the automatic controls in operation under normal conditions at moderate power to full load, the system control will be completely automatic. The proper response time for the various controllers will ultimately be determined from analog studies but, in view of the thermal inertia, no difficulty is envisioned in this power regime in controlling any of the system parameters, i.e., steam temperatures, steam pressure, or gas inlet or outlet temperature. The steam flow is controlled by the load and it is instructive to examine the effect of changes in load in the operation of the system controls in the moderate to full-load region.

8.2.1 Sequence of Automatic Control Actions Following a Decrease in Load:

a. Turbine generators will tend to speed up.
b. The turbine governor will cause steam flow to the turbine generators to decrease by closing the steam throttle valves.
c. The pressure and temperature of the steam at the boiler outlet will tend to increase which will cause the boiler feed-water regulator to decrease the feed-water flow and the desuperheater regulator to increase the desuperheater water flow.
d. The gas temperature leaving the steam generator will increase causing more gas to bypass the reactor.
e. The exit gas temperature will increase causing the rods to insert. The helium temperatures will stabilize with the reactor power matching the new load demand.

8.2.2 Sequence of Automatic Control Actions Following an Increase in Load:

a. The turbine generator tends to slow down.
b. The turbine governor will cause the steam flow to the turbine to increase by opening the inlet throttle valves.

c. This will cause the pressure (and temperature) of the steam at the steam generator outlet to decrease which will cause the boiler feed-water regulator to increase the water flow and the desuperheater regulator to decrease the water flow to the desuperheater.

d. The gas temperature leaving the steam generator will decrease leading to a reduction in gas flow through the bypass and an increase in gas flow through the reactor.

e. The gas temperature leaving the reactor will then drop causing the rods to be withdrawn. The helium temperatures will stabilize when the power production matches the new load demand.

8.3 Part Load Operation

Although it is assumed to be a base load plant, the power station is designed so that it can be operated for extended periods of time at part load conditions. The relationship between turbine steam flow and trubine load is indicated in Fig. 8.1 (Willans Line). As described in Section 8.4, the steam generator flow may exceed the turbine steam flow at low loads because part of the steam will be bypassed directly to the condenser during start-up. While variations in load above 40% of full power will be automatically handled by the control equipment described in the preceding section, should it be necessary to maintain reduced loads for extended periods it is reasonable to consider shutting down one or more of the four heat exchanger loops. The possible power savings are indicated by a number of typical cases indicated in Table 8.1.

Loads below 75% of full load can be maintained by only three steam generators while loads below 50% of full load can be maintained by two steam generators. The following procedure is concerned with removing one loop from operation and bringing it back into operation at a later time. (The operations would be similar whether two, three, or four circuits are initially in operation.)

8.3.1 Removing One Heat Exchanger Loop from Operation:

1. Disconnect automatic control operators on the helium by-pass valve and on the steam generator in the circuit to be removed from operation.

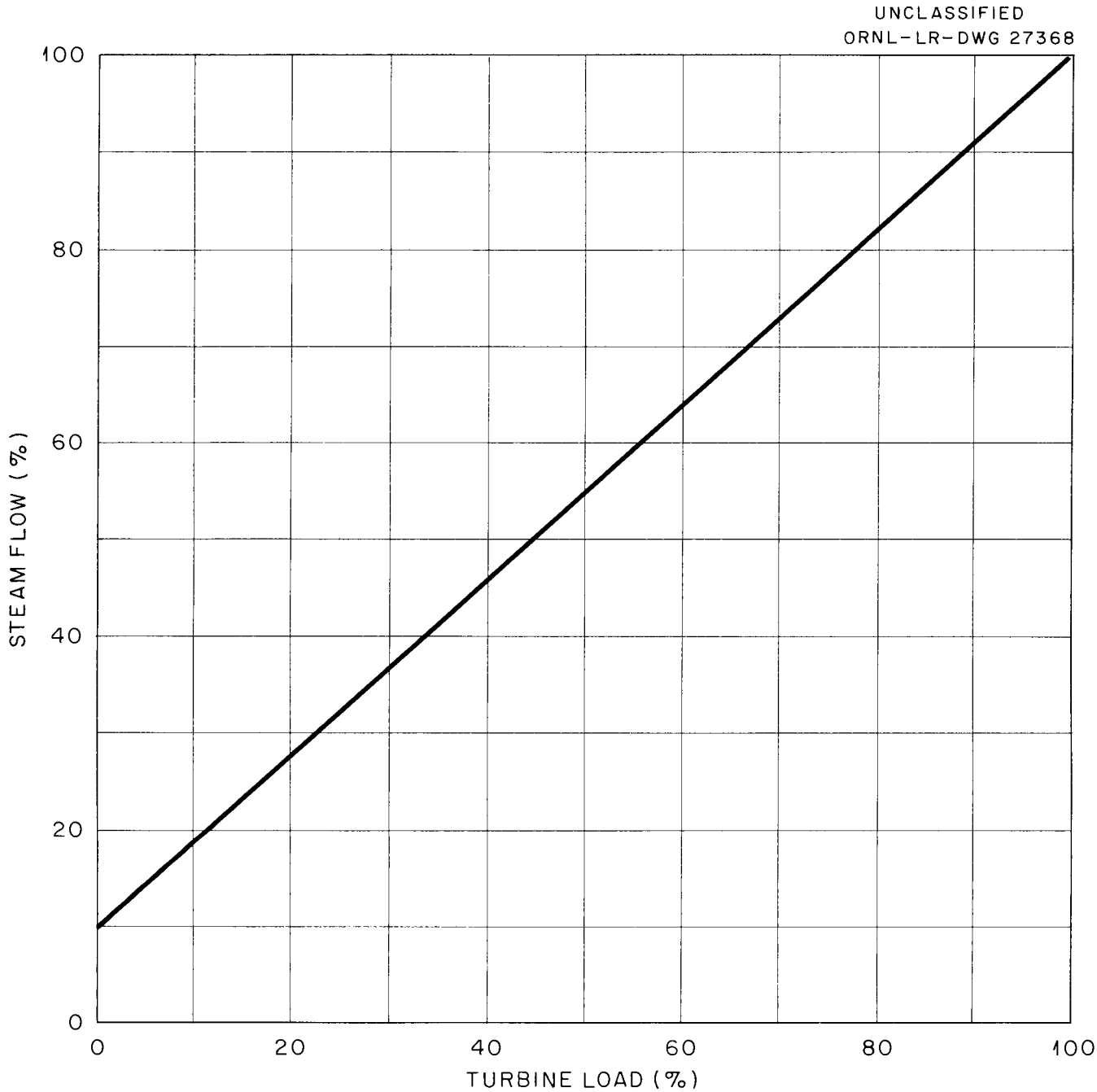

Fig. 8.1. Relationship Between Turbine Load and Steam Flow (Willans Line).

TABLE 8.1

REACTOR PLANT OPERATING CONDITIONS AT VARIOUS LOADS

Net Electrical Output-% of Full Load	100	75	75	50	50	50
Helium flow total, %	100	79.7	77.6	59.6	57.6	55.6
Blowers operating	4	4	3	4	3	2
Reactor power-Mw(T)	700	558	544	418	403	390
Gross electrical output-Mw	252	195	190	138	133	128
Net electrical output-Mw	225	169	169	113	113	113
Power to blowers-Mw	18	18	13.5	18	13.5	9
Power to blowers-% gross electrical output	7.9	10.6	7.1	13.0	10.1	7.0
Helium by-pass flow, %	0	25	0	50	33 1/3	0
Helium flow, % total	100	79.7	77.6	59.6	57.6	55.6
Hot helium Temp, °F	1000	1000	1000	1000	1000	1000
Cold helium Temp, °F	450	450	450	450	450	450
Boiler feed-water flow-%	100	79.7	77.6	59.6	57.6	55.6
Steam pressure-psia	950	950	950	950	950	950
Steam temperature-°F	950	950	950	950	950	950
Steam flow-%	100	79.7	77.6	59.6	57.6	55.6

2. Gradually reduce the flow to the reactor from that circuit and open the helium bypass until no gas from the reactor flows through that steam generator (the automatic controls on the remaining steam generator circuits will cause them to pick up the load). The water flow to the boiler being taken out of operation must be reduced manually to maintain the temperature of the exit gas and to keep the water level in the boiler between 1/4 and 1/2 full.
3. Shut off the blower and one of the two boiler feed pumps for that steam generator.
4. When the helium flow stops completely, the required water flow will drop to zero. The outlet steam valve should then be closed and the individual steam pressure relief valve for that steam generator set to 680 psia(the steam pressure corresponding to a saturated steam temperature of 500°F). The water level should be checked periodically to be certain the boiler does not run dry.

One heat exchanger loop will then be in stand-by condition. When it is desired to place this system back in operation, the procedure is as follows:

8.3.2 Placing Stand-by Heat Exchanger Loop in Operation:

1. Raise the setting on the pressure relief valve to 950 psia and open the block valve in the line to the turbine.
2. Start up the boiler feed pump.
3. Start up the blower with 100% bypass.
4. Manually open the block valve in the helium pipe to the reactor slightly to allow a small amount of helium from the reactor to flow through the steam generator so that it will gradually heat up to design conditions. The feed-water flow should be controlled manually to maintain the temperature of the helium entering the blower.
5. Gradually decrease the helium by-pass flow so as to obtain the same conditions in all of the operating circuits. The water flow will have to be increased manually as required to maintain the gas temperature and the water level. Note that

as this by-pass flow is decreased, the by-pass flow in the other loops which are under automatic control will increase; this will continue until they all arrive at the same value.

6. Transfer the control of the gas bypass and the boiler feed-water to automatic controllers.

8.4 Normal Start-up

A normal start-up is defined as a routine start-up after extended operation with no need for cleanup of the graphite, purification of the helium, cleanup of the steam system, critical experiments, rod calibrations, etc.

Inasmuch as the automatic system controls, i.e., by-pass gas flow, control rod, boiler feed water, and boiler desuperheater flow will probably not function satisfactorily at low powers (i.e., less than 20 to 40% design), these controls are all disconnected from their automatic controllers. (This should be the situation as a consequence of the previous shutdown.)

It is important to note that the automatic controls associated with one steam generator will function properly when its power production is 20 to 40% of its design value. Therefore, as there are four steam generators, any one would become controllable at 5 to 10% of design output for the plant if the other steam generators were not in operation. The situation is different at the reactor as the control of reactor outlet temperature will probably not respond properly to the automatic controller at reactor powers less than 20 to 40% of full design load. Utilizing these features of the system, it is proposed to start up the four steam generator circuits one at a time. When an adequate load is available (a minimum of 10% of plant design per circuit), other circuits may be placed in operation following the procedures described in the preceding sections. The reactor helium outlet temperature will, however, be manually controlled by rod position until the total reactor power is up to 20 to 40% of full load. System conditions corresponding to the various steps in the start-up are given in Table 8.2. The normal start-up procedure would be as follows:

1. Pressurize the gas system with helium to ~100 psia. (This pressure is calaulated so that the pressure will be somewhat less than 300 psia when the system reaches the design temperature.) Close the valve to the helium supply system.

TABLE 8.2

HELIUM AND STEAM CONDITIONS DURING NORMAL START-UP*

Parameters	Step. No. 1 – 6	7	8 – 9	10 – 11	12	18
Helium through flow reactor (% design)	25	12-1/2	12-1/2	12-1/2	12-1/2	50
Helium pressure, psia	100		increasing →			300
Blowers operating	1	1	1	1	1	4
Amount of helium bypassed (per operating loop), %	0	50	50	50	50	50
Hot helium temperature, °F	480	510	570	490	1000	1000
Cold helium temperature, °F	450	450	450	450	450	450
Position of control rods			increasing withdrawal →			
Boiler feed-water flow, lb/sec	10	10+	20	20-	90	360
Steam pressure, psia	500	500	500	550	950	950
Steam flow, lb/sec	10	10+	20	20-	90	360
Steam temp., °F	470	470	470+	480+	950	950
Reactor power, Mw	10	10	20	20	90	350

*All values approximate for illustrative purposes only.

2. Close the steam generator outlet steam valve and fill the steam generator half full of water (the differential pressure level indicator and the vent valve are employed in this operation). Close the valve to the water system.
3. Set the pressure relief valve to dump steam to the condensers at a pressure of 500 psia. This corresponds to a saturated steam temperature of 470°F.)
4. Start up one blower and set its by-pass helium flow valves to by-pass 0%. It is noted that each blower at design speed puts about 4 Mw into the helium so that the system temperature will start to increase.
5. Bring the reactor critical and increase the power to 5–10 Mw as indicated by the nuclear instrumentation. (With the helium blowers coupling the reactor and steam generator, this will cause the system temperature to rise at a rate of less than 1°F/min. Since the system heat loss is less than 1 Mw at design temperature, a heat production of greater than 1 Mw with no other heat loss would cause the system temperature to rise eventually to considerably above the design values.)
6. As the system temperature increases, steam will be generated which will pass to the condenser when the pressure reaches 500 psia. The water in the boiler will then be evaporated by the 9 Mw power input (i.e., 10 Mw produced -1 Mw heat losses) at a rate of ~5000 gal/hr. Therefore, add water to the boiler manually as required to maintain the water level in the steam generator between 1/4 and 1/2 full.
7. Gradually reduce the helium flow to 50% of the design value in the operating loop by opening the bypass while at the same time increasing the feed-water flow as required to hold the helium inlet temperature to the reactor at 460°F.
8. Withdraw the rods as required to increase the power to 20 Mw. This will raise the outlet temperature of the reactor about 60°F. The rate of rod withdrawal should be adjusted so that the rate of temperature increase does not exceed 5°F/min.
9. Now increase the water flow rate as required to maintain the cold helium temperature at 460°F. (Neither of these manual operations,

steps 8 and 9, should proceed rapidly nor should both be allowed to occur simultaneously. There will undoubtedly be some over-shooting or under-shooting in one circuit as a consequence of a change in the other, but because of the large thermal inertia of the system such transients are slow and quite tolerable. As the operators become more experienced and more familiar with the transient behavior of the system, these operations may be speeded up.)

Note that as the hot helium temperature exceeds the steam temperature by progressively greater amounts, the steam will become superheated. Superheated steam is indicated in Table 8.2 by a plus (+) after the saturated temperature. It is desirable to allow the steam to become superheated to at least 100°F above the saturation temperature. As this condition is achieved by the repetition of steps 8 and 9, the steam pressure may then be increased. Furthermore, as the water flow is increased as a consequence of steps 8 and 9 the water level will also rise. Raising the steam pressure will also increase the water level as well as decrease the inlet helium temperature so that the water flow will have to be reduced. Therefore:

10. Slowly increase the steam pressure by adjusting the pressure relief valve. This will cause the water level to rise and the reactor inlet helium temperature to decrease.
11. Reduce the water flow as required to maintain the helium inlet temperature at 460°F.
12. Steps 8 and 9 are now repeated and should be alternated with steps 10 and 11 until a helium temperature of 1000°F and a steam pressure of 950 psi are attained. Since the gas flow was 50% of one boiler, this corresponds to ~90 Mw.
13. The rods may be placed on automatic control tc hold the temperature of the helium leaving the reactor at 1000°F when the reactor power is greater than 40% of design power.
14. Place feed-water flow on automatic control to hold the boiler steam outlet pressure at 950 psia.
15. Place helium flow on automatic control to hold the temperature of the helium return to the reactor at 460°F.
16. Place desuperheater flow on automatic control to hold the boiler steam outlet temperature at 950°F.

17. Adjust helium pressure, if necessary, to 300 psia.
18. The three other loops may be placed in operation following the procedures outlined in the preceding section on part load operation. Note that at this time the rod is on manual control and will not be placed on automatic control until the reactor power is ~40% design.
19. Start turbine, increase speed, synchronize and increase generator load.
20. Put turbine on load control.
21. Shut off steam dumping to condenser.

8.5 Initial Start-up

The initial start-up of the plant is complicated by problems associated with cleaning and shaking down the system. Since there will be no large auxiliary source of steam at the plant site, neither the steam nor the gas system temperature can be increased until the reactor can be placed in operation as a heat source. Although the many detailed checks that need to be performed on the system when it is first heated will not be listed here, it is imperative that the high-pressure steam piping be "blown-down", and that the graphite be "baked-out". The initial start-up will also involve the usual nuclear problems of the critical loading, calibration of rods and instruments and measurement of the pertinent nuclear parameters of the system. Some of these procedures may have to be repeated at other times, as for example, after the gas system is opened to air. Preparatory to the initial start-up, the system will be checked out as much as possible at room temperature. The initial start-up may then be carried out by the following procedure:

1. Install the neutron source in the reactor and begin recording the count rate. If the nuclear instrumentation provided for power operation cannot sense this source adequately, additional instruments can be provided inside the pressure vessel.
2. Load fuel starting from the center with the rods completely inserted until 90% of the calculated critical mass is installed in the reactor. Record the counting rate at regular intervals.
3. Add additional fuel to the reactor and after each addition, withdraw the rods and record the counting rate at several positions; then fully insert the rods before adding additional fuel. The approach to criticality can then be predicted accurately.

4. Take the reactor critical and hold at a power level of a few watts.
5. Calibrate the rods using the in-hour relationship.
6. Add additional fuel to the reactor to provide the desired excess k, i. e., ~14.5% $\Delta k/k$.
7. Shut down the reactor.
8. Operate all four blowers at design speed. Since the density of atmospheric air is about the same as the operating helium density, the power input to the air from the blowers will be the same, i.e., 15 Mw.
9. The system will heat up at a rate of approximately 1°F/min and the system pressure should be reduced at such a rate as to permit the system temperature to level off at approximately 500°F.
10. The system should be operated in this condition until the point of diminishing returns is reached as determined by the rate of pressure rise when pumping is stopped.
11. Evacuate the gas system in order to remove the air and the occluded gases from the graphite. Continue evacuating the system until the point of diminishing returns is reached as determined by the rate of system pressure rise when the pumping is stopped.
12. Stop the blowers and fill the system with helium to ~100 psia.
13. Recheck the operation of mechanical components of the system, i.e., blowers, valves, etc.
14. The rod, boiler feed water, and helium by-pass flows should be on manual control.
15. Fill the steam generators half full of water and close the isolation valves.
16. Set the pressure relief valves on the steam generators for 500 psig, a value corresponding to a saturated steam temperature of 470°F.
17. Set all by-pass valves at 0% bypass.
18. Turn all blowers on. The heat input from the blowers will cause the system temperature to rise.

19. Set the by-pass boiler water supply valve to control the water level.[1] Since the temperature to which the system is to be heated in this step is ~ 470 °F and the steam valve is set for 500 psig there should be some steam flow because of the heat input from the blowers.
20. The system should be allowed to bake-out at this temperature. (It is estimated that about one half of the residual gases occluded in the graphite will evolve at this temperature after 50 hr.)
21. Open the steam line and blow it out. If there is not sufficient steam to obtain a good purge at this time, this step may have to be repeated at a higher power. In any event the boiler must not be allowed to run dry.
22. With this bake-out at 450°F the steps in the procedure unique to the initial start-up are completed, the reactor may be brought critical, and further increase in pressure and temperature to design conditions can then be carried out as described in the preceding section. It should be noted that gases will continue to evolve from the graphite, though in decreasing quantities, as the temperature is increased. The contamination of the gas should be closely monitored while the system temperature is raised as this may indicate difficulties such as leaks and require a more gradual approach to power than might otherwise be possible.

8.6 Normal Shutdown

A normal shutdown is defined as one that is planned in advance and throughout which all process equipment is operative and available. The occasion may be a routine inspection, fuel charging, removal of a defective fuel element, etc. In such an event the load (turbine and/or condenser) will

---

[1] It is assumed here that the boiler feed-water control valves will not operate satisfactorily at the low flow rates required by the removal of after-heat so that the by-pass valves herein referred to would be required for this purpose. Should the feed-water control valves be adequate the by-pass valves would be unnecessary.

be removed gradually so as to minimize the thermal transients to which the system would otherwise be subjected.

1. The turbine load should be reduced to below 50% of design and the helium by-pass flow controllers transferred to manual control.
2. The turbine load should then be reduced gradually to zero and simultaneously the manual bypass to the condensers should be opened and set to maintain a steam pressure of 950 psia.
3. The control rod should then be switched from automatic to manual control.
4. All but one of the heat exchanger circuits should now be taken out of operation (as described in the section on Part Load Operation). The remaining steam generator circuit should be operating at about 50% load with its boiler still under automatic control. The reactor power should be about 90 Mw(T) and the pressures and temperatures of the helium and the operating steam system at design values.
5. Switch the boiler feed water from automatic to manual control.
6. Slowly insert the rods a few inches, after which the water flow should be reduced gradually as required to maintain the reactor helium inlet temperature at 460°F.
7. At some point it may not be possible to raise the helium inlet temperature to 460°F without allowing the water level to drop below the minimum level. As this condition is approached, the steam pressure maintained by the by-pass controller to the condenser will have to be reduced to enable the steam system to dump enough reactor heat at the lower temperature level.
8. Slowly reduce the steam pressure, increasing the water flow as required to maintain the reactor helium inlet temperature at 460°F.
9. Steps 6, 7, and 8 should be repeated as required to bring the reactor outlet temperature down to 500°F.
10. The rods may be fully inserted, shutting down the reactor when the helium inlet and outlet temperatures are within 100°F of each other.
11. A heat dump will have to be kept in operation to remove the system afterheat. For this purpose one blower may be kept in operation with

a fixed bypass and the feed-water control turned over to a water flow controller operated from the differential pressure measurement on the boiler water. The steam may be dumped to the condenser or blown off.

12. Should it be desired to take the blower out of operation, this may be done but all bypasses would have to be closed (to permit thermal convection circulation) and the feed-water flow to all four boilers would have to be placed under level control.

8.7 Emergency Shutdown

The reactor will have no automatic emergency fast rod insertion above 10 Mw but the operator may initiate a fast rod insertion should he judge that a situation warrants it; for example, in the event of a major system leak. For the emergency situation considered here, it is assumed that all equipment is operative. Situations in which one or more component failures are experienced will involve changes in this basic procedure.

1. The operator may decide that the system must be shut down quickly and will activate a seal-in type emergency circuit. Actuation of this circuit automatically does the following:
   a. inserts rods at the rate of 0.10% Δk/sec,
   b. closes steam lines to the turbine generators,
   c. opens circuit breakers connecting the electric generators to the transmission system,
   d. sets the by-pass steam relief valve to the condensers to dump steam at 950 psia,
   e. switches the helium by-pass valves from automatic control, and sets the valves to zero per cent bypass,
   f. stops all four blowers,
   g. removes the normal boiler feed-water control valves from automatic control and closes them, and simultaneously actuates the by-pass water valves controlled from the differential pressure measurement on the steam generator.

2. These actions occurring simultaneously do the following:
   a. Inserting the rods reduces the temperature and power level of the reactor. This will reduce the pressure of the steam and the temperature of the inlet helium to the reactor so that if the boiler feed water and by-pass helium flow were to remain on their respective automatic controls, the water flow would increase and the percentage of gas bypassed would decrease.
   b-d. The transfer of the load from the turbines to the condensers reduces the steam consumption so that the steam generator outlet pressure will tend to increase with the result that the effect on the by-pass gas flow and boiler feed-water flow would tend to oppose the results of "a".
   e-g. The helium by-pass valves and the boiler feed-water valves are removed from normal automatic control and positioned so that the system is capable of removing the afterheat.

The system is of course subjected to severe transients in such a sequence. Should analog studies indicate that the transients are too severe, appropriate time constants will be introduced into the sequence. This type of shutdown is clearly an emergency; at all other times the system would be shutdown by the normal procedures in which the transients are relatively mild.

8.8 Inspection and Maintenance

8.8.1 Annual Shutdown: It is standard practice in steam power plants to accomplish as much repair work as possible during scheduled or forced shutdowns. The former usually take place once each year during periods when system operations are least affected by the outage of a unit and commonly require ten days to two weeks. Since fuel rearrangement and replacement will require about two weeks, it is proposed to schedule a single annual shutdown for fuel charging operations, inspection, and preventive maintenance on the turbine-generator plant. This procedure eliminates the need of fuel loading and unloading during operation except in the event of a fuel element leak which with the proposed fuel handling equipment, will require that the gas system be depressurized before the defective fuel element can be removed. Although the number of fuel elements is large, it does not appear at this time that fuel element failures will be frequent and the plant has been designed accordingly.

This will also provide an opportunity for inspection of the helium blower units. Tennessee Valley Authority operating personnel have stressed the advisability of inspection of motors periodically before a major failure occurs. Since the large valves on the 60-in. helium pipes and the smaller valves on the by-pass pipes to the heat exchanger are constantly in operation, inspection of these units would be scheduled for this period.

The steam generators should be inspected also to the extent that the tube matrix is accessible for inspection, and it would probably be well to test it hydrostatically during this inspection. The graphite must also be inspected with TV cameras and removable specimens should probably be provided during the original construction. A fuel loading outage would also allow servicing of control rod mechanisms and flux monitors.

8.8.2 Remote Inspection of the Reactor: Once assembled and operated, the graphite core of the reactor, and in particular, any fuel channel through the graphite, is inaccessible for direct inspection. It is not realistic to assume that such a system will operate for many years without incident.

Failure of some of the 67,074 fuel capsules must be expected. Distortion of the vertical channels as a result of Wigner growth in the graphite or thermal effects will certainly occur to some extent. One of the most troublesome consequences of these effects could be some difficulty in removing fuel elements by routine methods. Special grappling tools can be made up and lowered through the charging chute, but such an operation becomes pure guess work without visual knowledge of the situation. For this purpose a remote television inspection camera will be provided which can be lowered down the charging chute to inspect any region of the core. Preliminary investigation has shown that such a camera can be built within a 3-in.-dia cylindrical envelope. This camera which would be lowered using the charge chute would contain a light source, lense, vidicon tube, and preamplifier. The balance of the circuitry would be located externally at the viewing console. The coaxial cable from camera to console would be 5/8 in. dia. Full travel of the camera vertically would be about 60 ft and provisions should be made to take up or let out the coaxial cable without winding it on a drum which would require collector rings, an unsatisfactory method for signal transmission.

A further limitation exists in the form of a minimum bending radius for the coaxial cable. This is expected to be 6 in. or larger.

The camera can be designed to accommodate standard 16 mm movie camera lenses, making possible the use of standard telescopic, wide angle, or other lens systems as required. Remote focusing can be provided in the available space and lateral viewing for inspection of the graphite channel walls could be accomplished by attaching a mirror or prism system in front of the lens. Inspection of the helium inlet plenum region below the graphite support plate can be carried out by lowering the camera to the bottom of any unorificed graphite channel. The additional illumination required could be provided through an adjacent channel.

The camera system can be built to tolerate the after-shutdown gamma dose but darkening of lens glass is certain to result from prolonged exposure. More data are required on this problem. The vidicon tube must be protected against high temperatures. Present industry standards for standard vidicon tubes specify 125°F as the maximum ambient for continuous operation. It is probable that this figure could be increased for this application by development of a more temperature resistant tube and by accepting reduced tube service life.

8.9 Personnel

The approximate number of personnel required for the ORNL GCR-2 plant has been determined by constructing a suggested operating organization chart (see Table 8.3). This chart is developed on the basis of craft union maintenance and the control of both turbine-generator units, reactor, and outgoing transmission lines from a centralized plant control room. Items requiring regulation and adjustment during operation can be operated remotely from the unit control room. It is assumed that two operators would be required for each shift for the condenser water intake structure and the treatment plant. Because of the possible radiation hazard to unauthorized persons entering the building without escort, it is believed that control of entering personnel must be exercised on a 7 day/week, around-the-clock basis.

TABLE 8.3

GAS-COOLED REACTOR POWER PLANT ORGANIZATION CHART

PLANT SUPERINTENDENT	1
ASSISTANT SUPERINTENDENT	1

ADMINISTRATIVE		MAINTENANCE		OPERATING		ENGINEERING	
Administrative officer	1	Maintenance supervisor	1	Shift engineers	5	Supervisor	1
Payroll, clerical, stores*	12	Electricians	5	Assistant shift engineers	4	Performance, test, records	
Janitors	2	Machinists	5	Unit operators	13	Physicist	1
Public safety	6	Boilermakers	2	Assistant unit operators	9	Engineer	1
Grounds maintenance	1	Steamfitters	5	Intake structure and water treatment	9	Statistician	1
TOTAL	22	Painter	1	TOTAL	40	Instrument maintenance	2
		Carpenter	1			Chemical water treatment	6
		Laborers or helpers	3			Health physicist	1
		Other crafts	3			TOTAL	13
		TOTAL	26				

Total estimated staff = 101

*Stores personnel will also handle fuel element storage and accountability.

It is assumed that the unit control room will be manned by a supervisor and three unit operators: one who would be responsible for the reactor control and one for each of the two turbine-generator control stations. An assistant operator for each turbine-generator unit would be scheduled also to check physically the major items of operating equipment at intervals and record data as well as to perform certain manual operations such as occasional adjustment of feed-water chemical feed equipment, blowing out instrument and station air moisture separators, cleaning raw water pump strainers, perhaps occasional radiation monitoring duties, regeneration of the condensate demineralizers, and adjusting evaporator blowdown and deaerator vents.

In the engineering organization, allowance is made for full shift coverage by a chemical technician for feed-water control. It is assumed that the services of a professional health physicist would be required only on the day shift, while operators trained in the use of radiation monitoring equipment would be expected to be on the alert for unusual situations during routine operation on the evening and midnight shifts. Instrument maintenance personnel are scheduled only on day shift as in conventional plants. This is in keeping with operating practice at the ORNL graphite reactor.

Since many of the characteristics of the reactor after prolonged operation cannot be predicted at this time, the uncertainties in requirements for the maintenance staff are believed to be the largest. As can be seen from Table 8.3, a maintenance force of 26 craftsmen and supervisors is suggested.

In the administrative group, the number of personnel is somewhat dependent on the division of work between the plant personnel and the central office of the operating organization. The number of janitors may have to be increased in the event that the decontamination work load becomes more severe than presently anticipated.

SECTION 9

STEAM SYSTEM

9. STEAM SYSTEM

Contents

9.1 Design Specifications 9.1

9.2 Steam Cycle 9.2

9.3 Stages of Feed Heating 9.2

9.4 Steam Generator 9.5

9.4.1 Factors Affecting the Design 9.5

9.4.2 Design Calculations 9.9

9.4.3 Determination of Operating Steam Conditions 9.22

9.4.4 Vessel Diameter and Tube Matrix: Vessel Diameter 9.33

9.4.5 Additional Design Considerations: Generator Tubes 9.37

9.4.6 Insulation Optimization Data 9.42

9.4.7 Data for Steam Generator 9.45

9.4.8 Heat Transfer and Pressure Drop Equations - Cost Data: Heat Transfer 9.49

9.5 Feed Water Purity and Condenser Integrity 9.63

9. STEAM SYSTEM

9.1 Design Specification

As in the rest of the power plant, the first consideration in the design of the steam system was to employ the simplest and most reliable arrangement consistent with the production of low-cost power. Optimization studies were limited to the investigation of major parameters only, the primary objective being to obtain a well-balanced system to produce near minimum cost power. Although it was recognized that some improvement in over-all thermal efficiency might be obtained through the use of a dual pressure or a reheat cycle, it was decided that the small possible gains would be more than offset by the required additional complexities in the system. Thus, a simple steam cycle was chosen with sufficient superheat to permit expansion through a single turbine with no reheat and with no more than 12% moisture in the steam leaving the turbine. In this way the limited time and engineering effort available were conserved for work on the reactor rather than expended on optimization studies of the many possible minor variations in reheat arrangements. The use of regeneration by feed water heating with bleed-off steam is, of course, advantageous. However, higher feed water inlet temperatures to the heat exchanger conflict with the necessity of returning the helium coolant to the reactor at low temperature in order to minimize the power required to circulate the helium.

The principal problem in the design of the steam system was to match the steam and helium circuits to yield minimum power costs with the 1000°F to 460°F temperature range chosen for the reactor coolant. Power plant control considerations indicated that the steam temperature should approach the gas temperature within 50 to 100°F to minimize temperature cycling between full and part load operation. Minimum capital costs for the steam generators, on the other hand, would be obtained with much larger temperature differences between the helium and the steam. While steam-turbine costs increase slightly, condenser costs would be reduced by designing for the highest steam temperature obtainable with the 1000°F helium temperature.

In a study of such short duration, it was not possible to optimize the design in every way.

9.2 Steam Cycle

The heat balance diagram is given in Fig. 9.1. Steam is generated at 950 psia and 950°F in four steam generators, each of which has a capacity of 505,500 lb of steam per hour. The turbine generator plant consists of two identical units of 125,800 kw capacity each. The steam piping is cross-connected so that steam from any steam generator can be supplied to either turbine generator unit. Similar cross connections are provided in the feed water piping to the steam generators.

Three stages of regenerative feed water heating are employed in the design cycle. Feed water is supplied to the steam generators at a temperature of 325°F. The first and third stage feed water heaters are closed type heaters utilizing extraction steam from the turbine. The second stage of feed water heating serves also as the deaerating unit, and is a direct-contact-type heater utilizing extraction steam from the turbine. When the load on the turbine is reduced to the point that the pressure at the second extraction point is not sufficient to provide a temperature at the deaerator of 250°F, an additional supply of steam from the main steam line is provided through a reducing valve.

Makeup for water losses in the steam system is obtained from a supply of softened water which is evaporated and supplied as vapor to the deaerator. The evaporator coil steam supply is from the same turbine extraction point as the highest pressure feed water heater. The condensate from the coil drain is also returned to the deaerating heater.

9.3 Stages of Feed Heating

The final steam conditions of 950 psia and 950°F were chosen to give a 50°F difference between the helium and the steam at the top of the steam generator, and a 20°F minimum difference in the boiler region, that is, where the feed water reaches boiling temperature. The choice of these temperatures is discussed in Section 9.4.3. A brief study indicated that three stages of feed water heaters were close to the optimum for the final

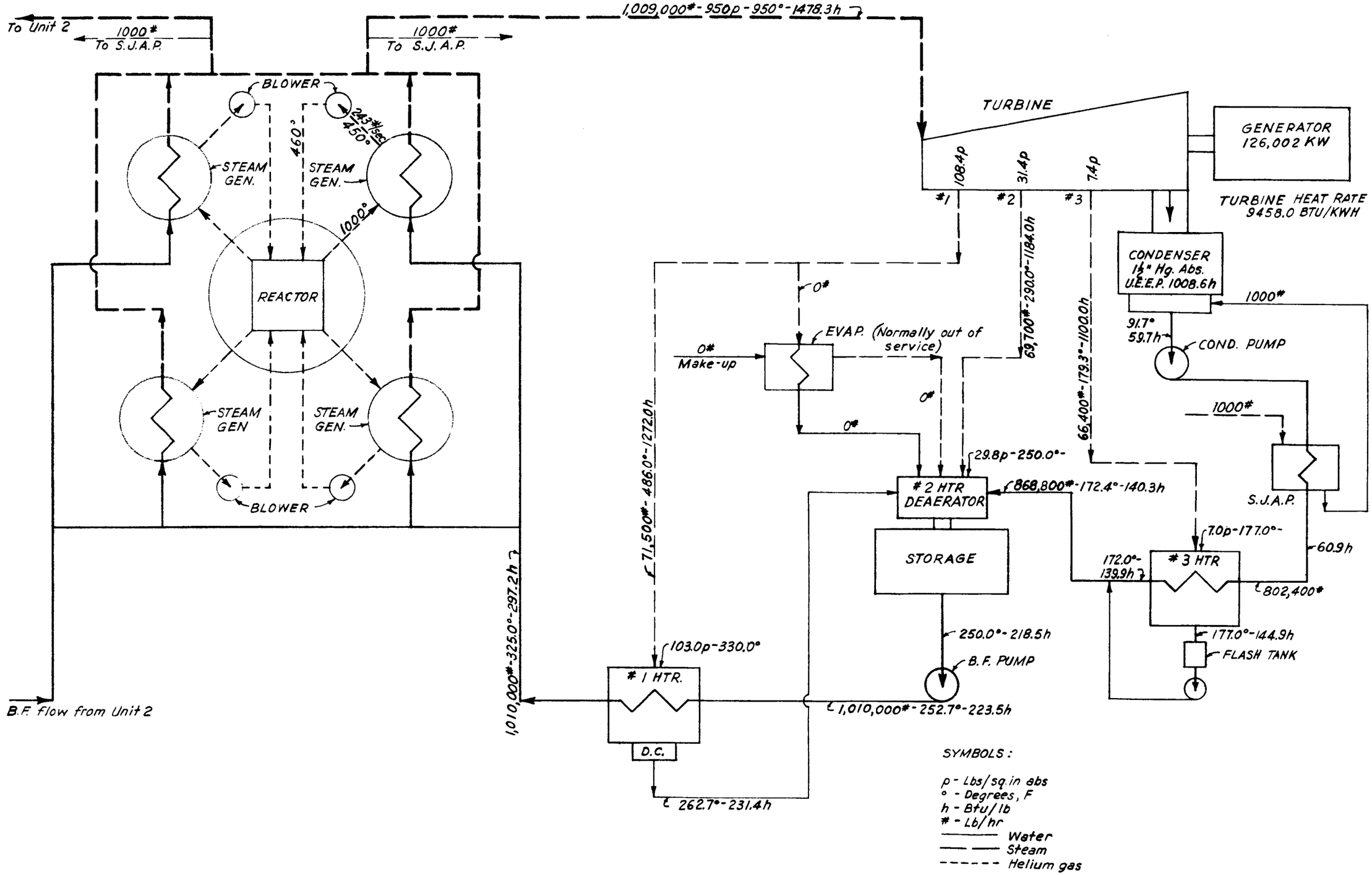

Fig. 9.1. GCR-2 Heat Balance Diagram (Design Div., Tennessee Valley Authority).

steam conditions. As can be seen in Fig. 9.2, the largest part of the maximum potential increase in steam cycle efficiency for 325°F feed water temperature is realized by the use of three feed water heaters.

9.4 Steam Generator

The steam generator design was basically concerned with the determination of the steam conditions for the plant, the determination of the number and size of the steam generator units, and a suitable tube configuration for the unit. The maximum temperature to which any section of the steam generator unit will be subjected is 1000°F. There will be no danger of hot spots in the unit. The gas-side of the unit will be clean in contrast with a conventional boiler for a coal-fired power plant where sooting up, slagging, hot spots, tube burnout and temperatures of 2000 to 3000°F must be considered in the design. Outside surface corrosion of the heat exchanger tubes which occurs in coal-fired plants will not occur in the reactor power plant. British experience has shown that after a year of operation the interior of the boilers at Calder Hall looked as clean as the day they were installed.

9.4.1 Factors Affecting the Design: The steam generator design has been discussed with engineers of several boiler manufacturers. A complete optimization of the steam generator unit could not be carried out in the time available for this study because many parameters which affect the detailed steam generator design can only be determined from an over-all system design. The important steam generator parameters are:

1. Helium inlet temperature
2. Helium exit temperature
3. Helium pressure
4. Water inlet temperature
5. Steam exit temperature
6. Steam exit pressure
7. Tube diameters
8. Fin sizes and thicknesses
9. Vessel diameter
10. Tube materials
11. Gas mass velocity
12. Gas pressure drop

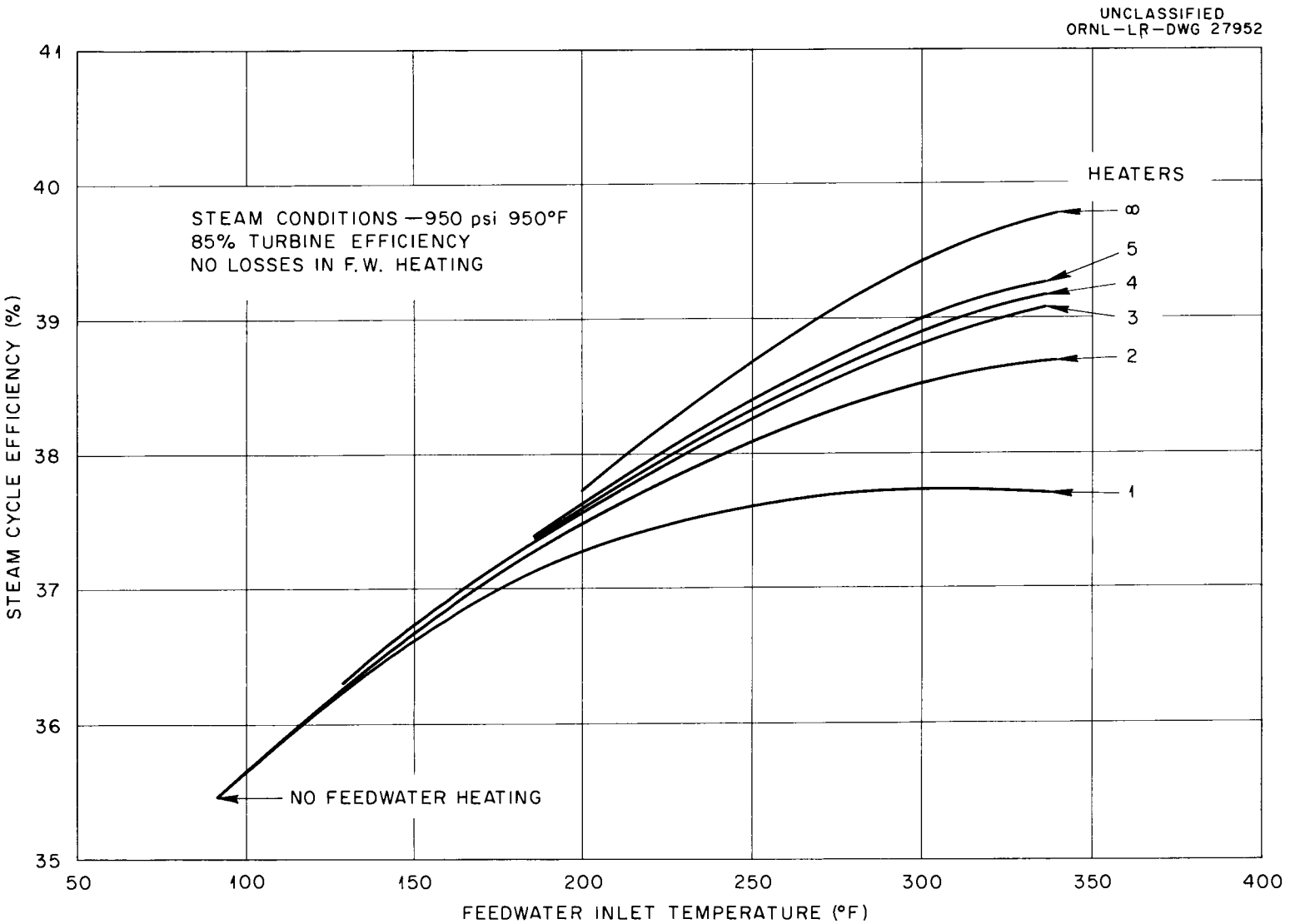

Feedwater Inlet Temperature vs Steam Cycle Efficiency for Various Numbers of Feedwater Heaters.

Fig. 9.2. Effect of Number of Feed-Water Heaters on Feed-Water Enthalpy.

13. Water pressure drop
14. Tubing, vessel, and pumping costs
15. Matrix arrangement of tube bundle and steam flow path
16. Effects of exit steam conditions on plant thermal efficiency
17. Maintenance requirements

Although the operating temperature and pressure of the helium system affect the steam generator performance, preliminary studies showed that reactor costs were dominant and hence the helium temperature and pressure were determined as discussed in Sections 5 and 6. A study which was made of the effect of vessel diameter on heat exchanger performance and cost is included in Section 9.4.4.

The most serious problem in optimizing the heat exchanger has been the lack of material and fabrication cost data. The detailed cost data utilized in the design of the steam generator are given in Section 9.4.8.

Because of its inherent simplicity and compatibility with the reactor system, it was decided to utilize a once-through monotube steam generator design as shown in Fig. 9.3. This choice eliminates the need for a large number of steam generator shell penetrations and should result in a low cost unit.

A serpentine coil with extended surfaces on the tubing is specified for the economizer and boiler section and a bare tube for the superheater section. This choice is based on the ratios of inside to outside heat transfer coefficients (steam-side to gas-side) which are large in the economizer and boiler section and small in the superheater sections. Preliminary cost information indicated that a savings in the fabricated tube bundle could be achieved by employing extended surfaces since the major portion of the tube bundle cost is fabrication cost rather than material cost. The difference in bare-tube vs extended-surface fabrication costs is small. Thus, although the efficiency of the extended surface is only about 40%, the effective additional surface per dollar has been increased. The cost of fabricating a typical tube bundle with 2.0-in. bare tube is estimated to be $5.21 per ft of tube as compared to $7.79 per ft for 1.75-in. extended-surface tubing. After taking account of all factors, such as surface area and effectiveness, the extended-surface tubing is approximately 40% cheaper. This advantage is

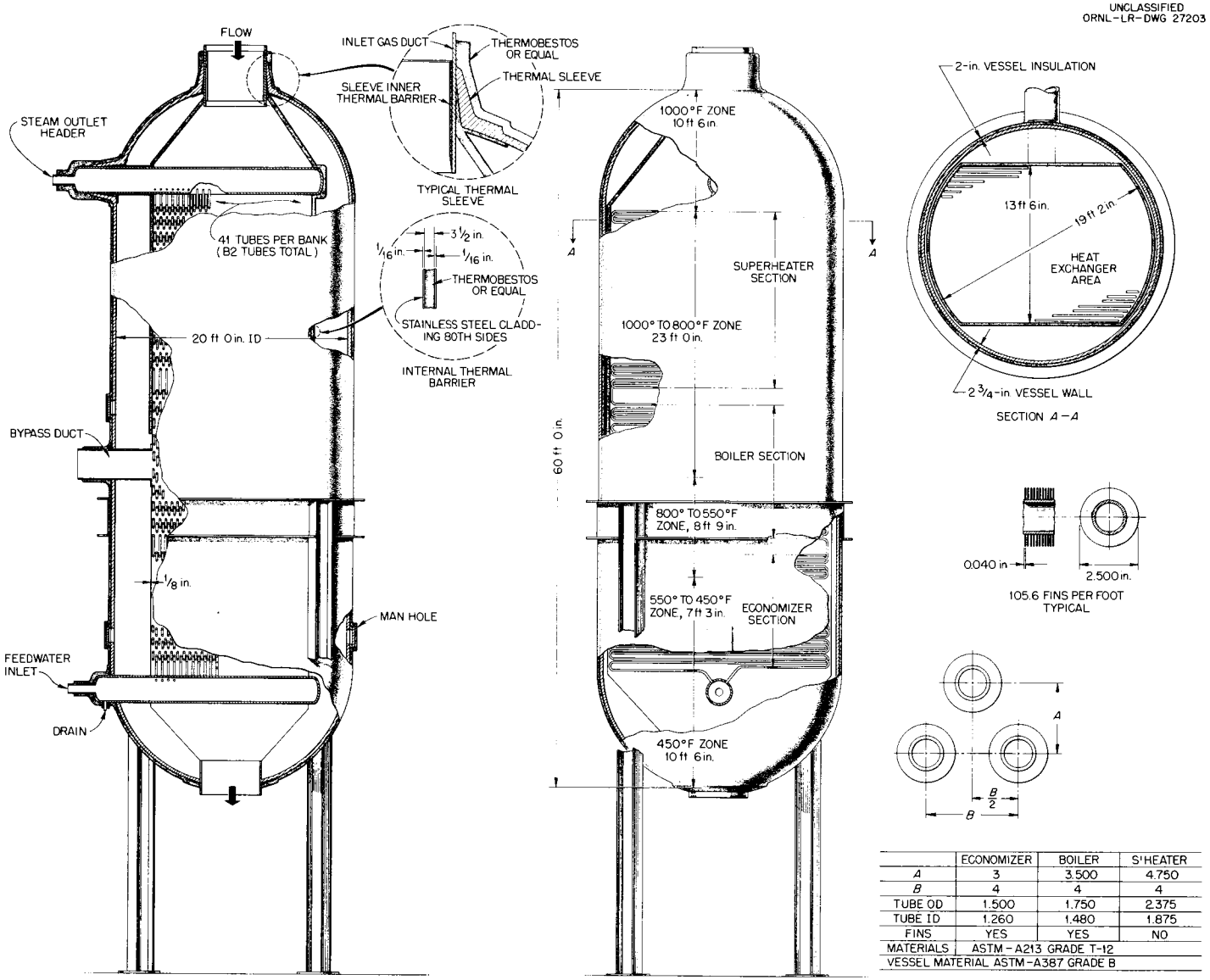

	ECONOMIZER	BOILER	SUPERHEATER
A	3	3.500	4.750
B	4	4	4
TUBE OD	1.500	1.750	2.375
TUBE ID	1.260	1.480	1.875
FINS	YES	YES	NO
MATERIALS	ASTM-A213 GRADE T-12		
VESSEL MATERIAL ASTM-A387 GRADE B			

Fig. 9.3. GCR-2 Steam Generator.

sufficient to warrant the use of extended-surface tubing in the boiler and economizer regions but not in the superheater section where the extended surface cannot be as effectively utilized because of the relatively poor inside-surface coefficient.

9.4.2 Design Calculations: Typical calculations are presented for the required surface areas in the economizer, boiler, and superheater sections of the steam generator. The steam temperature and pressure and helium temperature and pressure are given in Table 9.1.

In order to establish the operating temperatures in the separate generator sections, the calculations were initially based on assumed tube-side-pressure drops. It was intended that the generator size, the pressure drop, and the pressures and temperatures would be established by iteration, but the final pressure drops were so nearly those estimated that a recalculation based on corrected temperatures was not carried out.

For a given set of helium and steam conditions and a fixed tube matrix, calculations on the steam generator were carried out as indicated below. The results are summarized in Tables 9.1 and 9.2.

1. Determination of heat loads and fluid flows

   a. Total heat load $Q = 700$ Mw

   $= 2.389 \times 10^9$ Btu/hr Total

   $= 5.97 \times 10^8$ Btu/hr for each of four heat exchangers

   b. Tube-side flow

   Water flow $\frac{\text{lb}}{\text{hr}} = \frac{\text{Heat load Btu/hr}}{\text{Net heat gain Btu/lb}}$

   Water temperature in 325°F

   Steam temperature out 950°F

   Steam pressure out 950 psia

$$\text{Water flow } \frac{\text{lb}}{\text{hr}} = \frac{5.97 \times 10^8}{\text{Enthalpy out - Enthalpy in}}$$

$$= \frac{5.97 \times 10^8}{1477.6 - 295.5} = \frac{5.97 \times 10^8}{1182.1}$$

$$= 5.050 \times 10^5 \text{ lb/hr per exchanger}$$

$$= 140.3 \text{ lb/sec per exchanger}$$

TABLE 9.1

HELIUM AND STEAM TEMPERATURES AND HEAT BALANCE CALCULATIONS FOR STEAM GENERATOR

	Economizer	Boiler	Superheater
Steam exit temperature, °F			950
Steam exit pressure, psia			950
Helium temperature in, °F			1000
Helium temperature out, °F	450		
*Estimated water-side pressure drop, psi	5	40	25
Initial estimated pressure tube side, psia	1020	1015	975
Final estimated pressure tube side, psia	1015	975	950
Steam temperature, °F			
Initial	325	546.4	541.5
Final	546.4	541.5	950.0
Enthalpy in, Btu/lb	295.5†	544.6	1192.9
Enthalpy out, Btu/lb	544.6	1192.9	1477.6
Δh, Btu/lb	249.1	648.3	284.7
Total Δh, Btu/lb	1182.1		
Per cent of heat load	0.211	0.548	0.241
Heat load in Btu-hr/Ex.	1.260×10^8	3.271×10^8	1.439×10^8
Total per steam generator = 5.97×10^8 Btu/hr			
Helium ΔT, °F	116.1	301.4	132.5
Helium temperature in, °F	566.1	867.5	1000
Helium temperature out, °F	450.0	566.1	867.5
Tube side - shell side			
Initial temp. difference, °F	125.0	19.7	326
Final temp. difference, °F	19.7	326	50
Mean-temperature difference, °F	57.0	109.2	147.2
Helium pressure 300 psia			

*From previous calculations.

†This value neglects the correction for compressed liquid. The error is ~ 0.5%.

c. Shell-side flow

Helium temperature in	1000°F
Helium temperature out	450°F

$$Q = w\ c_p\ \Delta T$$

$$w = \frac{5.97 \times 10^8\ \text{Btu/hr}}{1.24\ \frac{\text{Btu}}{\text{lb °F}} \times 550\text{°F}} = 8.753 \times 10^5\ \text{lb/hr}$$

$$= 243\ \text{lb/sec per exchanger}$$

2. Superheater calculations

a. Geometry

Tube diameter outside	2.375 in.
Tube diameter inside	1.875 in.
Tube-well thickness	0.250 in.
Transverse pitch	4.00 in.
Longitudinal pitch (staggered rows)	4.75 in.
Total number of tubes	82
Face area of matrix	236
Free flow area of matrix	95.82

$$\text{Outside surface area} = \frac{\pi \times 2.375 \times 12}{144} = 0.622\ \frac{\text{ft}^2}{\text{ft pipe}}$$

$$\text{Inside surface area} = \frac{\pi \times 1.875 \times 12}{144} = 0.491\ \frac{\text{ft}^2}{\text{ft pipe}}$$

$$\text{Mean wall area} = \frac{A_o + A_1}{2} = 0.557\ \frac{\text{ft}^2}{\text{ft pipe}}$$

b. Temperatures and pressures

Estimate of tube-side-pressure drop	25 psi
Corresponding entering pressure to superheater	975 psia
Fluid saturation temperature corresponding to pressure	541.5 °F
Enthalpy entering superheater (975 psia saturated)	1192.9 Btu/lb
Enthalpy leaving superheater (950 psia and 950°F)	1477.6 Btu/lb

Enthalpy change through superheater 284.7 Btu/lb

Per cent heat exchanger load in superheater

$$= \frac{\text{Enthalpy change in superheater}}{\text{Total enthalpy change in steam generator}}$$

$$\doteq \frac{284.7}{1182.1} = 0.241$$

Helium temperature drop through superheater

= Total temperature drop x per cent heat load in superheater

Helium temperature drop = 550 x 0.241

= 132.5 °F

Helium temperature leaving superheater = 1000 - 132.5

= 867.5 °F

Log mean temperature difference

$$= \frac{(867.5-541.5)-(1000-950)}{\ell n \frac{867.5-541.5}{1000-950}}$$

$$= \frac{326 - 50}{\ell n \frac{326}{50}} = 147.2°F$$

Estimated log mean temperature difference correction factor 0.95

Corrected log mean temperature difference 139.8°F

c. Heat load

Superheater heat load = Total heat load x per cent of load in superheater

$$= 5.97 \times 10^8 \text{ Btu/hr} \times 0.241 = 1.439 \times 10^8 \text{ Btu/hr}$$

d. Tube-side heat transfer coefficient[1]

$$h_s = \frac{0.0266}{(d_i/12)^{0.2}} G^{0.8} c_p \mu^{0.2}$$

$$h_s \doteq \frac{0.0266}{(1.875/12)^{0.2}} \left(\frac{5.050 \times 10^5}{82 \times 0.01916}\right)^{0.8} 0.65 \times 0.066^{0.2}$$

$$h_s = 586.8 \text{ Btu/hr-ft}^2\text{-°F}$$

---

[1] R. A. Bowman, A. C. Mueller, and W. M. Nagel, "Mean Temperature Difference in Design," Trans. ASME, (May 1940).

Thermal properties are taken at average steam conditions of 745°F and 950 psia.

e. Gas-side heat transfer coefficient

$$\frac{h_m D_o}{k_f} = 0.33 \left[\frac{c_p \mu}{k}\right]_f^{1/3} \left[\frac{D_o G_{max}}{\mu_f}\right]^{0.6}$$

$$h_m = \frac{0.33 \times 0.1565}{0.1979} \left[0.669\right]^{1/3} \left[\frac{0.1979 \times 2.536 \times 3600}{0.0840}\right]^{0.6}$$

$$h_m = 95.4 \text{ Btu/hr-ft}^2\text{-°F}$$

Average film temperature taken as 850°F.

f. Wall resistance

$$R_{wall} = \frac{1}{\frac{k}{x}} = \frac{1}{\frac{18 \times 12}{0.250}} = 0.00116 \text{ (Btu/hr-ft-°F)}^{-1}$$

g. Assumed fouling factor

$$R_{fouling} = 0.0005 \text{ (Btu/hr-ft-°F)}^{-1}$$

h. Over-all U

$$\frac{1}{UA_o} = \frac{1}{h_s A_i} + \frac{1}{h_m A_o} + \frac{R_{wall}}{A_m} + \frac{R_{foul}}{A_i}$$

$$\frac{1}{U} = \frac{1 \times 0.622}{586.8 \times 0.491} + \frac{1 \times 0.622}{95.4 \times 0.622} + \frac{0.622}{0.557} \times 0.00116$$

$$+ \frac{0.622}{0.491} \times 0.0005$$

$$\frac{1}{U} = 0.01456$$

$$U = 68.7 \text{ Btu/hr-ft}^2\text{-°F}$$

i. Area requirements

$$Q = U A (\Delta T)_{\text{log mean}}$$

$$A = \frac{1.439 \times 10^8}{68.7 \times 139.8} = 15{,}000 \text{ ft}^2$$

Add 5% for loss in bends and face area at perimeter of heat exchanger surface

$$A = 15{,}750 \text{ ft}^2$$

j. Height of superheater section

Area/ft height = Area/ft pipe x ft pipe/ft vessel height

$$= 0.622 \times \frac{12 \times 12}{4 \times 4.75} \times 236 = 1112 \text{ ft}^2/\text{ft-height}$$

$$\text{Height required} = \frac{\text{Area required}}{\text{Area/ft height}} = \frac{15{,}750}{1112} = 14.2 \text{ ft}$$

Superheater height = 14.2 ft

k. Tube-side pressure drop (maximum)

$$\text{Number Tube Bends} = \frac{\text{matrix height}}{\text{longitudinal spacing}}$$

$$= \frac{14.2 \times 12}{9.5} \sim 18 \text{ bends}$$

Approximate maximum tube length = 19 x 18 = 342 ft

$$\Delta P = \left[\frac{1.5}{12} + \frac{fL}{d} + N_b/12\right] v \left(\frac{G}{10^5}\right)^2$$

$$\Delta P = \left[\frac{1.5}{12} + \frac{0.018 \times 342}{1.875} + \frac{18 \times 0.28}{12}\right] 0.687 \left(3.21\right)^2$$

$$\underline{\Delta P = 27.2 \text{ psi}}$$

(1) Helium side pressure drop

$$\text{Mass Velocity} = 2.536 \frac{\text{lb}}{\text{ft}^2 \text{ sec}}$$

$$\Delta P = \frac{4 f'' N.G^2}{2 g_c \rho}$$

$$f'' = \left[0.23 + \frac{0.11}{(x_t - 1)^{1.08}}\right] \left(\frac{D_o G}{\mu_f}\right)^{-0.15}$$

$$= \left[0.23 + \frac{0.11}{(\frac{4}{2.375} - 1)^{1.08}}\right] \left(\frac{\frac{2.375}{12} \times 2.536 \times 3600}{0.0840}\right)^{-0.15}$$

$$f'' = 0.089$$

$$\Delta P = \frac{4 \times 0.089 \times 36 \times 2.536^2}{2 \times 32.2 \times 0.080}$$

$$= 16.00 \text{ psf}$$

$$= 0.111 \text{ psi}$$

3. Boiler calculations

a. Geometry

Face area $236\ ft^2$

Total number tubes 82

$$\text{Fin area/ft pipe} = \frac{\frac{\pi}{4}(D_F^2 - D_T^2)\ 105.6}{144} \times 2$$

$$= 3.670\ ft^2$$

$$\text{Tube area/ft pipe} = \frac{\pi\ D_T\ (12 - 105.6 \times 0.040)}{144}$$

$$= 0.297\ ft^2$$

Total outside area/ft pipe $= 3.967\ ft^2$

Inside area/ft pipe $= 0.408\ ft^2$

Mean area/ft pipe $\doteq 0.422\ ft^2$

$$\%\ \text{Free gas flow area} = \sigma = 1 - \frac{[12 \times D_T + t\ (D_F - D_T)\ N_f] \times 12}{144\ S_T}$$

$\sigma = 0.50$

b. Temperatures, pressures, and flows

Method of calculation is indicated in Table 9.1

From Table 9.1 L.M.T.D. = 109.2°F

Apply estimated correction factor of 0.95

Corrected L.M.T.D. = 109.2 x 0.95

= 103.7°F

$$\text{Water mass velocity} = \frac{140.3 \times 144}{82 \times 1.719} = 143.3\ lb/ft^2\text{-sec}$$

$$\text{Gas mass velocity} = \frac{243}{118} = 2.06\ lb/ft^2\text{-sec}$$

c. Heat load

Boiler heat load $= 3.271 \times 10^8$ Btu/hr

d. Tube-side heat transfer coefficient

$$h_i = 2000\ Btu/hr\text{-}ft^2\text{-}°F$$

e. Gas-side coefficient

$$h_g = \frac{71}{D_o^{0.302}}\ G^{0.72}\ D_o^{0.283}$$

$$= \frac{71}{(1.75)^{0.302}}\ 2.06^{0.72}(1.75)^{0.283}$$

$$h_g = 110\ Btu/hr\text{-}ft^2\text{-}°F$$

f. Wall resistance

$$R_{wall} = \frac{1}{k/x} = \frac{1}{\frac{18 \times 12}{0.135}} = 0.000625 \text{ (Btu/hr-ft-°F)}^{-1}$$

g. Assumed fouling factor

$$R = 0.0005 \text{ (Btu/hr-ft-°F)}^{-1}$$

h. Over-all U

$$\frac{1}{UA_o} = \frac{1}{h_g(A_T + \phi A_F)} + \frac{1}{h_i A_i} + \frac{R_{wall}}{A_m} + \frac{R_{foul}}{A_i}$$

Fin efficiency[2]

$$w\sqrt{\frac{h}{ky_b}} = \frac{0.375}{12} \sqrt{\frac{110 \times 12}{18 \times 0.20}} = 1.89$$

$$\frac{x_e}{x_b} = 1.43$$

Fin efficiency ϕ = 0.45

$w = \pm (x_b - x_e)$ = fin height feet

x_b = spiral fin radius feet

x_e = tube outside radius feet

y_b = half thickness of fin feet

h = prime surface heat transfer coefficient $\frac{\text{Btu}}{\text{hr ft}^2\text{°F}}$

k = thermal conductivity Btu/hr-ft-°F

$$\frac{1}{U} = \frac{3.967}{110(0.297 + 0.45 \times 3.670)} + \frac{3.967}{2000 \times 0.408}$$

$$+ \frac{3.967}{0.422} \times 0.000625 + 0.0005 \times \frac{3.967}{0.408}$$

$$U = 29.4 \text{ Btu/hr-ft}^2\text{-°F}$$

i. Area requirements

$$Q = U\,A\,(\Delta T)_{\text{log mean}}$$

$$A = \frac{3.271 \times 10^8}{103.7 \times 29.4} = 107{,}300 \text{ ft}^2$$

---

[2] Karl A. Gardner, "Efficiency of Extended Surface," Trans. ASME (November 1945)

Add 5% for area loss in bends, etc.

$A = 112{,}700\ ft^2$

j. Height of boiler section using calculations similar to that for superheater section

$$\text{Area/ft-height} = 3.967 \times \frac{12 \times 12}{4 \times 3.5} \times 236$$

$$= 9629\ ft^2/ft$$

$$\text{Height} = \frac{112{,}700}{9629} = 11.7\ ft$$

k. Tube-side pressure drop

$$\text{Water } \Delta P = \frac{f\ L\ G^2}{2\ g_c\ D\ \rho^2}\ psf$$

$$\frac{DG}{\mu} = \frac{\frac{1.48}{12}\ 143.3}{0.235/3600} = 270{,}700$$

ρ and μ are evaluated at entering conditions of temperature and pressure

$f = 0.016$ for $Re = 270{,}000$ and smooth tubing

$$\text{Approximate maximum tube length} = \frac{19 \times 11.7 \times 12}{7}\ ft$$

$$= 381\ ft$$

$$\Delta P = \frac{0.016 \times 381 \times 143.3^2}{2 \times 32.2 \times \frac{1.48}{12} \times 46.8^2} = 7.195\ ft\ head$$

$$\Delta P = \frac{7.195 \times 46.8}{144} = 2.34\ psi$$

Bend loss

$$\Delta P = B_p \times \frac{v}{12} \left(\frac{G}{100{,}000}\right)^2$$

$$= \frac{0.27}{12} \times \frac{1}{46.8} \left(\frac{143.3 \times 3600}{10^5}\right)^2 \text{per bend}$$

$\Delta P = 0.0127$ psi/bend

$$\text{Number bends} = \frac{11.7 \times 12}{7} \sim 20$$

$\Delta P = 0.254$ psi

Two phase flow factor $\Delta P_{tpf} = 17$

Total pressure drop $= \Delta P \times \Delta P_{tpf}$

$= 2.59 \times 17 = 44$ psi

(1) Helium pressure drop

$$\Delta H = \frac{f\ A\ G^2}{2\ \rho_m^2\ g_c\ A_c}$$

$A = 112{,}700\ ft^2$

$A_c = 118\ ft^2$

$G = 2.06\ lb/ft^2\text{-sec}$

$\rho_m = 0.0985$ based on avg. film temp. $= 675°F$

$$f = \frac{4.94\ D_H^{0.506}\ G^{-0.253}}{\mu^{-0.253}}$$

$$= \frac{4.94 \times (0.049)^{0.506} \times (0.077)^{0.253}}{(2.06 \times 3600)^{0.253}}$$

$$\doteq \frac{4.94 \times 0.2175 \times 0.522}{2 \times 9.3} = 0.060$$

$$\Delta H = \frac{0.060 \times 112{,}700 \times 2.06^2}{2 \times 0.0985^2 \times 32.2 \times 118}$$

$\Delta H = 389$ ft

$\rho_{avg} = 0.095\ lb/ft^3$ mean bulk density

$\Delta P = 0.257$ psi

4. Economizer calculations

a. Geometry

Face area $236\ ft^2$

Total number tubes 82

$$\text{Fin area/ft pipe} = \frac{\frac{\pi}{4}(D_F^2 - D_T^2)\ 105.6 \times 2}{144}$$

$= 4.61\ ft^2$

$$\text{Tube area/ft pipe} = \frac{\pi\ D_T\ (12 - 105.6 \times 0.040)}{144} = 0.254\ ft^2$$

Total outside area/ft pipe = 4.86 ft^2

Inside area/ft pipe = 0.330 ft^2

Mean area/ft pipe = 0.361 ft^2

$$\text{Per cent free flow area} = \sigma = 1 - \frac{[12\ D_T + t(D_F - D_T)\ N_f]\ 12}{144\ S_T}$$

$$\sigma = 0.537$$

b. Temperatures, pressures and flows

L.M.T.D. = 57°F

L.M.T.D. correction factor = 0.95

Corrected L.M.T.D. = 54.2°F

$$\text{Water mass velocity} = \frac{140.3}{82 \times 0.00865} = 197.8\ lb/ft^2/sec$$

$$\text{Gas mass velocity} = \frac{243}{236 \times 0.537} = 1.92\ lb/ft^2/sec$$

c. Heat load

Economizer heat load = 1.260×10^8 Btu/hr

d. Tube-side heat transfer coefficient

$$\frac{hD_i}{k} = 0.023 \left(\frac{D_i G}{\mu}\right)^{0.8} \left(\frac{c_p \mu}{k}\right)^{0.4}$$

Average bulk temperature 435°F

$$h = \frac{0.023 \times 0.3743}{0.105} \left(\frac{0.105 \times 197.8 \times 3600}{0.300}\right)^{0.8} (0.882)^{0.4}$$

$$h = 0.0820\ (20{,}632)\ (0.951)$$

$$h = 1609\ \text{Btu/hr-ft}^2\text{-°F}$$

e. Gas-side coefficient

$$h_g = \frac{71}{D_o^{0.302}}\ G^{0.72}\ D_o^{0.283}$$

$$= \frac{71}{(1.5)^{0.302}}\ (1.92)^{0.72} \times (1.5)^{0.283}$$

$$h_g = 106\ \text{Btu/hr-ft}^2\text{-°F}$$

f. Wall resistance

$$R_{wall} = \frac{1}{k/x} = \frac{1}{\frac{18 \times 12}{0.120}} = 0.000555 \text{ (Btu/hr-ft-°F)}^{-1}$$

g. Assumed fouling factor

$$R = 0.0005 \text{ (Btu/hr-ft-°F)}^{-1}$$

h. Over-all U

$$\frac{1}{UA_o} = \frac{1}{h_g(A_T + \phi A_F)} + \frac{1}{h_i A_i} + \frac{R_{wall}}{A_m} + \frac{R_{foul}}{A_i}$$

Fin efficiency ϕ

$$w\sqrt{\frac{h}{ky_b}} = \frac{0.5}{12}\sqrt{\frac{106 \times 12}{18 \times 0.020}} = 2.48$$

$$\frac{x_e}{x_b} = 1.667$$

$$\phi = 0.33$$

$$\frac{1}{UA_o} = \frac{1}{106(0.254 + 0.33 \times 4.61)} + \frac{1}{1609 \times 0.33} + \frac{0.000555}{0.361} + \frac{0.0005}{0.330}$$

$$\frac{1}{UA_o} = 0.00531 + 0.00188 + 0.00154 + 0.00151$$

$$U = 20 \text{ Btu/hr-ft}^2\text{-°F}$$

i. Area requirements

$$Q = UA(\Delta T)_{\text{log mean}}$$

$$A = \frac{1.26 \times 10^8}{20 \times 54.2} = 116{,}200 \text{ ft}^2$$

Add 5% for area bend loss

$$A = 122{,}000 \text{ ft}^2$$

j. Height of Boiler

Using calculations similar to that for superheater section

$$\text{Area/ft height} = \frac{4.86 \times 12 \times 12}{4 \times 3} \times 236$$

$$= 13{,}760 \text{ ft}^2\text{/ft height}$$

$$\text{Height} = \frac{122,000}{13,760} = 8.87 \text{ ft}$$

k. Tube-side pressure drop

$$\Delta P = \frac{f\ L\ G^2}{2\ g_c\ D\ \rho^2} \text{ ft}$$

$$\frac{DG}{\mu} = \left(\frac{0.105 \times 197.8 \times 3600}{0.300}\right) = 256,000$$

Properties evaluated at average bulk temperature of water

$f = 0.0165$ at Re = 256,000 for smooth tubing

$$\text{Approximate maximum tube length} = \frac{8.87 \times 12}{6} \times 19$$

$$= 337 \text{ ft}$$

$$\Delta P = \frac{0.0165 \times 337 \times 197.8^2 \times 12}{2 \times 32.2 \times 1.26 \times 52.3^2}$$

$$\Delta P = 11.8 \text{ ft}$$

$$= \frac{11.8 \times 52.3}{144} = 4.28 \text{ psi}$$

Bend loss

$$\Delta P = B_p \times \frac{v}{12} \left(\frac{G}{100,000}\right)^2$$

$$= 0.27 \ \frac{1}{52.3 \times 12} \left(\frac{197.8 \times 3600}{100,000}\right)^2$$

$$= 0.022 \text{ psi/bend}$$

$$\text{No bends} = \frac{8.87 \times 12}{6} \sim 18$$

$$\Delta P = 0.4 \text{ psi}$$

$$\text{Total } \Delta P = 4.28 + 0.40 = 4.68 \text{ psi}$$

(1) Helium pressure drop

$$\Delta H = \frac{f\ A\ G^2}{2\ \rho_m^2\ g_c\ A_c}$$

$$A = 122,000 \text{ ft}^2$$

$$A_c = 126.7 \text{ ft}^2$$

$$G = 1.92 \text{ lb/ft}^2\text{-sec}$$

$$\rho_m = 0.114 \text{ lb/ft}^3 \text{ based on average film temp. = 520°F}$$

$$f = \frac{4.94 \times D_H^{0.506} \, G^{-0.253}}{\mu^{-0.253}}$$

$$f = \frac{4.94 \, (0.037)^{0.506} \, (1.92 \times 3600)^{-0.253}}{(0.071)^{-0.253}}$$

$$f = \frac{4.94 \times 0.1888 \times 0.512}{9.36}$$

$$f = 0.051$$

$$\Delta H = \frac{0.051 \times 122{,}000 \times 1.92^2}{2 \times 0.114^2 \times 32.2 \times 126.7}$$

$$= 216.2 \text{ ft}$$

$$\rho_{avg} = 0.1153 \text{ at mean bulk density}$$

$$\Delta P = 0.173 \text{ psi}$$

A summary of the results of the above calculations appears in Table 9.2 and in Section 9.4.7.

9.4.3 Determination of Operating Steam Conditions: The determination of design operating conditions for the steam system was carried out by an evaluation of the effects of variations of steam temperature and pressure on steam generator costs and on over-all plant thermodynamic efficiency.

Two studies were carried out to determine the steam conditions. For the first study, the steam pressure was assumed constant and the steam helium approach temperature was varied. In the second part, the steam temperature was held constant and steam pressures were varied.

Effect of Steam-Helium Approach Temperatures. For a steam pressure of 900 psia, steam generator calculations were carried out for a series of steam-helium approach temperatures at the top of the steam generator with helium inlet temperatures of 950, 1000, and 1100°F. The results have been plotted in Fig. 9.4 to show that for a helium inlet temperature of 1000°F, an approach temperature of approximately 10°F is optimum. The studies were carried out for the tube matrix as shown in Fig. 9.3. Tables 9.3 and 9.4 show the principal items included in the calculation and indicate the method employed.

TABLE 9.2

STEAM GENERATOR DESIGN DATA

	Economizer	Boiler	Superheater	Total
Shell-Side Surface Area, ft^2	122,000	112,700	15,750	250,500
Tube-Side Surface Area, ft^2	8,280	11,580	12,400	32,300
Linear ft Tubing (Straight)	25,100	28,400	25,300	78,800
Maximum Tube Length, ft	337	381	342	1,060
Tube Size OD in.	1.50	1.75	2.375	--
Tube Size ID in.	1.26	1.48	1.875	--
Fin OD in.	2.5	2.5	--	--
Fins/ft	105.6	105.6	--	--
Transverse Pitch, in.	4.00	4.00	4.00	--
Longitudinal Pitch, in.	3.0	3.5	4.75	--
Number of Tube Rows	36	40	36	112
Height of Matrix, ft	8.9	11.7	14.2	34.8
Gas Mass Velocity, lb/ft^2 sec	1.92	2.06	2.54	--
Gas Pressure Drop, psi	0.17	0.26	0.11	0.54
Water-Side Mass Velocity, lb/ft^2 sec	197.8	--	--	--
Water Pressure Drop, psi	4.7	44.0	27.2	75.9*
Heat Load Btu/hr per Exchanger	1.260×10^8	3.271×10^8	1.439×10^8	5.97×10^8
Heat Flux Btu/hr-ft^2 Inside Area	15,200	28,200	11,600	--
Over-all U Btu/hr-ft^2-°F	20	29.4	68.6	--

* To this a static head of approximately 5 psi must be added.

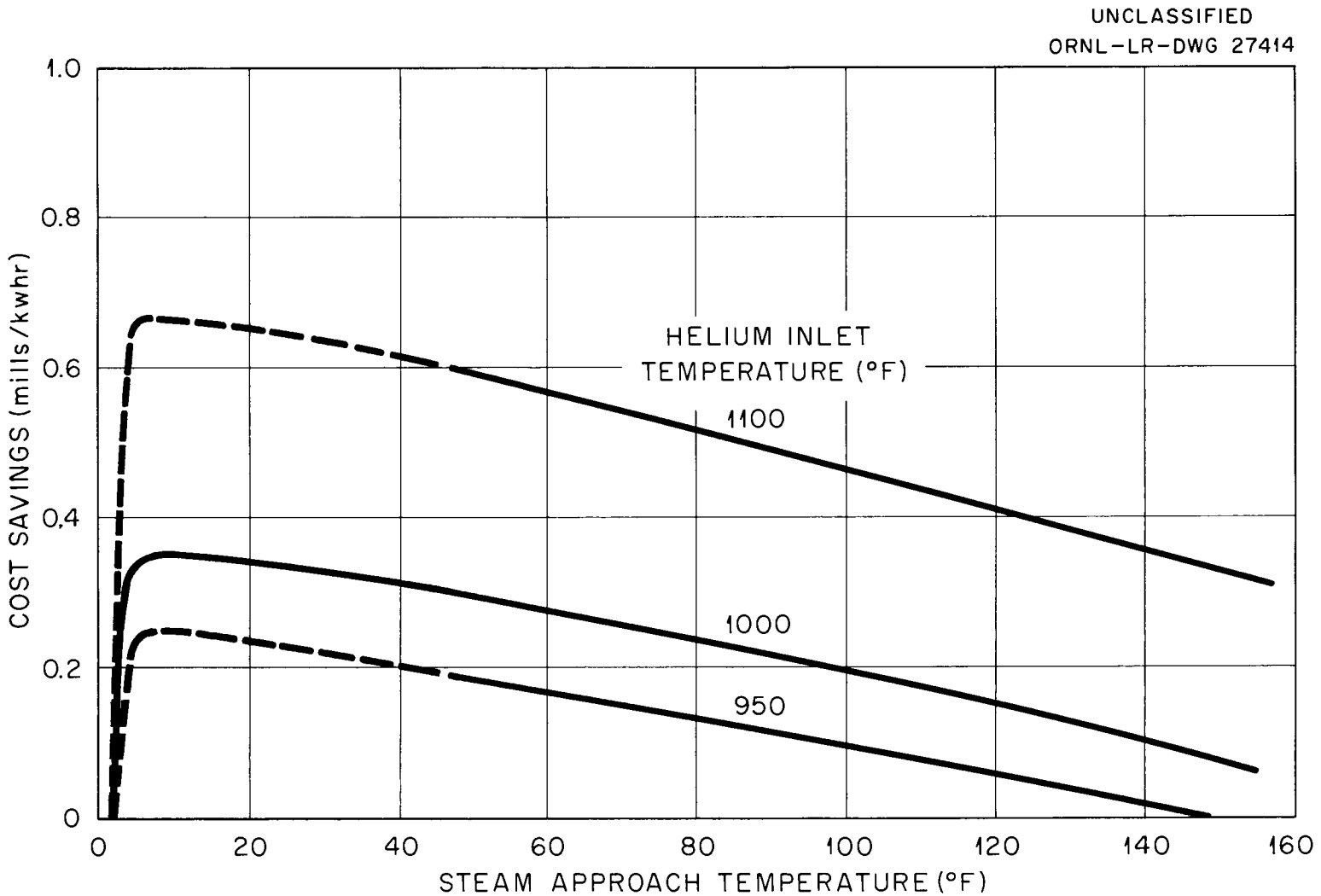

Fig. 9.4. Power Cost Savings as a Function of Approach Temperature.

TABLE 9.3

EFFECTS OF STEAM TEMPERATURE ON GROSS ELECTRICAL REVENUE

Steam temperature, °F	800	900
Steam pressure, psia	900	900
Enthalpy of exit steam (assumed entering turbine-generator), Btu/lb	1392.9	1451.1
Enthalpy leaving turbine-generator, Btu/lb (2 in. Hg condition pressure)	882.0	908.0
Total effective enthalpy change (assuming 85% turbine-generator efficiency), Btu/lb	434.3	462.5
Enthalpy of return feed water, Btu/lb	69.72	69.72
Total enthalpy change, Btu/lb	1323.2	1381.4
Total thermodynamic cycle efficiency, per cent	0.328	0.335
Gross Mw output at 700 Mw, thermal load	229.6	234.5
Assumed fixed auxiliary and blower load, Mw	25	25
Net Mw output	204.6	209.5
Δ Mw from 800°F steam condition	0	4.9
Dollar value of Δ Mw in 20 yr at 10 mills/kwh (increased revenue)	0	7.296×10^6

TABLE 9.4

STEAM GENERATOR COST AND ASSOCIATED NET POWER COSTS FOR TWO STEAM TEMPERATURES

Helium inlet temperature, °F	950	950
Steam exit temperature, °F	800	900
Steam exit pressure, psia	900	900
Inlet water temperature, °F	250	250
Economizer area per exchanger*, ft^2	60,500	61,700
Boiler area per exchanger*, ft^2	56,100	58,600
Superheater area per exchanger*, ft^2	7,100	14,200
Cost tube bundle plus shell (4 units)**, $	3,616,000	4,068,000
Helium pumpingcost (4 units), $	2,423,000	3,114,000
Water pumping cost (4 units), $	227,000	283,000
Total relative costs, $	6,266,000	7,465,000
Cost difference from 800°F steam condition, $	0	1,199,000
Net extra electrical revenues from Table 9.3, $		7,296,000
Net savings, $		6,097,000
Net savings, mills/kwh		0.19

* In computing these areas no fouling factor was included.
** Cost of heads, headers, insulation, support structure and miscellaneous not included in these values.

Steam exit conditions were assumed to be those entering the turbine generator. The turbine-generator performance was computed on the basis of an over-all efficiency of 85%. The net electrical-plant output was obtained by assuming a connected plant load of 25 Mw.

The cost savings indicated in reducing the steam approach temperature from 150°F to approximately 10°F show that the increased thermodynamic efficiency produced by higher steam temperatures to the turbine-generator units more than offsets the increased costs of the steam generator. The steam generator costs do not include such items as insulation costs, pipe support and structural costs, and miscellaneous incremental costs. These items will tend to shift the optimum point of the curve toward somewhat larger steam-helium approach temperatures. Since the net potential savings between a 50°F approach temperature and the 10°F optimum is only of the order of 0.05 mills/kwh, a steam approach temperature of 50°F was selected for the design.

A comparison of the curves for various helium inlet temperatures indicates the potential savings to be realized by an increase in the helium inlet temperature. For a 50°F approach temperature a potential savings of 0.3 mills/kwh could be achieved by increasing the helium temperature from 1000°F to 1100°F. This figure does not take into account extra costs accruing from materials changes required by the higher temperature. Fig. 9.5 shows the effects of helium inlet temperature on the log mean temperature differences for various steam-helium approach temperatures. Figure 9.6 shows the effect on the over-all heat transfer coefficient for the same variables. As would be expected, the effects of steam approach temperature on the over-all heat transfer coefficient are small.

Effect of Steam Pressure on Steam Generator Design. The effects of steam pressure on steam generator size and cost have been investigated for a constant steam exit temperature of 950°F. The results are shown in Tables 9.5 and 9.6. A net cost reduction can be achieved by raising the steam pressure to 1400 psia, as shown in Fig. 9.7.

A preliminary investigation of steam-piping costs and turbine-generator costs in the 950 psia to 1400 psia range indicated no large change in capital costs, so it was assumed for purposes of analysis that the total capital

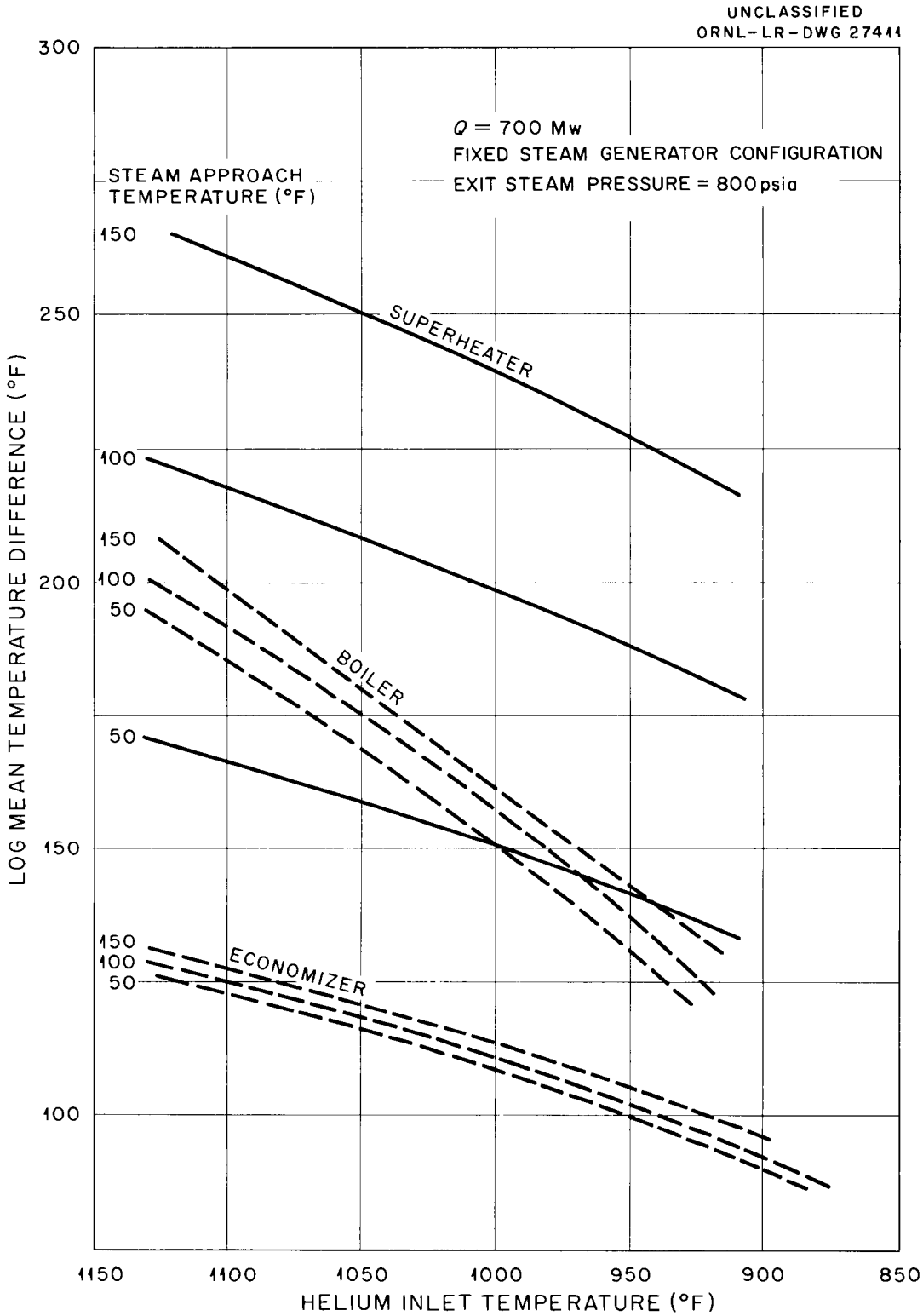

Fig. 9.5. L.M.T.D. vs Helium Temperature.

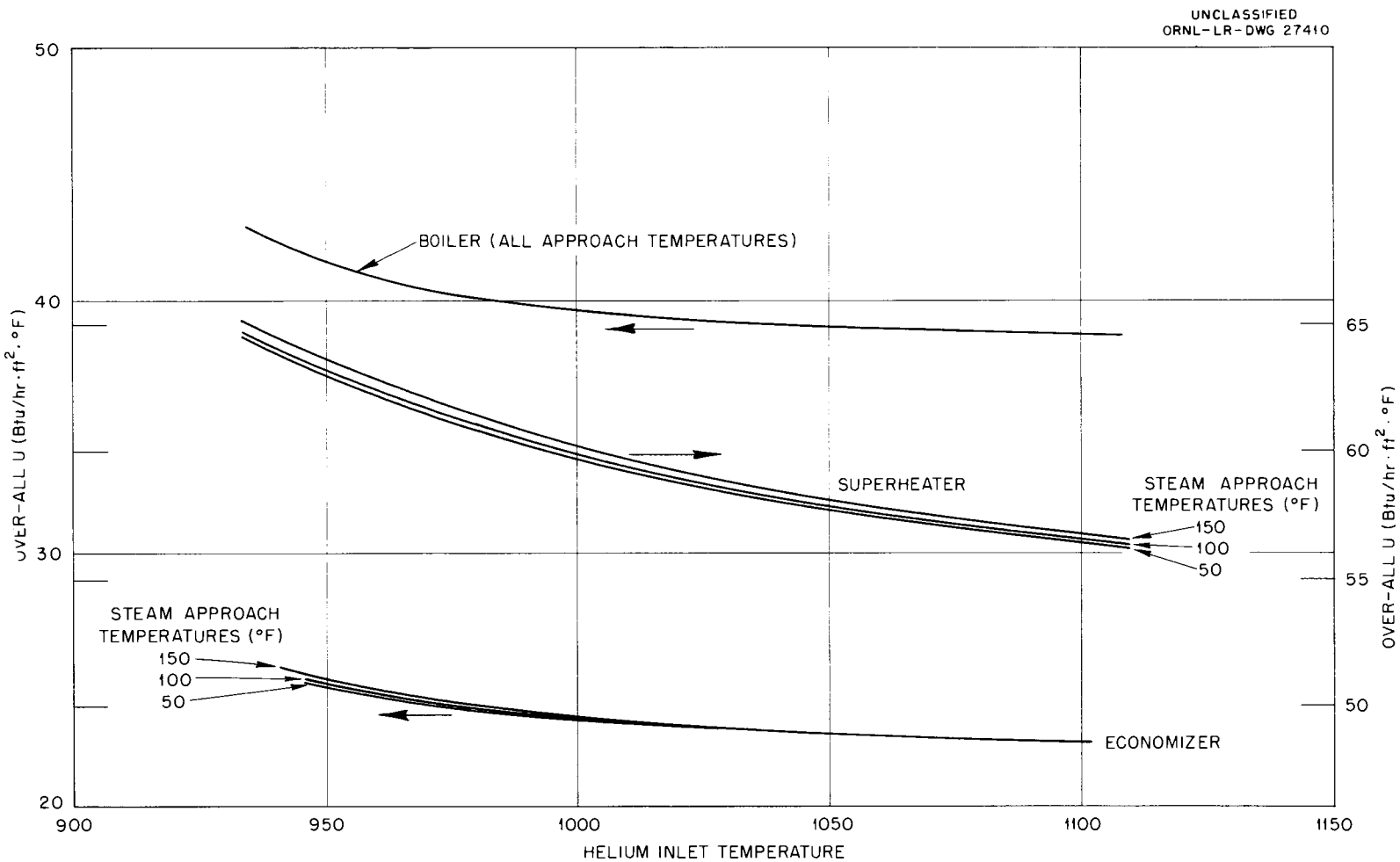

Fig. 9.6. Over-all Steam Generator Heat-Transfer Coefficient vs Helium Inlet Temperature.

TABLE 9.5

EFFECTS OF STEAM PRESSURE ON GROSS ELECTRICAL REVENUE

	Steam Pressure (psi)			
	950	1000	1200	1400
Steam temperature, °F	950	950	950	950
Enthalpy of exit steam, Btu/lb	1477.7	1475.2	1469.3	1462.3
Enthalpy leaving turbine-generator, Btu/lb (2 in. Hg condition pressure)	917	913	900	887
Enthalpy change in turbine-generator, Btu/lb	560.7	562.2	569.3	575.3
Effective enthalpy change (85% turbine-generator efficiency) Btu/lb	476.6	477.9	483.9	489.0
Enthalpy of feed water, Btu/lb	69.7	69.7	69.7	69.7
Total enthalpy change, Btu/lb	1408.0	1405.5	1399.6	1392.6
Total thermodynamic cycle efficiency, %	33.85	34.00	34.57	35.11
Gross Mw output with 700 Mw thermal load	237.0	238.0	242.0	245.8
Assumed fixed auxiliary and blower load in Mw	25	25	25	25
Net Mw output	212	213	217	220.8
ΔMw from 950 psia steam pressure		1	5	8.8
Total kwh in 20 yr	3.157	3.171	3.231	3.288×10^{10}
Dollar value of ΔMw in 20 yr at 10 mills/kwh, $1,489,000/Mw		1.489	7.445	13.10×10^{6}

TABLE 9.6

EFFECTS OF STEAM PRESSURE ON STEAM GENERATOR SIZE AND COST

	Steam Pressure (psi)			
	950	1000	1200	1400
Steam temperature, °F	950	950	950	950
Log mean temperature difference, °F				
Economizer	58.9	56.2	47.1	37.3
Boiler	112.2	106.5	86.7	67.0
Superheater	147.2	145.4	138.2	131.5
Heat load Btu/hr/exchanger				
Economizer	1.227×10^8	1.270×10^8	1.420×10^8	1.570×10^8
Boiler	3.304×10^8	3.270×10^8	3.090×10^8	2.914×10^8
Superheater	1.438×10^8	1.440×10^8	1.460×10^8	1.487×10^8
Over-all heat transfer coefficient, Btu/hr-ft^2-°F				
Economizer	20.5	20.5	20.5	20.5
Boiler	28.0	28.0	28.0	28.0
Superheater	64.5	64.5	64.5	64.5
Area required x 1.1[1]), ft^2				
Economizer[2])	111,800	121,200	169,900	237,200
Boiler[2])	115,700	120,600	140,000	170,800
Superheater[2])	16,600	16,900	18,000	19,300
Heights required, ft				
Economizer, (13,760 ft^2/ft height)	8.12	8.81	12.3	17.2
Boiler, (9,630 ft^2/ft height)	12.0	12.5	14.5	17.7
Superheater, (1,110 ft^2/ft height)	15.0	15.2	16.2	17.4
Vessel costs[3] $				
Economizer, ($81,289/ft height)	660,000	716,000	1,000,000	1,398,000
Boiler, ($70,576/ft height)	847,000	882,000	1,023,000	1,249,000
Superheater, ($2108/ft height)	316,000	320,000	342,000	367,000
Total cost per unit, $	1,823,000	1,918,000	2,365,000	3,014,000
Cost difference from 950°F as base per unit, $		95,000	542,000	1,191,000
Cost difference from 950°F base for four units, $		380,000	2,168,000	4,764,000
Net savings from 950 psi condition $ x 10^6		1.109	5.277	8.336
Total kwh produced in 20 yr		3.171×10^{10}	3.23×10^{10}	3.288×10^{10}
Savings in mills/kwh		0.035	0.163	0.253

1. L.M.T.D. values not corrected for divergence from true counter flow. Used 1.1 factor on area. This value was later shown to be conservative.
2. A fouling factor of R = 0.0005 was used on the inside of the tubes.
3. These costs include only tube bundle and vessel costs. Later cost data indicate values above are low.

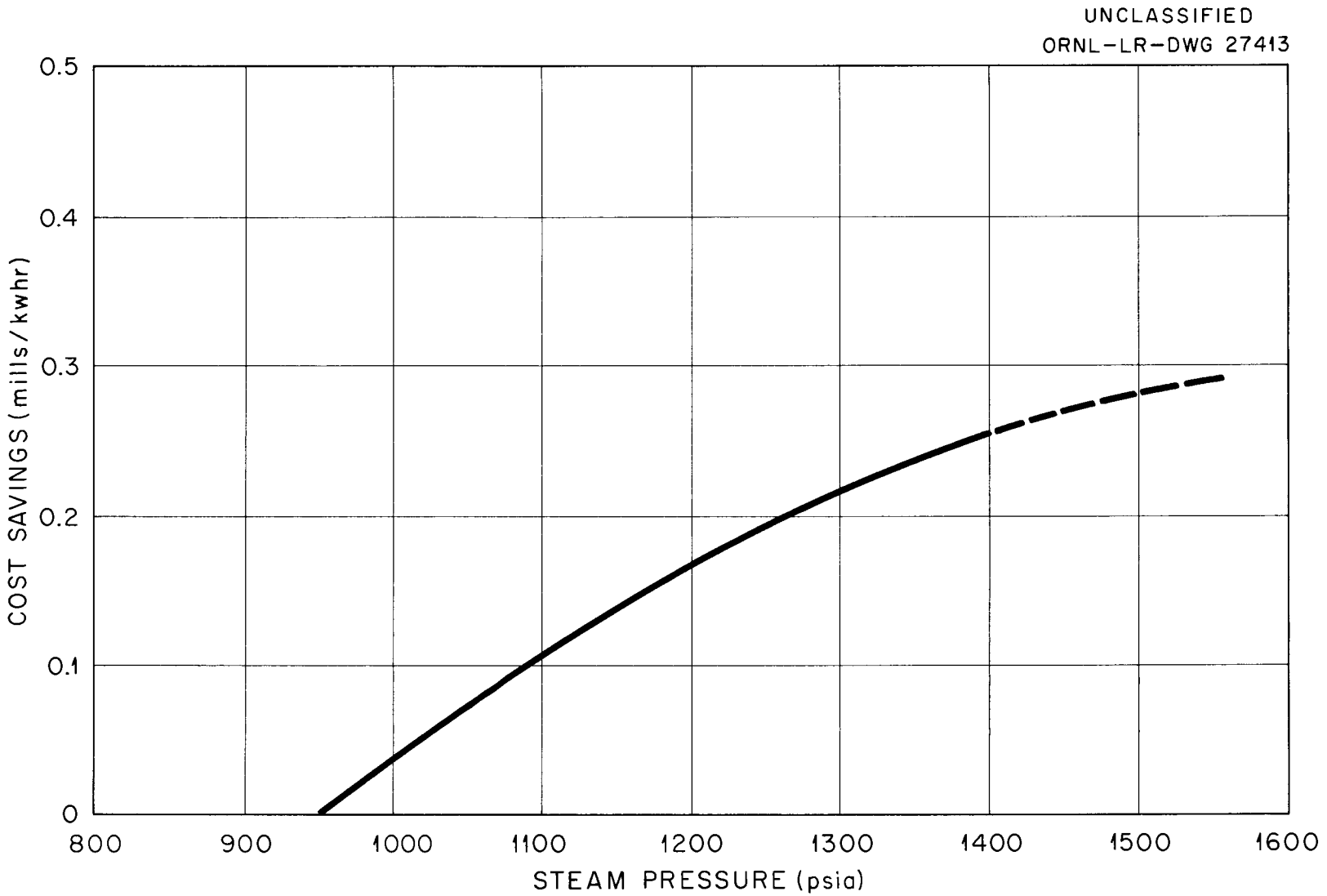

Fig. 9.7. Power Cost Savings vs Steam Pressure.

cost increase could be taken as equal to the increased steam generator costs. As discussed earlier, certain cost items, such as insulation, headers, structural supports, and thicker tube walls, were omitted in computing the cost estimates. These factors will have the effect of depressing the curve in Fig. 9.7 and reducing the net potential savings.

Although increased savings were indicated by higher operating steam pressures, an exit steam pressure of approximately 950 psia was selected. This decision was reached to insure a minimum temperature difference of 20°F between the water and the helium in the economizer. Figure 9.8 shows the minimum value for this temperature difference as a function of steam pressure. As the minimum water-helium approach temperature decreases below this value, the log mean temperature difference becomes extremely sensitive to small changes in this minimum temperature difference. Thus, small errors in predicting items such as water-side pressure drop could cause significant changes in the minimum approach temperature and the log mean temperature difference. This would result in significant changes in area requirements for the various generator sections, and would change the exit steam conditions under design load.

A later and more detailed investigation, carried out by TVA, of the effect of steam pressure on steam plant costs, including turbine generators, condensers, feed-water equipment, piping and accessories, indicated a strong incentive for higher steam pressures to reduce steam plant costs and decrease turbine heat rates. The TVA information became available at a time which precluded its incorporation into this report.

9.4.4 Vessel Diameter and Tube Matrix: Vessel Diameter. Early in the design study it was necessary to fix the diameter of the heat exchanger vessel in order that the layout of the reactor plant could proceed. A tube matrix design was selected and studied in vessels of 12-, 16-, 18-, and 20-ft diameters for a four-heat-exchanger system. Heat transfer calculations were carried out for each diameter to determine the required surface areas and exchanger heights for the mass velocity through each diameter vessel. Total costs were based on tube bundle costs, vessel costs, and helium and water pumping costs available at that time. Figure 9.9 summarizes these studies.

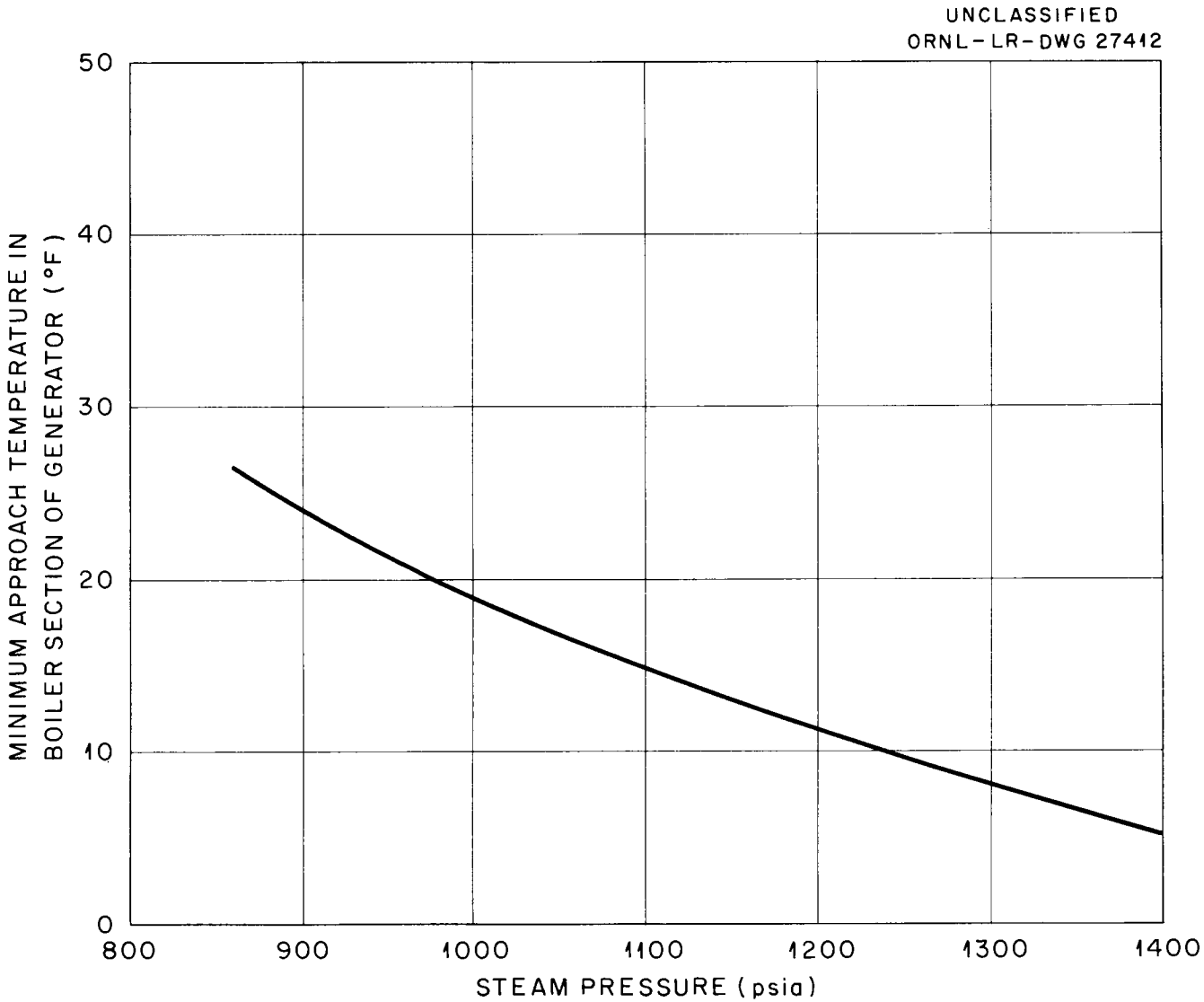

Fig. 9.8. Minimum Approach Temperature in Boiler Section of Steam Generator vs Steam Pressure.

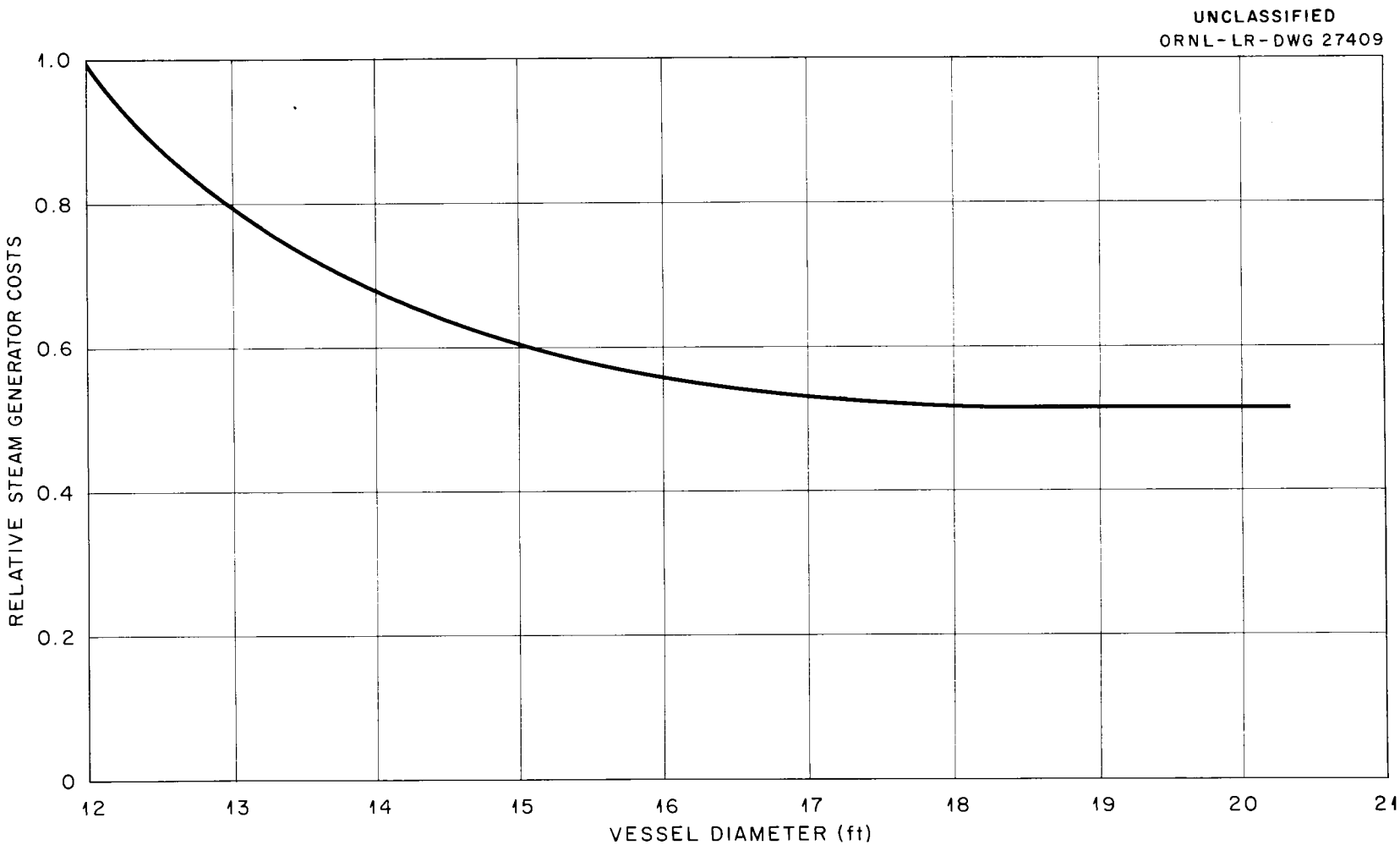

Fig. 9.9. Relative Steam Generator Costs vs Steam Generator Vessel Diameter.

Changes in base capital costs that have occurred since the study was made tend to shift the curve to a minimum at a slightly smaller vessel diameter, but the costs are relatively insensitive to vessel diameter as the diameter increases.

A parallel study was carried out for a gas system having only two main heat exchangers but it was apparent that, in order to reduce helium pumping power to a reasonable value, vessel diameters well in excess of 20 ft would be required. Uncertainties in commercial capabilities for fabricating such large sizes lead to the decision to limit vessel diameters to 20 ft.

Tube Matrix. In the initial matrix study, the economizer, boiler, and superheater sections were designed separately with the intention that either internal or external manifolds would be used to connect the generator sections together. This permitted an individual optimization of each generator section. Initial work indicated little performance advantage for this approach, so it was decided to employ a continuous tube design with no intermediate manifolds, and thus obtain a marked simplification in the mechanical construction and fabrication. With a continuous tube design, the number of degrees of design freedom is restricted and the design approach is more complicated. This can be seen from an examination of the heat transfer coefficients in each of the three steam generator sections and the calculations for the gas- and water-side pressure drops.

If the water is carried in a single long tube of uniform diameter through the economizer and boiler, the pressure drop through the boiler will be from 15 to 30 times the pressure drop through the economizer section. To reduce this pressure drop, a larger tube can be employed in the boiler region. This reduces the net free-flow area on the gas-side and increases the gas-side pressure drop. The need to employ the same number of tubes in parallel in each section makes it impossible to obtain an optimum design for each section. The best design is one giving the best over-all compromise. Time prevented an extensive study, but earlier individual section studies indicated that no great savings could be achieved through a complete tube-matrix parametric study. The arrangement chosen consists of a double bank entry of tubes with forty-one tubes per horizontal row. The water flow proceeds in opposite directions in adjacent tube rows. With the proposed

tube layout the center tubes will be longer than the side tubes, but orificing of the shorter tubes will avoid unbalanced flows and temperatures in the system.

9.4.5 Additional Design Considerations: Generator Tubes. The material selected for the tubes is SA 213, Grade T-12, a low-cost alloy containing 1% chromium and 1/2% molybdenum. This material is widely used in steam service up to 1000°F. Calculations of the required tube-wall thickness were carried out following the prescription used in the ASA and ASME codes.

$$P = \frac{2\,t_{mc}}{D - 2\,Yt_{mc}} \times S$$

or

$$t_m = \frac{DP}{2\,(S+YP)} = C$$

where

D = outside tube diameter, in.

P = design pressure, psia

S = allowable stress at operating temperature, psi

C = corrosion allowance, in..

Y = a constant determined by the metal and temperature and prescribed by code

t_m = minimum tube-wall thickness required.

An allowance for tube-wall variation must be added to the minimum tube-wall thickness. ASTM specifies a zero under tolerance allowance on SA 213-T-12 cold-drawn tubing. A corrosion allowance of 0.063 in. was selected and added to the calculated tube-wall thickness as indicated above. This value is believed to be quite conservative for the selected steel for this application.[3] Further investigation might allow a reduction in this corrosion allowance with a consequent savings in pressure drop and a slight improvement in heat transfer. Table 9.7 lists the values used for the generator design

---

[3] H. H. Uhlig, The Corrosion Handbook (New York: John Wiley and Sons, 1948).

and the calculated tube-wall thicknesses. In general, the nearest standard tube-wall thickness available was selected for the unit.

TABLE 9.7

DESIGN DATA FOR DETERMINATION OF TUBE-WALL THICKNESSES IN STEAM GENERATOR

	Economizer	Boiler	Superheater
Design temperature, °F	550	900	1000
Design pressure, psia	1000	975	950
Tube outside diameter, in.	1.5	1.750	2.375
Allowable stress, psi	15,200	13,100	7,500
Y value	0.4	0.4	0.7
Corrosion allowance, in.	0.063	0.063	0.063
Under-thickness allowance	0	0	0
Calculated tube-wall thickness, in.	0.111	0.126	0.201
Tube-wall thickness employed, in.	0.120	0.135	0.250

Vessel. The heat-exchanger pressure-vessel thickness and material were determined from ASME code requirements for the various materials investigated and from the cost data available on these materials. Figure 9.10 shows typical costs as a function of vessel diameter for operation at both 800°F and 1050°F. As discussed in Section 9.4.6, it was determined economically practical to limit the maximum temperature of the vessel to 800°F, thus permitting the use of higher allowable stresses.

Maintenance and Repair. In the event of a steam generator leak to the helium system, detection devices will indicate which generator unit is leaking. Repairs on the generator unit may be carried out by inspection from within the steam-outlet header drum and the water-inlet header drum. These header drums are sufficiently large to permit a man to enter, inspect, and plug the leaking tube. The following sequence of events will occur if a steam generator leak develops.

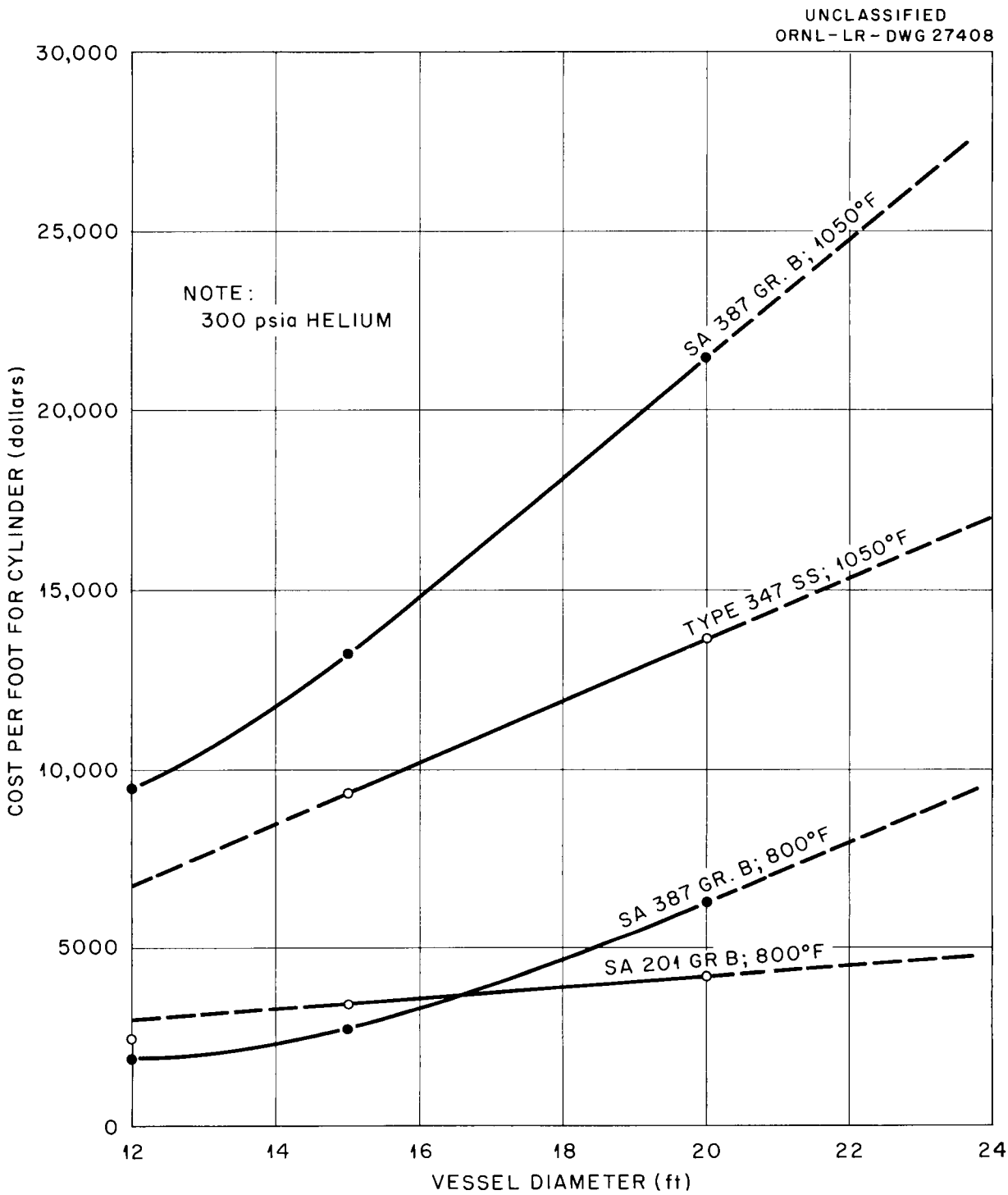

Fig. 9.10. Steam Generator Vessel Shell Costs.

1. Leak detection device indicates a steam leak to the helium system in a given steam generator unit.
2. Reactor plant is shut down and the leaking steam generator drained.
3. The header drums are opened for inspection.
4. For small leaks, the helium-system pressure can be maintained slightly above atmospheric. A man entering the steam exit header with a helium-leak-detection device can determine from which tube helium is entering the system.
5. The helium is evacuated from the helium system.
6. The leaking tube is then blown out with dry air and pierced below the point at which the tube enters the header.
7. The tube is then plug-welded shut at both header sheets. Assuming a linear relationship between generator capacity and surface, each plug-welded tube will reduce the steam generator capacity by 1.2%.

Table 9.8 shows a record of tube failures in boiler units of TVA coal-fired steam plants. Note the remarkably small incidence of tube failures, and hence the low probability that a tube will have to be plugged. Only 15 joints out of a total of 50,000 leaked in a cumulative total of one and one-half million tube-joint years of service. The joints that failed did so as a result of either faulty welds originally, or as a result of repeated water splashing against the outside of the lower wall headers at the bottom ash hoppers.

Even with the very large number of tube-to-header joints employed in the Calder Hall heat exchangers, namely, thirty-five times as many tube-to-header joints as employed in the ORNL design, no tube-to-header joint leakage has occurred in more than a year of operating experience.

Access doors and ladders are provided in the generator unit for entry and inspection.

Vapor Separator Unit. The present design does not provide for a vapor separator unit between the boiler and superheater sections of the steam generator unit. Information available at the time of this report indicated that the unit would operate satisfactorily without a separator.

TABLE 9.8

RELIABILITY OF BOILER TUBE-TO-HEADER WELDED JOINTS

Plant Units	Total Welds Per Unit: Evaporator Type Service	Total Welds Per Unit: Superheater and Reheater	Number of Leaks Per Plant
Johnsonville 1-6	2,388	913	0
Kingston 1-4	1,512	1,224	0
Kingston 5-9	2,864	2,792	0
John Sevier 1-4	2,864	2,792	0
Colbert 1-4	2,466	1,944	0
Shawnee 1-10	1,713	1,814	10*
Gallatin 1-2	3,924	3,080	0
Widows Creek 1-4	1,394	1,074	6*
Widows Creek 5-6	1,842	2,033	0

* Approximate. Obtained from plant maintenance supervisors.

9.4.6 Insulation Optimization Data: The insulation requirements for each generator include two general areas, the outer vessel surface and its protuberances, including the insulation at the thermal sleeves, and the inner vessel thermal barrier. The outer insulation requirements were investigated for five temperature-zone sections because of the helium temperature gradient through the heat exchanger. Both the 1000°F and 1000 to 800°F zones were evaluated in conjunction with an inner thermal barrier which was terminated at the 800°F helium level. Insulation for the 1000°F zone was optimized as shown on Fig. 9.11. The vessel inner-wall maximum temperature was established at 800°F on the basis of the allowable stress characteristics of the vessel material, SA 387-B, low-alloy steel. By adhering to standard insulation thicknesses, and considering the effect of convection currents in the space between the vessel and the inner thermal barrier, outer and inner thicknesses of 2 in. and 3.5 in., respectively, were chosen. Figure 9.12 is included to show the effects of outer and inner insulation thicknesses on heat losses in the 1000°F zone.

The remainder of the insulation thicknesses chosen for the 800 to 550°F, 550 to 450°F, and 450°F zones are shown in Table 9.9, as well as the heat losses anticipated.

TABLE 9.9

INSULATION AND HEAT-LOSS COSTS PER STEAM GENERATOR AT DESIGN CONDITIONS

Zones (°F)	Insulation Thickness Outer (in.)	Insulation Thickness Inner (in.)	Vessel Length (ft)	Insulation Area Outer (ft^2)	Insulation Area Inner (ft^2)	Total Insulation costs[c] ($/20 yr)	Heat Losses (Btu/hr)	Heat Loss Costs[d] ($/20 yr)
1000, 1000–800	2[a]	3-1/2[a]	33.5	2187	1775	40,700	278,000	42,800
800–550	3[a]	-	8.8	572	-	6,300	49,200	7,600
550–450, 450	3[b]	-	17.7	1159	-	7,700	72,000	11,100
		TOTALS	60.0			54,700	339,000	61,500

Notes:
a J-M Thermobestos or equivalent
b J-M 85% Magnesia or equivalent
c From cost estimates supplied by the Brooks-Fisher Insulating Company, Knoxville, Tennessee
d Based upon a $0.154/Btu/20 yr heat cost.

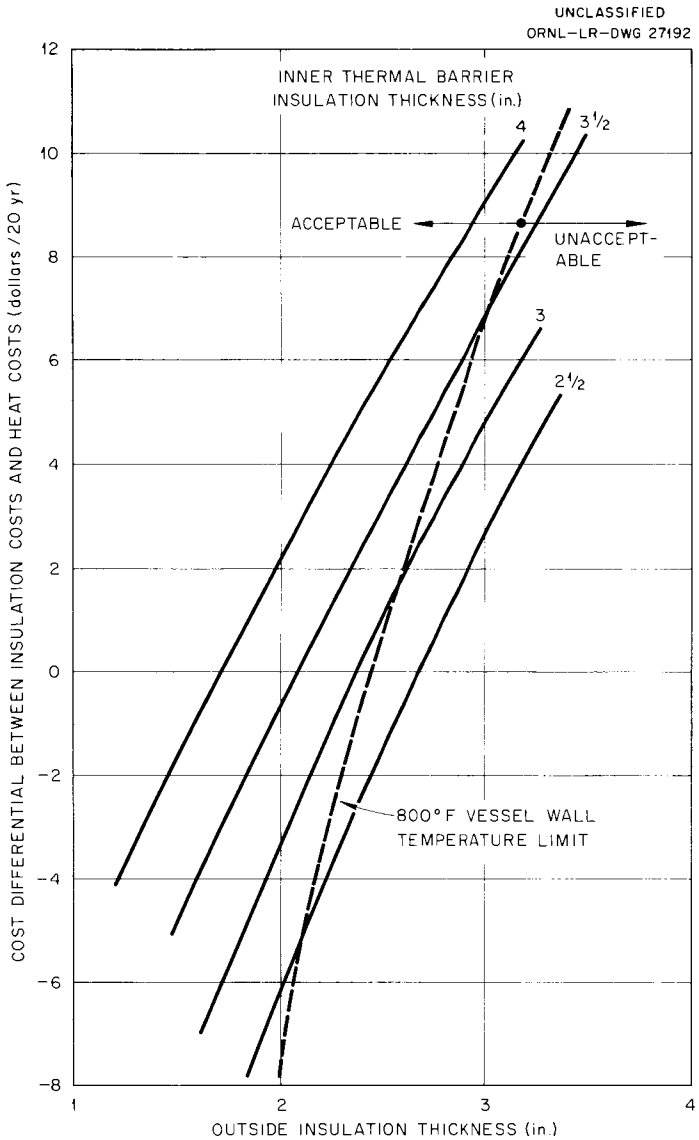

Fig. 9.11. Optimum Insulation Thickness in 1000°F Zone of Steam Generator.

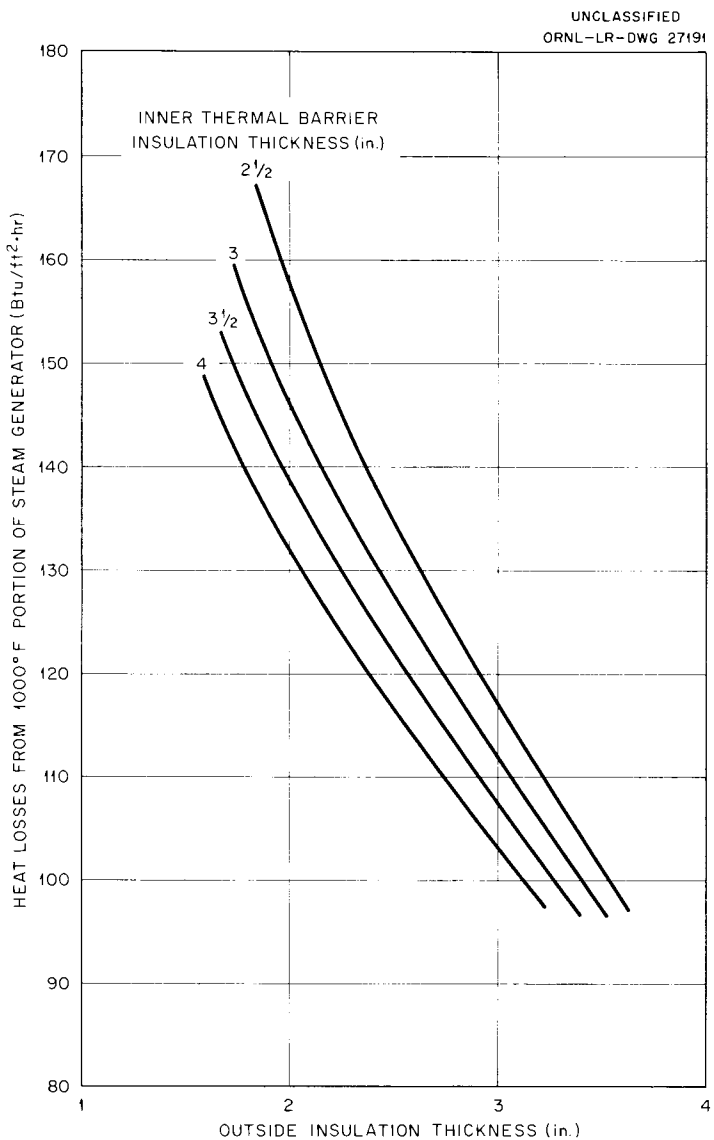

Fig. 9.12. Heat Losses from Insulated 1000°F Zone of Steam Generator.

The inner thermal barrier, comprised of insulation sandwiched between 1/16-in.-thick stainless steel plates, is an integral part of the heat exchanger gas enclosure, which extends unbroken from the helium inlet duct to the outlet duct. Thermal barrier venting will be required to permit pressure equalization. Replacement of the air in the insulation with helium results in an increase in thermal conductivity. The accepted thermal conductivity in air was multiplied by three to obtain the thermal conductivity values used. This rough value of three is indicated by the limited experimental data available.[4] A sample calculation is shown below:

Sample Insulation Calculation for 1000°F Zone

Assumptions

1. All metal thermal resistances considered negligible.
2. Heat exchanger side of thermal barrier at bulk helium temperature.
3. Opposing surfaces of vessel wall and thermal barrier at the same temperature, 800°F.
4. The ambient temperature 96°F at 6 mph wind velocity.
5. Thermal conductivity of the insulation in helium equal to three times the conductivity in air.
6. Insulation of J-M Thermobestos or equal.

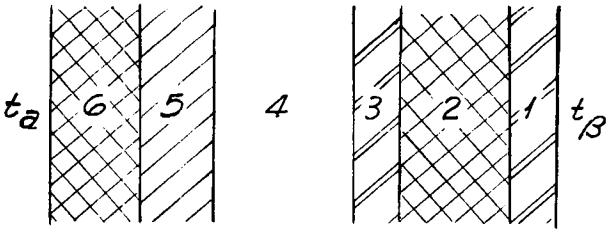

Layers 1, 2, and 3 form thermal barrier.

Layer 4 is a stagnant helium layer.

Layers 2 and 6 are inner and outer insulation.

Layer 5 is the vessel wall.

$$Q = \frac{t_\beta - t_a}{\frac{L_2}{K_2 A_2} + \frac{L_6}{K_6 A_6} + \frac{R_a}{A_a}}$$

[4] B. E. Short et al, Heat Loss Experiments for Package Reactor Loop, ORNL CF-57-11-127, (November 14, 1957)

where

Q = Heat losses, Btu/hr/ft of vessel

t_β = Bulk helium temperature, °F

t_a = Ambient temperature, °F

L = Thickness of layers, in.

K = Thermal conductivity, Btu in./hr-ft^2°F

A = Mean area, ft^2/ft of vessel

R_a = Ambient surface resistance at 6 mph wind velocity, ft^2-°F-hr/Btu

Δt_2 = Layer 2 temperature differential, °F

$$Q = \frac{1000-96}{\frac{3.5}{0.705(3)(58.21)} + \frac{3}{0.485(64.97)} + \frac{0.29}{65.75}} = \frac{904}{0.0284 + 0.0952 + 0.0044}$$

= 7060 Btu/hr/ft of vessel

Temperature check Δt_2 = 200°F; Δt_5 = 672°F; Δt_s = 31°F

K check within 1/2%

R_a check within 3%

The effects of variations in insulation thickness were not included previously in the steam generator optimization. Since these costs are substantial they must be considered in future steam generator optimization work. Further, the possibility of maintaining a vessel wall temperature much lower than 800°F, thereby permitting the use of cheaper vessel materials, should be investigated. In the case considered, the combined fabrication and materials cost for the stainless steel enclosure was estimated to be about $3.00/lb, or approximately $50,000 per steam generator including the steam generator structural allowance.

9.4.7 Data for Steam Generator: Table 9.2 gives the dimensions chosen for the heat exchanger together with water-side and gas-side flows, tube lengths and pressure drops. Figure 9.13 shows graphically the intermediate water and gas temperatures while 9.14 presents the heat balance for the unit.

Table 9.10 shows the estimated costs of the various components of the heat exchanger unit. The final estimated cost of $1,369,400 per unit is substantially in excess of earlier estimates used for parametric design studies. The basis for this final cost estimate is included in Table 9.10.

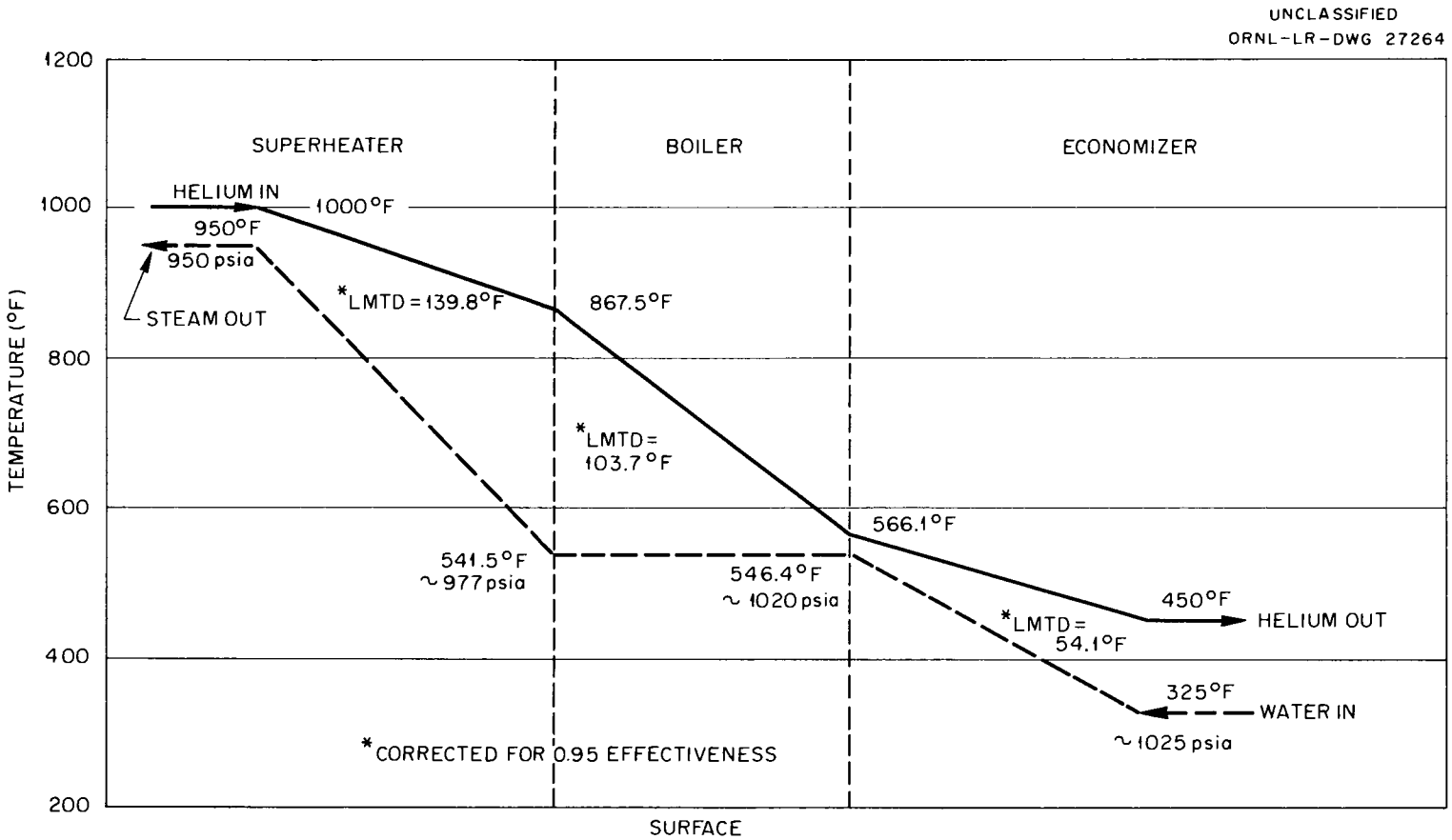

Fig. 9.13. Steam Generator, Helium and Steam Temperature Diagram.

UNCLASSIFIED
ORNL-LR-DWG 27265

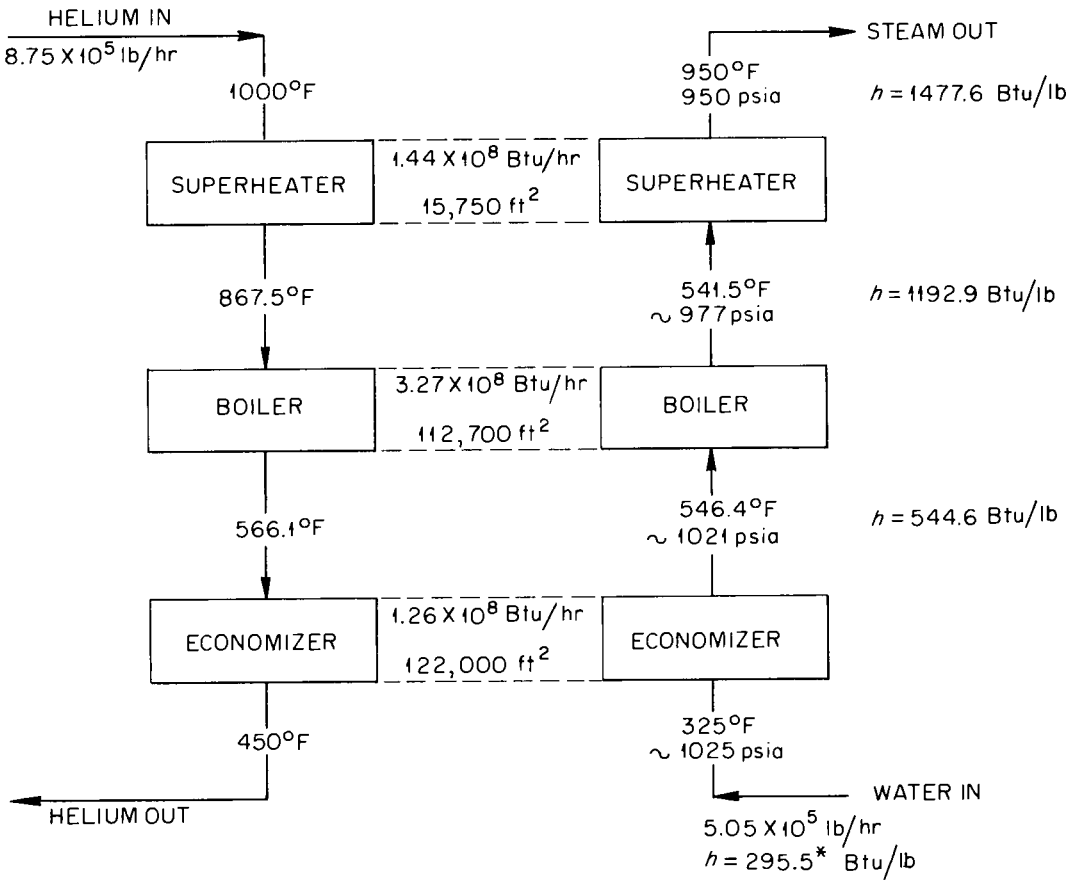

ALL VALUES ARE PER HEAT EXCHANGER

*THIS VALUE NEGLECTS THE EFFECT OF A COMPRESSED LIQUID WHICH AMOUNTS TO ~1.5 Btu/lb

Fig. 9.14. Steam Generator Heat Balance.

TABLE 9.10

COMPONENT COSTS AND WEIGHTS PER STEAM GENERATOR

Portion of Generator	Additional Weight During Hydrostatic Tests (lbs)	Weight (lbs)	Cost ($)
Cylindrical section of vessel[1]	-	285,200	427,800
Top head and thermal sleeves[2,1]	-	40,800	55,000
Bottom head and thermal sleeves[2,1]	0	37,200	50,000
Superheater tubing[3]	34,500	153,200	150,400
Boiler finned tubing[4]	22,200	158,300	235,100
Economizer finned tubing[5]	14,600	141,000	211,200
Steam outlet manifold[6]	4,200	14,200	28,400
Steam inlet manifold[6]	4,800	7,600	15,100
Manholes[7]	-	2,100	3,600
By-pass, inlet and outlet ducts[8,9]	-	7,500	8,300
External structural steel[10]	-	90,200	45,000
Internal structural steel[11,2]	-	60,000	70,000
Insulation[12,13,14,15]	-	12,600	19,500
Heat exchanger area gas enclosure[16]	-	16,700	50,000
TOTAL	80,300	1,026,600	1,369,400

Notes:

1. $ 1.50/lb Cr-Mo steel costs - ORNL estimate
2. $ 1.25/lb internal Cr-Mo structural steel - ORNL estimate
3. $ 5.57/ft interpolated from vendor cost data
4. $ 7.89/ft interpolated from vendor cost data
5. $ 8.06/ft interpolated from vendor cost data
6. $ 2.00/lb Cr-Mo steel costs - ORNL estimate
7. $ 150/manhole cover - manufacturers catalog prices
8. $ 1.00/lb Cr-Mo steel costs - ORNL estimate
9. $ 1.25/lb Cr-Mo steel costs - ORNL estimate
10. $ 0.50/lb external structural steel - ORNL estimate
11. $ 1.00/lb internal structural steel - ORNL estimate
12. $ 4.43/ft^2, 3.5 in. J-M Thermobestos
13. $ 3.05/ft^2, 2 in. J-M Thermobestos
14. $ 3.94/ft^2, 3 in. J-M Thermobestos
15. $ 2.37/ft^2, 3 in. J-M 85% Magnesia
16. $ 3.00/lb stainless steel - ORNL estimate

9.4.8 Heat Transfer and Pressure Drop Equations - Cost Data: Heat Transfer. Heat transfer performance calculations for the steam generator employed the following correlation equations:

A. Gas-Side Heat Transfer

Since all of the designs under consideration employed gas flow across staggered tube banks, the following correlation equations were used.

Bare Tubes. Colburn recommends the following equation for gas flow across banks of staggered bare tubes:

$$\frac{h_m D_o}{K_f} = 0.33\left[\frac{C_p \mu}{k}\right]^{1/3}\left[\frac{D_o G_{max}}{\mu_f}\right]^{0.6}$$

h_m = mean surface heat transfer coefficient, Btu/hr-ft^2-°F

D_o = tube outside diameter, ft

k = thermal conductivity, Btu/hr-ft^2-°F/ft

C_p = specific heat, Btu/lb-°F

μ = absolute viscosity, lb/ft-hr

G_{max} = mass velocity of fluid, lb/hr-ft^2

Subscript f refers to average film-temperature conditions through minimum free-flow area.

Fin Tubes. For tubes with circular spiral fins,[5] Kays includes graphs of data for various tube diameters, fin diameters, fin pitches, and fin thicknesses. These give Colburn's j factor against Reynolds number across the tube bank. In order to utilize this information more effectively, the data from the various spiral fin matrices were tabulated and correlated to permit predictions for spiral fin arrangements not given by the reference text.

The basic correlation equation used for spiral circular fin surfaces with flow across banks of staggered tubes is as follows:

$$\frac{h}{G\,C_p}\left(\frac{C_p\,\mu}{k}\right)^{2/3} = K\left(\frac{D_H G}{\mu}\right)^n$$

---

[5] W. M. Kays and A. L. London, Compact Heat Exchangers, (London: National Press, 1955).

where

D_H = hydraulic diameter in ft = $4\ (A_c L/A)$

L = flow length of the heat exchanger, ft

A_c = exchanger minimum free-flow area, ft^2

A = total heat transfer area, ft^2

h = prime surface heat transfer coefficient, Btu/hr-ft^2-°F

other symbols retain their previous definitions

The determination of K and n for a wide variety of fin and tube dimensions was required.

For a specified gas operating at equivalent temperatures in each geometry, the above equation can be reduced to the following:

$$h = K_1 G^{n+1}$$

where

$$K_1 = \frac{K\ C_p^{1/3}\ D_H^n\ k^{2/3}}{\mu^{2/3+n}}$$

n = slope of j vs Re curve

K = intercept of j vs Re curve

By assuming an average gas temperature, the above equation reduces to:

$$K_1 \doteq \frac{K_2\ D_H^n}{\mu^n}$$

From the data given, the variation in n was sufficiently small that μ^n is approximately constant for a specified gas temperature for the surfaces studied. Then:

$$K_1 = K_3\ D_H^n\ .$$

Thus, h can be correlated as a function of the hydraulic diameter and mass velocity. A cross plot of K_3 vs D_H^n, for each surface listed[6] is shown in Fig. 9.15. It is evident that no correlation was obtained.

The function $K_3\ D_H^n$ was then plotted against tube outside diameter, as shown in Fig. 9.16 together with the slope, n, plotted against the same

---

[6] Ibid, p. 9.49.

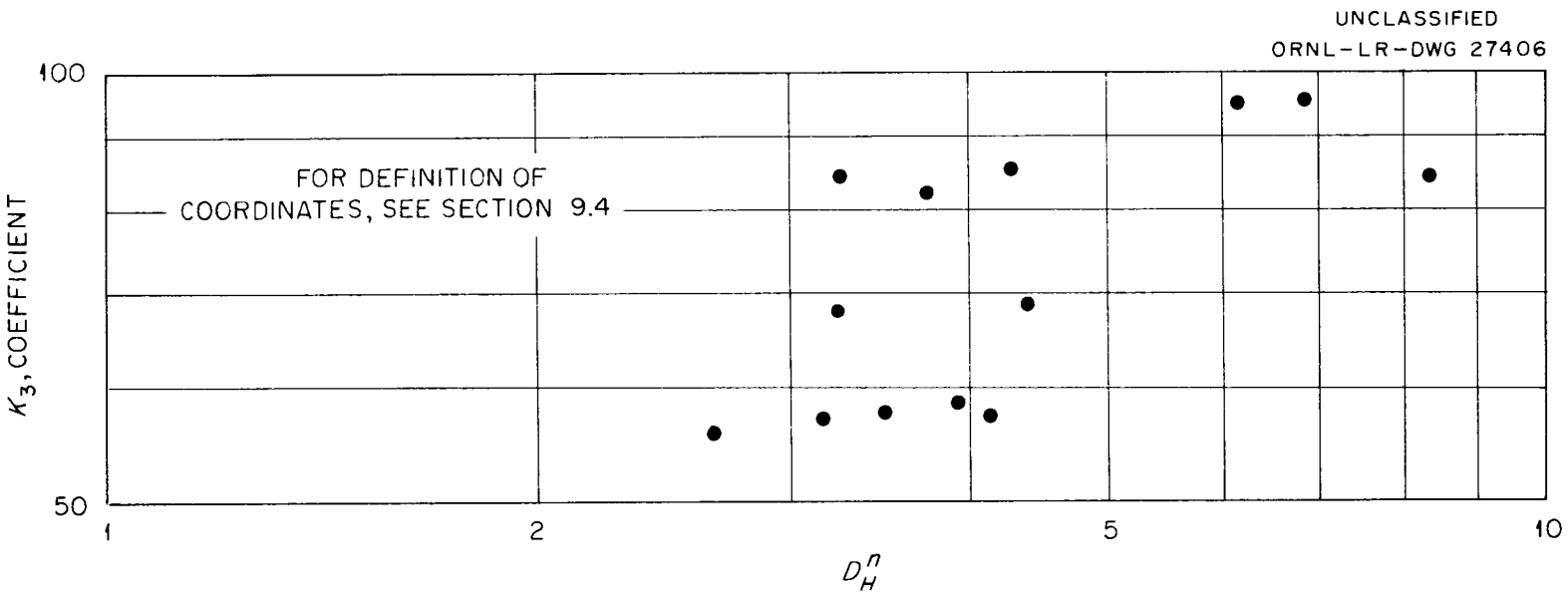

Fig. 9.15. Correlation of Hydraulic Diameter for Helium Heat Transfer to Spiral Fins.

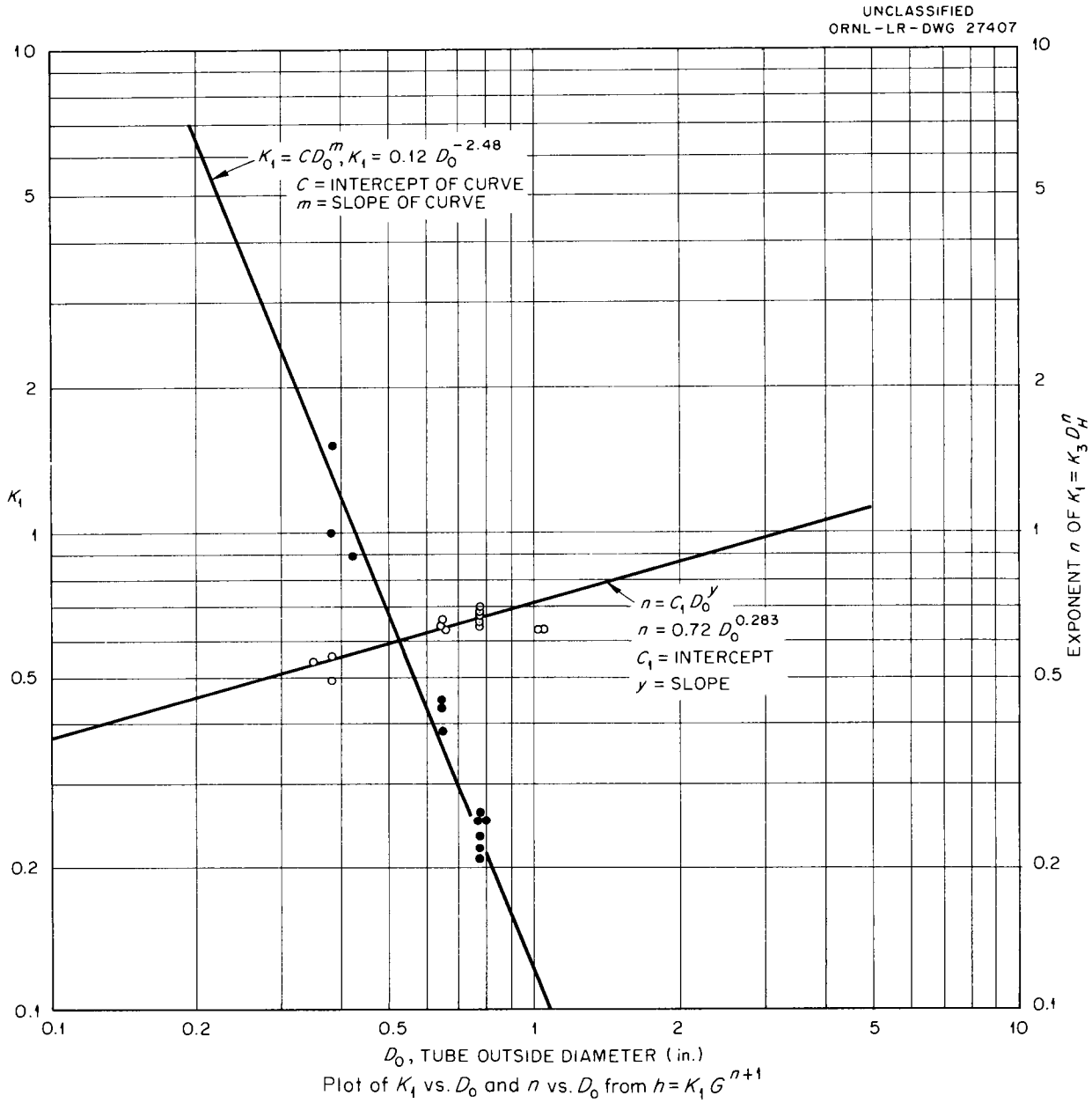

Fig. 9.16. Graph of K_1 vs D_0 and n vs D_0 from $h = K_1 G^{n+1}$.

diameter. Reasonable expressions were obtained for K_1 and n as function s of tube diameter, as follows:

$$K_1 = 0.12\ D_o^{-2.48}$$

$$n = 0.72\ D_o^{0.283} - 1$$

The basic correlating equation for h could then be written:

$$h = K_1\ G^{n+1}$$

$$h = \frac{0.12}{D_o^{2.48}}\ G^{0.72}\ D_o^{0.283}$$

G = mass velocity in lb/ft^2-hr

Rewriting for G in lb/ft^2-sec

D_o = outside diameter in inches

$$h = \frac{71}{D_o^{0.302}}\ G^{0.72}\ D_o^{0.283}$$

A plot of this equation is shown in Fig. 9.17

The above equation was derived from data for tube diameters up to 1.024 in. and the correlation was utilized on tubes up to 2-in. diameter.

Fin Efficiency. Fin efficiencies were calculated using the method of Gardner[7] for annular fins of constant thickness.

B. Tube-Side Heat Transfer

Water. The following correlating equation was used for the prediction of the water-side heat transfer coefficient:

$$\frac{h\ D_i}{k} = 0.023 \left(\frac{D_i G}{\mu}\right)^{0.8} \left(\frac{C_p\ \mu}{k}\right)^{0.4}$$

D_i = tube inside diameter, ft

Other symbols which have been defined previously are evaluated at bulk fluid temperatures.

---

[7]Karl A. Gardner, "Efficiency of Extended Surface," Trans. ASME, 67, 621 (1945).

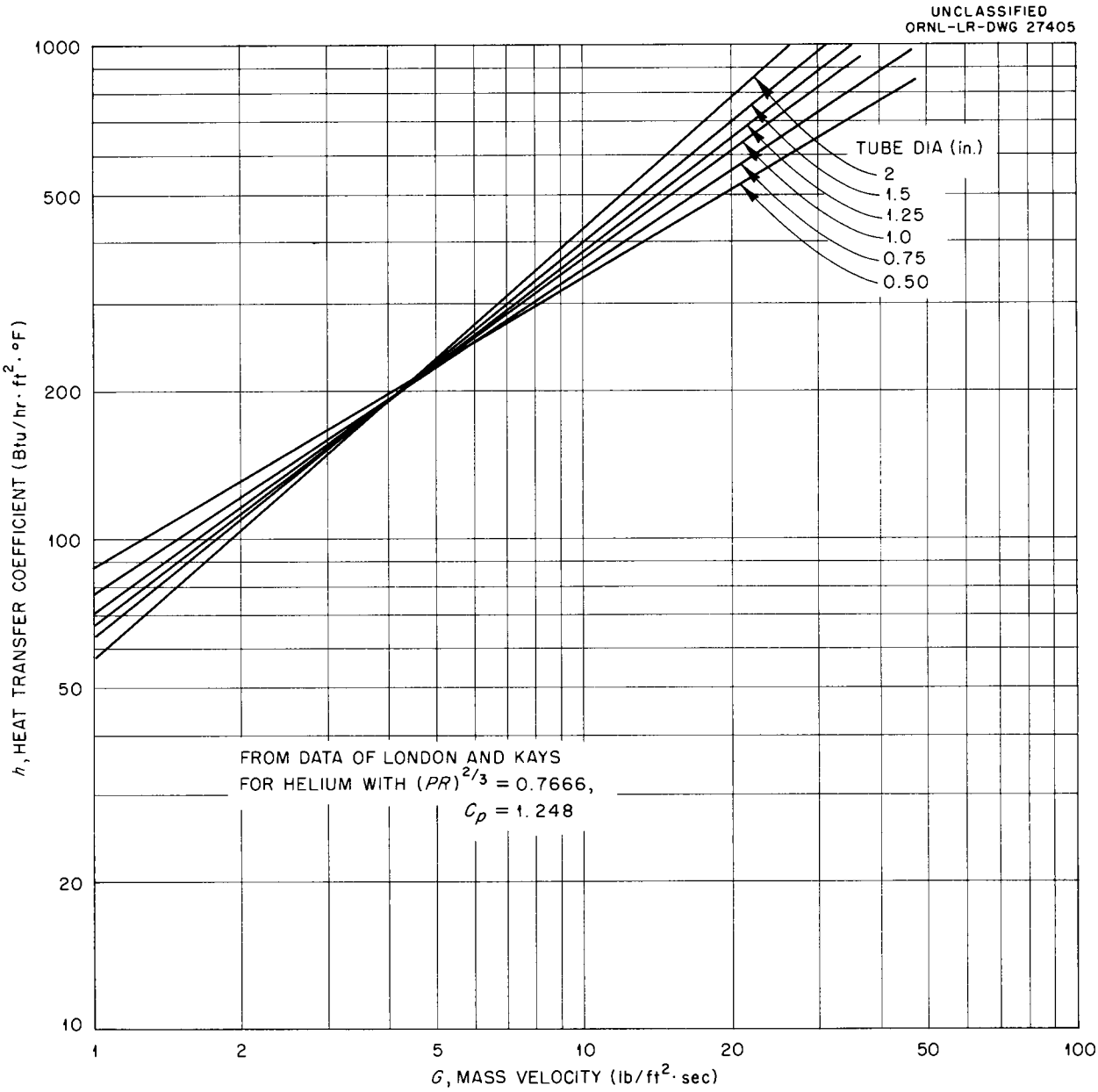

Fig. 9.17. Helium Heat-Transfer Coefficient for Spiral-Finned Tubes.

For a reasonable range of water temperatures, the above equation can be reduced to a much simplified form. Thus, at 400°F:

$$h = \frac{14.2\ G^{0.8}}{D_i^{0.2}}$$

Boiling. In attempting to predict a boiling heat transfer coefficient, a conservative value of 2000 Btu/hr-ft^2-°F was adopted for all calculations.

C. Steam Heat Transfer Coefficient.

The following modified equation[8] for steam-side coefficients was used for the prediction of all steam heat transfer coefficients.

$$h_s = \frac{0.0266}{(d_i/12)^{0.2}}\ G^{0.8}\ C_p\ \mu^{0.2}$$

d_i = inside tube diameter, in.

G = mass velocity, lb/hr-ft^2

Other symbols which have previously been defined are evaluated at mean bulk temperature.

D. Tube-Wall Resistance.

For all calculations, a constant value of thermal conductivity equal to that of the 1% Cr, 1/2% Mo alloy was used. The bare tube-wall resistance was sufficiently unimportant that errors occurring due to variation in materials had only a slight effect on the over-all heat transfer resistance. The effect of the variable thermal conductivity on the fins was not negligible. The design calculations assumed a homogeneous tube and fin material. The temperatures encountered by the finned sections are low enough that a higher alloy steel is not required.

The possible use of high-alloy steels such as 347 stainless steel having a lower conductivity would occur only in the bare tube superheater section where the effect of reduced thermal conductivity is trivial.

$K = 18$ Btu/ft^2-hr-°F/ft

Tube-Side Scale Factor. A constant resistance value of 0.0005 (Btu/ft^2-°F)$^{-1}$ has been used.

---

[8] Steam, Its Generation and Use, The Babcock and Wilcox Co. (1955).

E. Determination of Over-all U.

All coefficients have been converted to gas-side total heat transfer areas using the following equation:

$$\frac{1}{U\,A_o} = \frac{1}{h_{Gas}(A_t+\Phi A_F)} + \frac{1}{h_{fluid}A_i} + \frac{1}{(\frac{K}{x})A_M} + \frac{R_W}{A_i}$$

U = Over-all coefficient of heat transfer, Btu/hr-ft^2-°F

A_o = Total outside surface area, ft^2

A_T = Total outside tube surface area, ft^2

A_F = Total outside fin area, ft^2

Φ = Fin efficiency

A_i = Total inside tube area, ft^2

A_M = Mean tube wall area, ft^2

K = Thermal conductivity of wall, Btu/hr-ft^2-°F/ft

x = Tube-wall thickness, ft

Pressure Drop. Calculations on the water-side and gas-side pressure drop have been carried out using the equations and methods described below.

A. Gas-Side Pressure Drop

Pressure Drop Across Staggered Banks of Bare Tubes. McAdams[9] gives the following equations based on Grimison's data for evaluating turbulent pressure drop across banks of staggered tubes:

$$(P_1 - P_2) = \frac{4\,f''\,N\,G_{max}^2}{2\,g_c\,\rho}$$

$$f'' = \left(0.23 + \frac{0.11}{(X_T - 1)^{1.08}}\right)\left(\frac{D_o G}{\mu_f}\right)^{-0.15}$$

where

P_1 = Initial absolute pressure, lb force/ft^2

P_2 = Final absolute pressure, lb force/ft^2

N = Number of tube rows

---

[9] W. H. McAdams, Heat Transmission, 3rd Ed., (New York: McGraw Hill, 1954)

G_{max} = Mass velocity through minimum area, lb/ft^2-sec

g_c = Conversion factor 32.2 $\frac{\text{lb mass ft}}{\text{lb force sec}^2}$

ρ = Density, lb/ft^3

X_T = Ratio of transverse pitch to D_o

D_o = Tube outside diameter, ft

μ_f = Fluid viscosity at film temperature, lb/ft-sec

The above equation takes into account no momentum change of the gas as it passes across the tube bank. This change has already been shown to be small.

Pressure Drop Across Banks of Staggered Finned Tubes. The gas pressure drop across banks of finned tubes was computed by using equations and friction factors given by Kays.[10]

The following equation was employed:

$$\frac{\Delta P}{P_1} = \frac{G^2}{2\,g_c}\,\frac{v_1}{P_1}\left[(1+\sigma^2)\left(\frac{v_2}{v_1}-1\right) + f\frac{A}{A_c}\,\frac{v_m}{v_1}\right]$$

f = Friction factor across finned tubes

ΔP = Pressure drop across bank, lb/ft^2

P_1 = Absolute initial pressure, lb/ft^2

v_1 = Specific volume initial, ft^3/lb

v_2 = Specific volume final, ft^3/lb

v_m = Specific volume mean, ft^3/lb

σ = Mean free-flow area in per cent

Other symbols have been defined previously.

By employing the universal gas equation and the definition of free-flow area, the above equation may be written as follows:

$$\Delta H = \frac{G^2}{2\,g_c\,\rho_M^2\,T_M}\left[\left(1+\frac{A_c}{A_F}\right)(T_2 - T_1) + f\frac{A}{A_c}\,T_M\right]$$

ΔH = Heat loss in ft

ρ_M = Mean gas film density in tube bank, lb/ft^3

T_M = Mean bulk temperature of gas, °F

---

[10] W. M. Kays, op cit, p. 9.49.

T_1 = Initial temperature, °F

T_2 = Final temperature, °F

A_F = Face area of tube bank, ft^2

Other symbols have been defined previously.

The effect of the first two terms is less than one per cent in most cases so the above equation can be simplified to give:

$$\Delta H = \frac{fG^2 A}{2 g_c \rho_M^2 A_c} ,$$

from the definition of D_H the equation can be written

$$\frac{A}{A_c} = \frac{4 L}{D_H}$$

or

$$\Delta H = \frac{2 f L G^2}{\rho_M^2 g_c D_H}$$

which is a familiar form of the pressure drop equation.

L = Height of tube bundle, ft.

B. Friction Factor Determination

The proper friction factor for finned spiral tubes had to be determined in order to use the formulation above. From the relation of f to Re[11] for the matrices discussed under the section on heat transfer, a correlation of the friction factor vs hydraulic diameter was attempted.

The following equation was assumed:

$$f = K \left(\frac{D_H G}{\mu}\right)^n .$$

Kays[12] gives an average value for n of 0.253. The values for K were then calculated from the known f values and constant n value. A graph was constructed of K vs D_H^{+n}.

Thus,

$$K = C(D_H^n)^p .$$

The constants are determined from Fig. 9.18.

---

[11] W. M. Kays, op cit, p. 9.49.

[12] Ibid.

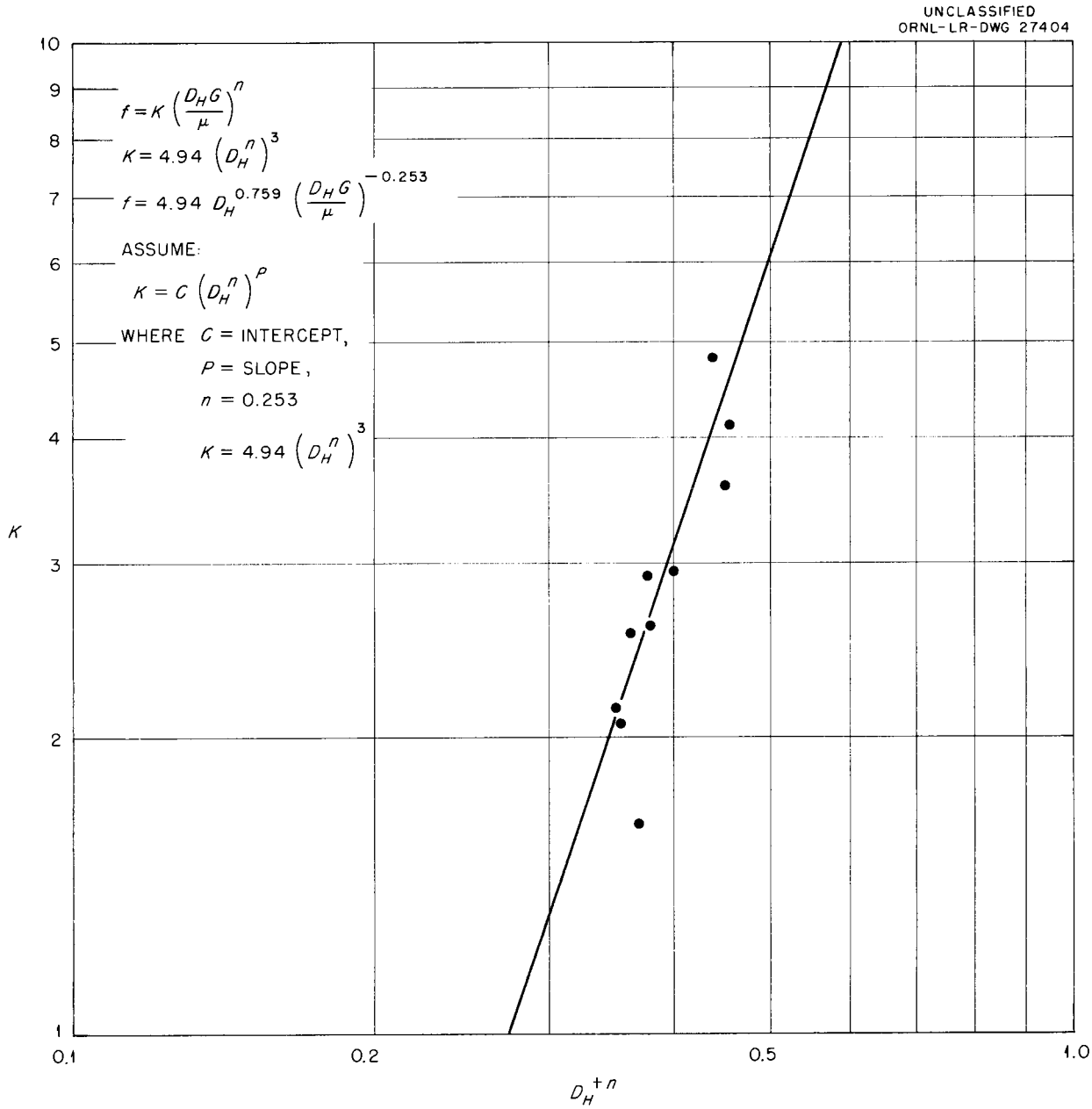

Fig. 9.18. D_H^n vs K in Friction Factor Equation.

$$K = 4.94\ (D_H{}^n)^3$$

$$K = 4.94\ D_H{}^{0.759},$$

then

$$f = K\ \left(\frac{D_H G}{\mu}\right)^n$$

$$f = \frac{4.94\ D_H{}^{0.506}\ G^{-0.253}}{\mu^{-0.253}}\ .$$

For a fixed average temperature of the gas through the tube bank, the expression can be written as

$$f = \frac{0.33\ D_H{}^{0.506}}{G^{0.253}} \sim \frac{0.33\ D_H{}^{0.5}}{G^{0.25}}$$

C. Tube-Side Pressure Drop.

Water Drop.[13] The following equation was used to compute the water-pressure drop.

$$\Delta P = \frac{f\ L\ G^2}{2\ g_c\ D\ \rho^2}\ .$$

ΔP = Pressure drop in ft. fluid

L = Tube length, ft

f = Darcy Weisback friction factor

G = Mass velocity, lb/ft^2-sec

ρ = Fluid density at mean temperature, lb/ft^3

g_c = Conversion factor, ft-lb mass/lb force sec^2

D = Tube inside diameter, ft.

Boiling-Water Pressure Drop. The relationships used for the determination of the two-phase flow pressure drop occurring in the

---

[13] Calculation of bend losses was as indicated by term three in the equation for steam flow pressure drop $\Delta P = \frac{N_b}{12}\ v\ \left(\frac{G}{10^5}\right)^2$.

boiler section of the steam generator are those given by Martinelli and Nelson.[14] The pressure drop is expressed in terms of a two-phase flow factor $\Delta P_{TPF}/\Delta P_o$ which relates the pressure drop during two-phase flow to that occurring for single-phase flow. Graphs have been prepared to permit the determination of $\Delta P_{TPF}/\Delta P_o$ as a function of the absolute pressure level of the system and the exit quality of the vapor leaving. For all calculations an exit quality of 100 per cent was assumed in the determination of the two-phase flow factor. Any reduction in exit quality will reduce this factor.

Steam Flow Pressure Drop. The steam pressure drop was calculated using the following equation.[15]

$$\Delta P = \left[0.125 + \frac{f\ L}{d} + N_b/12\right] v \left(\frac{G}{10^5}\right)^2$$

ΔP = Pressure drop, psi

L = Tube length, ft

d = Tube inside diameter, in.

N_b = Bend factor x No. bends

f = Friction factor

G = Mass velocity, lb/ft^2-hr

v = Specific volume, ft^3/lb at average temperature

Determination of Costs for Pumping. All pumping costs were computed on the basis of power costs of 10 mills/kwh with the pumps operating 85% of the time over a 20-yr period.

A. Water-Pumping Costs

Water-pumping costs were computed on the basis of motor efficiency of 95% and a pump efficiency of 70%.

$$\text{Cost} = \text{h.p. x cost/h.p. per 20 yr}$$

$$= \frac{w\ \Delta H}{550 \times 0.95 \times 0.7} \times 0.01 \times 24 \times 365 \times 20 \times 0.746$$

$$= \$502.41/\text{ft heat at the pump}$$

w = 140.6 lb/sec for 20 yr under original conditions

---

[14] R. C. Martinelli, D. B. Nelson, "Prediction of Pressure Drop During Forced Circulation Boiling of Water," Trans. ASME, (August 1948).

[15] The Babcock and Wilcox Co., op cit, p.9.55.

B. Helium-Pumping Costs

Helium-pumping costs assumed a 95% motor efficiency and an 80% blower efficiency.

$$\text{Cost} = \frac{w\ \Delta H}{550 \times 0.95 \times 0.8} \times 0.01 \times 24 \times 365 \times 20 \times 0.746$$

= \$830/ft heat at blower

w = 266 lb/sec per system under original conditions.

The above values were based on steam and helium flows as determined by plant conditions assumed at the beginning of the design study. These conditions are as given below:

Helium inlet	950°F
Helium exit	450°F
Steam exit temperature	800°F
Steam exit pressure	810 psia
Water to economizer	250°F
Steam pressure from turbine	2 in. Hg
Thermal load capacity	700 Mw

These conditions yielded the following flows per system:

W_{H_2O} = 140.6 lb/sec

W_{He} = 266 lb/sec

The effect of variations in cost caused by slight changes in flows was not incorporated in the parametric studies until the final design was selected. The latest actual equipment costs are tabulated in Table 9.10 where a summary of the steam generator cost is shown.

C. Tubing Costs

Table 9.11 gives the costs used in the studies of Section 9.4.3. They are for 1% Cr, 1/2% Mo fabricated in a serpentine coil. The costs include x-ray inspection, vacuum testing,and special cleanliness requirements. Costs were obtained from vendors familiar with such manufacture.

TABLE 9.11

COST OF SERPENTINE COILS AS A FUNCTION OF SIZE

OD (in.)	Wall Thickness (in.)	Fin Thickness (in.)	No. of Fins	Fin OD (in.)	Total Linear Pipe Length (ft)	$/ft
1-1/2	0.095	0.040	105/ft	2.5	15,000	8.03
1-3/4	0.095	0.040	105/ft	2.5	12,000	7.79
2	0.154	0	0	0	1,000	5.21

9.5 Feed Water Purity and Condenser Integrity

Because the steam generators selected for this plant are of the "once-through" type, some special provisions are required to provide the extremely pure feed water necessary for this equipment since the amount of solids deposited on the heat-transfer surfaces on the water side must be held to a minimum. Table 9.12 lists specifications for feed-water purity.

TABLE 9.12

SPECIFICATIONS FOR FEED-WATER PURITY

Recommended Limits:	
Total dissolved solids	0.1 ppm
Suspended solids	0 ppm
Hardness	0
Free caustic	0
Dissolved O_2	0.005 cc/l max.,preferably 0
Carbon dioxide	minimum, perferably 0
Total Silica as SiO_2	0.01 ppm max.
Total iron, Fe	0.01 ppm max.
Total copper, Cu	0.005 ppm max.
pH adjusted to obtain 0.01 ppm Fe max. PH of 8.5 to 9.5 at 77°F	This would normally require a

The special provisions required to meet the feed-water specifications consist of the addition of a demineralizer unit in the condensate system, and extra leak-tightness provisions in the main condenser. Since condenser leakage is

the largest single source of feed-water contamination in conventional power plants, capital expenditures to reduce expected condenser leakage would be reflected in reduced capital expenditures for equipment required to remove condenser-leakage contamination from the condensate.

Condenser leakage may occur either from failure of a cooling water tube between the tube sheets, or through the tube-to-header joint. It is believed that 100% inspection of condenser tubes by electronic, ultrasonic, or radiographic methods would reduce the probability of tube failure between the tube sheets to essentially zero. The use of welded tube-to-tubesheet joints, as used in the Portland Station of Metropolitan Edison Company,[16] the use of double tube sheets, the use of a sprayed neoprene coating over rolled tube-to-tubesheet joints,as used in the American Gas and Electric Company Philo Plant,[17] or some combination of these methods should also be capable of reducing leakage at these joints well below usual standards. For these reasons, it is believed demineralization facilities in the condensate system can have capacity of five per cent of full-load condensate flow. The cost of demineralizers to handle five per cent of the condensate flow from both units is $270,000. The cost of 100% tube inspection for the condenser plus the addition of extra tight tube-to-tubesheet joints is not expected to add more than 10% to the cost of the condensers or about $40,000 per unit.

This study has not included a cost comparison of the "once-through" steam generator plus the added costs for condenser tightness and water purity as opposed to the drum-type boiler with standard condensers and no demineralizers required in the condensate system. A detailed cost study of both cases should be made to determine whether this decision affects the cost optimization.

Chemical feed-water treatment will consist of hydrazine for oxygen scavenging and ammonia or morpholene for pH control.

---

[16] G. T. Jones, The Condenser at Portland, ASME Paper No. 57-PWR-14.

[17] S. N. Fiala, "First Commercial Supercritical Pressure Steam Electric Generating Unit for Philo Plant," Trans. ASME, (February 1957).